MOLECULAR FUNCTION OF A TRANSLESION DNA SYNTHESIS COMPLEX

DETERMINING THE MOLECULAR FUNCTION OF A TRANSLESION DNA SYNTHESIS COMPLEX

By ANDRIANA TETENYCH, H.B.Sc.

A Thesis Submitted to the School of Graduate Studies in Partial Fulfilment of the Requirements for the Degree Master of Science

McMaster University MASTER OF SCIENCE (2022) Hamilton, Ontario (Biochemistry and Biomedical Sciences)

TITLE: Determining the molecular function of a translesion DNA synthesis complex

AUTHOR: Andriana Tetenych, H.B.Sc. (McMaster University)

SUPERVISOR: Professor Sara Andres

NUMBER OF PAGES: xiii, 96

ABSTRACT

Translesion DNA Synthesis (TLS) is a mechanism that promotes DNA damage tolerance during DNA replication using an error-prone DNA polymerase complex. The complex is comprised of the ImuA, ImuB, and ImuC proteins that are found in approximately one-third of bacteria, including high priority antimicrobial resistant pathogens, such as *Pseudomonas aeruginosa*. Previous *in vivo* studies have shown that TLS increases beneficial bacterial mutations as the error-prone DNA polymerase, ImuC, lacks proof-reading activity. However, how ImuA and ImuB proteins contribute to the polymerase mechanism is unknown. Thus, the goal of this study is to characterize the TLS proteins *in vitro* to determine how ImuA and ImuB associate with ImuC to promote error-prone replication.

ImuA and $ImuB_{N\Delta34}$ were successfully purified for biochemical characterization from the homolog *Myxococcus xanthus*. Using size-exclusion chromatography coupled to multi-angle light scattering, both ImuA and $ImuB_{N\Delta34}$ are trimers in solution. Each protein also binds DNA independently as assessed by fluorescence polarization. Interestingly, both proteins bind ssDNA and a 3' overhang substrate mimicking the DNA replication intermediate with the highest affinity. DNA binding assays further confirm these proteins can form a DNA-ImuA-$ImuB_{N\Delta34}$ complex. Using bacterial two-hybrid assays, the ImuA-ImuB interaction occurs in the C-terminal region of both proteins. Overall, these results suggest that ImuA and ImuB may recruit and stabilize ImuC on DNA for replication past damaged DNA, providing the first insights into the ImuA and ImuB molecular mechanism.

ACKNOWLEDGEMENTS

Albert Einstein once said “Failure is success in progress” which I took throughout my masters trying to solve a problem researchers all over the world have encountered with TLS: insolubility of proteins.

First and foremost, I’d like to thank my supervisor Dr. Sara Andres for her ongoing support, guidance, expertise, and mentorship throughout my masters. I would also like to thank my committee members, Dr. Xu-Dong Zhu and Dr. John Whitney, for their valuable feedback and guidance.

Thank you to my undergraduate students- Sahil Karnani, Noorisah Khan, and Nethmi Rajapakse for their help on this project. Thank you to my parents and my brother for the constant support throughout my masters.

Finally, a big thank you to Dana Sowa and Monica Warner, PhD students in the Andres Lab and life-long friends, who taught me how to purify protein and brought me Starbucks after my committee meetings.

TABLE OF CONTENTS

LIST OF TABLES

LIST OF FIGURES

LIST OF ABBREVIATIONS

6-FAM: 6-Carboxyfluorescein

aa: amino acids

AIM: autoinduction media

Amp: ampicillin

BAC2H: bacterial adenylate cyclase two-hybrid system

bp: base pair

dsDNA: double-stranded DNA

E. coli: Escherichia coli

EMSA: electrophoretic mobility shift assay

FP: fluorescence polarization

HRP: horseradish peroxidase

IMAC: immobilized metal-affinity chromatography

ImuABC: ImuA, ImuB, and ImuC as a protein complex

IPTG: isopropyl β-d-1-thiogalactopyranoside

Kan: kanamycin

K_D: dissociation constant

LB: Luria-Bertani

LIC: ligation independent cloning

M. tuberculosis: Mycobacterium tuberculosis

M. xanthus: Myxococcus xanthus

Ni-NTA: nickel-nitriloacetic acid

nt: nucleotide

P. aeruginosa: Pseudomonas aeruginosa

PCR: polymerase chain reaction

PM: polymerization motif

PolIII: DNA Polymerase III

RE: restriction enzyme

SAXS: small-angle x-ray scattering

S. cerevisiae: *Saccharomyces cerevisiae*

SDM: site directed mutagenesis

SDS-PAGE: sodium dodecyl sulfate polyacrylamide gel electrophoresis

SDS: sodium dodecyl sulfate

SEC-MALS: Size-exclusion chromatography coupled to multi-angle light scattering

SOE: splicing by overlap extension

SSB: single-stranded DNA-binding protein

ssDNA: single-strand DNA

TB: Terrific Broth

TLS: Translesion DNA Synthesis

UV: ultraviolet

WT: wildtype

X-Gal: 5-Bromo-4-Chloro-3-Indolyl β-D-Galactopyranoside

DECLARATION OF ACADEMIC ACHIEVEMENT

Study design, experiments, data analysis, and thesis writing were completed by Andriana Tetenych, under supervision of Dr. Sara Andres. Dr. Sara Andres designed *P. aeruginosa* primers for full-length and N-terminal truncations of proteins for cloning in Table S1. Monica Warner designed twelve genomic deletion primers in Table S1. Lucas Koechlin cloned three full-length plasmids in Table S3. Noorisah Khan contributed to the creation of five genomic DNA knockout strains in Table S4 and Sahil Karnani was responsible for the UV mutagenesis assay (Figure 17, 18). Dr. Sara Andres analyzed the SAXS data.

INTRODUCTION

DNA Replication

Faithful DNA replication is essential for the continuation of life, where the machineries involved in the replication of DNA are conserved among all three domains of life: Bacteria, Archaea, and Eukarya (Oakley, 2019). To ensure high fidelity, DNA replication is a highly regulated process and must overcome obstacles such as active transcription and damaged DNA (Oakley, 2019). The loss of fidelity of DNA replication may lead to a variety of consequences including mutations that affect cellular processes, genomic instability, and cell death (Mertz et al., 2017). However, DNA replication pathways also remain a source of developing new mutations, which can lead to bacterial antibiotic resistance (Oakley, 2019; Robinson et al., 2012). Currently, only one class of antibiotics target bacterial DNA replication, even though it is a fundamental process in bacteria (Bradbury & Pucci, 2008; Robinson et al., 2012). Thus, the study of DNA replication in bacteria not only provides insight on the most important process for the continuation of life, but also how it can be exploited for novel therapeutics to target infectious diseases.

DNA replication in bacteria is carried out by the replisome, a large multi-protein complex to ensure high-fidelity DNA replication. With one origin of replication, DNA synthesis continues bidirectionally with two replication forks. Initially, an ATP-dependent DNA helicase, DnaB, unwinds the double-stranded DNA (dsDNA) duplex and the primase DnaG lays down RNA primer (Figure 1A) (Oakley, 2019; O'Donnell, 2006; Wegrzyn et al., 2016). Single-stranded DNA binding proteins (SSB) then stabilize and protect the

single-stranded DNA (ssDNA) unwound by the primase. However, the major factor used to synthesize DNA is the DNA Polymerase III holoenzyme. This holoenzyme is made up of 3 proteins: DNA Polymerase III (PolIII), a clamp loader, and the β-sliding clamp (O'Donnell, 2006; Wegrzyn et al., 2016). The clamp loader binds to the template RNA primer and loads the β-clamp. This clamp is important as it acts as a tether for PolIII to DNA. The β-clamp also serves as a protein interaction hub in various cellular processes such as DNA replication, regulation of DNA replication, and the repair of DNA damage (Hedglin et al., 2013; Katayama et al., 2010; Rangarajan et al., 1999; Wegrzyn et al., 2016). PolIII, on the other hand, is responsible for elongating the DNA chain by reading the DNA template in a 3'-5' direction but carrying out the addition of nucleotides in a 5'-3' direction (Wegrzyn et al., 2016). Overall, these proteins come together to form a replisome where PolIII carries out faithful DNA replication (Figure 1A).

DNA Polymerases

PolIII is responsible for duplicating bacterial chromosomal DNA. In *Escherichia coli* (*E. coli*), PolIII is divided into three functional parts – a heterotrimer composed of α, ε, and θ subunits. The α subunit is responsible for DNA replication which contains aspartate residues (D^{401}, D^{403}, and D^{555}) that are essential for catalysis, while the ε subunit has 3′- 5′ exonuclease activity that excises incorrect bases to ensure replication fidelity (Bailey et al., 2006; Lamers et al., 2006; Oakley, 2019). Finally, the θ subunit stabilizes the catalytic core (Taft-Benz & Schaaper, 2004). PolIII has two binding sites for the β-clamp, which prevents dissociation from DNA and produces high processivity (Bailey et al., 2006; Oakley, 2019).

Given its high fidelity, PolIII belongs to the C-class polymerase family (Bailey et al., 2006; Filée et al., 2002). However, there are a total of six families of DNA polymerases that are involved in DNA replication and repair – A, B, C, D, X, and Y. Each family varies in overall function, but all families share a common structure regardless of amino acid sequence (Table 1) (Filée et al., 2002). The general structure of DNA polymerases resembles an open right hand, which includes the palm, thumb, and finger domains. Generally, the palm domain contains the catalytic site, the thumb binds the dsDNA duplex, and the fingers interact with the incoming nucleotides and the ssDNA, which acts as a template (Bailey et al., 2006; Bębenek & Ziuzia-Graczyk, 2018; Filée et al., 2002; Ollis et al., 1985). In coordination, these three domains allow for the extension of the DNA. Families A-D have proofreading activity, which include bacterial, archaeal, and eukaryal DNA replication polymerases, producing high-fidelity replication (Table 1) (Bailey et al., 2006; Filée et al., 2002). In both prokaryotic and eukaryotic cells, this means that in DNA replication, there is approximately one wrong nucleotide incorporation per 10^8–10^{10} nucleotides, which keeps mutation rates low (Bębenek & Ziuzia-Graczyk, 2018). In contrast, X and Y polymerases are specialized in DNA repair or DNA damage tolerance, even during DNA replication, which will be discussed later (Table 1) (Bailey et al., 2006; Filée et al., 2002).

DNA Replication Stress

During DNA replication, genomic integrity is highly vulnerable and is threatened by exogenous and endogenous sources of DNA damage, as bacteria are in constantly changing environments (Aguilera & Gómez-González, 2008). Endogenous DNA damage

includes reactive metabolites such as reactive oxygen species that are generated by cells themselves, which can lead to depurinations and depyrimidinations (Lindahl & Barnes, 2000; Waters et al., 2009). In contrast, outside factors, including ionizing or UV radiation and chemical agents, cause DNA strand breaks and base alterations such as methylation and cross-linking (Lindahl & Barnes, 2000; Waters et al., 2009). The variety of DNA lesions induced by DNA-damaging agents threaten DNA replication by stalling PolIII and replication forks, which leads to fork breakdown, chromosomal instability, and genetic loss. Ultimately, this can lead to cell death (Aguilera & Gómez-González, 2008; Goodman & Woodgate, 2013; Knobel & Marti, 2011).

DNA Damage Repair and Tolerance During Replication

Stalling of PolIII at DNA lesions results in long stretches of ssDNA, as the DNA helicase continues to unwind dsDNA during replication. These long DNA strands activate the SOS response (Mckenzie et al., 2000; Waters et al., 2009). The SOS response is a cellular mechanism to restart DNA replication and avoid cell death. Under normal growth conditions, the genes responsible for the SOS response are repressed by the transcriptional repressor, LexA, binding to SOS boxes. Once PolIII stalls, RecA, an ATP-dependent recombinase, 1) accumulates on ssDNA by forming polymer chains and becomes activated and 2) interacts with LexA to promote its self-cleavage (Leite et al., 2016; Lin-Ling & Little, 1988; Mckenzie et al., 2000; Podlesek & Žgur Bertok, 2020). Inactivation of the LexA repressor leads to induction of over 50 genes to promote DNA damage repair, so that DNA replication continues. Early in the SOS response, nucleotide excision repair, mismatch excision repair, base excision repair, homologous recombination, and non-

homologous end-joining repair the DNA damage, as their genes have weak LexA-binding sites (Waters et al., 2009). These repair processes are considered error free, apart from non-homologous end-joining, although not as accurate as DNA replication (Knobel & Marti, 2011).

However, sometimes the DNA damage surpasses the cell's ability to repair it. Once all DNA repair mechanisms have been exhausted, the continual stalling of the replication fork activates a bypass mechanism to tolerate the damage. This bypass mechanism, known as translesion DNA synthesis (TLS), has tighter LexA-binding sites and is induced as a late-stage response to DNA damage (Goodman & Woodgate, 2013; Sommer et al., 1993; Waters et al., 2009). TLS allows for DNA lesion bypass to restart DNA replication and avoid replication fork collapse by switching out PolIII for a specialized polymerase to incorporate nucleotides based on the damaged template (Figure 1B) (Freidberg et al., 2005; Waters et al., 2009). While PolIII incorporates a wrong nucleotide (nt) every 10^8–10^{10} nucleotides synthesized, TLS polymerases have error rates of one wrong nt per 10^1–10^3 nucleotides (Bębenek & Ziuzia-Graczyk, 2018; Knobel & Marti, 2011; McCulloch & Kunkel, 2008). This is primarily because TLS polymerases lack the PolIII ε subunit that has 3′- 5′ exonuclease activity. Due to this lack of proof-reading ability, TLS increases mutation rates, which leads to genetic adaptation and diversity of the bacteria (Bębenek & Ziuzia-Graczyk, 2018; Knobel & Marti, 2011; McCulloch & Kunkel, 2008).

Discovery of TLS Polymerases in DNA Damage Tolerance

In the 1970's, it was widely believed all DNA polymerases had been discovered. However, Jeffery Lemontt discovered a set of genes that increased mutagenesis after UV

irradiation in *Saccharomyces cerevisiae (S. cerevisae)* yeast (Lemontt, 1971; Waters et al., 2009). These genes became known as *REV1* and *REV3* (Lemontt, 1971; Waters et al., 2009). In 1977, similar UV irradiation screens were tested on *E. coli* to discover the *umuC* and *umuD* genes (Kato & Shinoura, 1977; Knobel & Marti, 2011). Given that PolIII was unable to bypass DNA lesions *in vitro*, it was believed that these newly discovered genes allowed PolIII to be modified and bypass the damage (Fuchs & Fujii, 2013). This was believed for almost thirty years, as no biochemical evidence supported the discovery of additional polymerases, largely due to the insolubility of the now known TLS proteins and lack of primary sequence homology with high fidelity polymerases (Fuchs & Fujii, 2013; Goodman & Woodgate, 2013; Waters et al., 2009). In the 1990's, sequence conservation and homology searches discovered orthologs of the Rev1/Rev3 (*S. cerevisae)* and UmuC/UmuD (*E. coli*) proteins in other archaea, prokaryotes, and eukaryotes, which prompted scientists to suggest an enzymatic function for these proteins (Table 2) (Goodman & Woodgate, 2013; Nelson et al., 1996; Waters et al., 2009). It was not until the late 1990's that the first biochemical analysis showed that yeast Revl protein has deoxycytidyl transferase activity and that the $UmuD_2C$ complex was able to replicate both damaged and undamaged DNA without PolIII, concluding that these proteins are polymerases (Nelson et al., 1998; Tang et al., 1998, 1999). Since then, through genetic studies, TLS polymerases have been found across all domains of life: Bacteria, Eukarya, and Archaea (Table 2) (Goodman & Woodgate, 2013).

Most TLS polymerases that have been discovered belong to the Y-family of polymerases, which lack 3'-5' proofreading activity, however some B-family TLS

polymerases have been observed in eukaryotes (Filée et al., 2002; Waters et al., 2009). Polymerases of the A- and X-families have minor roles in TLS; however, their TLS polymerase activity is weak and is not their primary function (Filée et al., 2002; Waters et al., 2009).

Bacterial TLS Polymerases

There are two known main TLS polymerase complexes that exist in bacteria and function as a mechanism to bypass DNA damage. They are Pol V, made up of $UmuD_2C$, and the ImuAImuBImuC (ImuABC) complex, which are functionally homologous and activated later in the SOS response (Goodman & Woodgate, 2013; Sheng et al., 2021). Based on 6,107 sequenced bacterial strains, approximately one third of bacteria use Pol V for TLS, such as *E. coli*, while another third use the ImuABC complex in organisms such as *Pseudomonas aeruginosa* (*P. aeruginosa*) and *Mycobacterium tuberculosis* (*M. tuberculosis*) (Sheng et al., 2021). It is important to acknowledge the other TLS polymerases, Pol II and Pol IV, which have been observed to be back-up polymerases to $UmuD_2C$ and ImuABC. However, Pol II and Pol IV are not a universal DNA damage bypass mechanism. Instead, they have a slightly higher fidelity and only bypass certain DNA damage such as abasic sites or create frameshift mutations in *E. coli* (Fuchs & Fujii, 2013; Goodman & Woodgate, 2013; Jaszczur et al., 2016; Sheng et al., 2021).

Pol V

The discovery of *umuC* and *umuD* genes preceded the identification of these genes as TLS polymerases for decades as Pol V suffered from insoluble recombinant protein expression. To circumvent this, UmuC initially was purified from inclusion bodies by

denaturing and renaturing the protein. Then in 1996, after overexpression in 200 L of media, UmuD'$_2$C complex was purified (Bruck et al., 1996; Goodman & Woodgate, 2013). Since then, Pol V purification was optimized through the additional of an N-terminal His-tag and low expression levels, where 1 mg of pure Pol V can be obtained from 4 L of *E. coli* culture (Karata et al., 2012). Pure Pol V allowed its mechanism to be extensively studied. Briefly, when PolIII encounters a DNA lesion, it stalls either one nt before the lesion or at the lesion, while DNA helicase continues unwinding DNA (Fuchs & Fujii, 2013). As previously mentioned, the accumulation of ssDNA allows for the activation of RecA polymers. Similar to the mechanism of LexA, a single RecA monomer interacts with UmuD$_2$, a homodimer in regular growth conditions, and promotes self-cleavage of the 24 N-terminal amino acids of UmuD$_2$ to form UmuD'$_2$ (Burckhardt et al., 1988; Fuchs & Fujii, 2013). This allows for association of UmuD'$_2$ with ATP and UmuC, the catalytic polymerase, to form an active UmuD'$_2$C-RecA-ATP complex, known as Pol V mutasome (Burckhardt et al., 1988; Fuchs & Fujii, 2013; Goodman & Woodgate, 2013; Jiang et al., 2009). During the recruitment, UmuC interacts with the β-clamp through 357Q^{LNLF}361 and UmuD'$_2$ associates with the α subunit of PolIII where Pol V is able to translocate and replace PolIII (Patoli et al., 2013; Sutton et al., 1999). The binding of an ATP molecule also triggers a conformational change to allow for Pol V to bind the template DNA (Gruber et al., 2015; Joseph & Badrinarayanan, 2020). After replacing PolIII, Pol V bypasses a variety of DNA lesions such as pyrimidine dimers and abasic sites (Hawver et al., 2011). Once lesion bypass is complete, Pol V deactivates by the dissociation of ATP, allowing PolIII to once

again bind the β-clamp, allowing high-fidelity replication to resume (Goodman & Woodgate, 2013; M. Jaszczur et al., 2019).

ImuABC

A second set of genes forming an ImuABC TLS polymerase complex were discovered in the early 2000's in *M. tuberculosis* and *Caulobacter crescentus (C. crescentus)* (Boshoff et al., 2003; Galhardo et al., 2005). In *M. tuberculosis,* the catalytic core of PolIII – the α subunit - is encoded by *dnaE1.* However, a second copy of *dnaE1*, *dnaE2,* was upregulated by DNA damaging agents contributing to drug resistance: mitomycin-C and ultraviolet (UV) radiation (Boshoff et al., 2003). This was supported by work in *C. crescentus* where DnaE2 was identified as a potential functional ortholog of UmuD'$_2$C. In *C. crescentus,* mitomycin-C and UV damage not only induced expression of DnaE2 but also two other hypothetical genes, *imuA* and *imuB,* which all transcribed from a single operon. These genes were named after inducible mutagenesis; however, their function was not known at the time (Galhardo et al., 2005). Later on, DnaE2 was renamed ImuC, and together these proteins form the ImuABC complex.

The ImuABC complex is primarily found in Actinobacteria and Proteobacteria. This classification is based on the Kyoto Encyclopedia of Genes and Genomes database, where 2,062 out of 6,107 genomes contain the *imuC* gene. 1,249 of these genomes belong to Proteobacteria and 632 belong to Actinobacteria (Kanehisa et al., 2021; Sheng et al., 2021). The complex is usually transcribed from a three gene cassette with the order of *imuA-imuB-imuC* in organisms such as *P. aeruginosa* and *C. crescentus* or is a part of a split gene cassette (*imuA-imuB/imuC)* where *imuC* is a few kilobases downstream in

organisms like *M. tuberculosis* or *Myxococcus xanthus* (*M. xanthus*) (Erill et al., 2006; Ippoliti et al., 2012; Sheng et al., 2021). However, due to the insoluble nature of the ImuABC recombinant proteins expressed *in vitro*, early studies of ImuABC have consisted of *in silico* and *in vivo* work discussed below.

ImuC has been characterized as a C-family low-fidelity polymerase lacking 3'-5' exonuclease activity, the main characteristic of TLS polymerases (Goodman & Woodgate, 2013; Luján et al., 2019; Warner et al., 2010). As part of the TLS pathway, the ImuC polymerase is dispensable for cell survival, unlike PolIII which is responsible for DNA replication (Peng et al., 2017). As previously mentioned, the active site in *E. coli* PolIII was composed of three acidic aspartates (Lamers et al., 2006). Using the *E. coli* PolIII sequence as a search model, the catalytic triad of ImuC was identified and consists of D^{439}, D^{441}, D^{579}. This catalytic triad was confirmed to be essential for the polymerase activity of ImuC in *M. tuberculosis* (Warner et al., 2010).

The two additional proteins, ImuA and ImuB are both essential for TLS to occur (Warner et al., 2010). ImuA has minor sequence homology to the RecA protein that activates Pol V, yet its primary function in TLS and as part of the ImuABC complex is unclear (Jiang et al., 2009; Pei et al., 2008). Based on secondary structure and domain prediction using InterPro, ImuA has a RecA domain, spanning almost the entire protein, that is predicted to bind ATP (Figure 2A) (Blum et al., 2021). In addition, yeast two-hybrid screens show that ImuA does not associate with ImuC, making it unlikely that ImuA is the activator of catalytic activity like RecA in the Pol V mutasome (Warner et al., 2010). Recently, Sheng et al. suggest that ImuA of *M. xanthus* may play a role in initiating TLS

(2021). In the SOS response, RecA forms a head-to-tail polymer chain through the use of two polymerization motifs (PM): the N-terminal PM and the Core-PM (Figure 2A) (del Val et al., 2019; Leite et al., 2016). However, *M. xanthus* ImuA has only one conserved Core-PM where it is predicted that ImuA binds to the RecA polymer thus possibly inhibiting the RecA extension and error-free pathways, such as template switching and enabling the switch to TLS (Figure 2A) (Sheng et al., 2021). Although these predictions are useful to begin identifying potential functions of ImuA and the mechanism, the structure of the protein may provide greater insight. Unfortunately, there are no existing structures of ImuABC proteins, likely due to their insolubility when expressed *in vitro*. ImuA's structure has been predicted by Alphafold (Figure 2B). ImuA is predicted to have a disordered C-terminus, while a DALI search supports the InterPro prediction that the ImuA core is most similar to the core of RecA, even though sequence identity is low (Gáspári, 2020; Jumper et al., 2021).

ImuB is an inactive Y-family polymerase (Warner et al., 2010). In *M. tuberculosis*, ImuB lacks the catalytic aspartate residues conserved in DNA polymerases as mentioned previously, where two aspartate residues are replaced with a leucine and tryptophan (Warner et al., 2010). ImuB is predicted to maintain the "open right hand" conserved structure of a polymerase which includes the palm, finger, and thumb subdomains (Pata, 2010; Timinskas & Venclovas, 2019). However, Y-family polymerases are unique to other DNA polymerases as they also contain a regulatory region: the little finger domain, which affects polymerase processivity, fidelity, and lesion-bypassing capabilities (Boudsocq et al., 2004; Pata, 2010; Timinskas & Venclovas, 2019). Interestingly, Y-family polymerases

possess a C-terminal extension beyond the little finger domain, which does not resemble any known protein structures (Warner et al., 2010). This little finger domain is also conserved in ImuB. ImuB proteins also contain a UmuC domain, the catalytic core of Pol V, which is labelled in *M. xanthus* (Figure 3A) (Blum et al., 2021). Alphafold has predicted the structure of ImuB of *M. xanthus* with the open right-hand conformation and little figure domain, along with this C-terminal extension (Figure 3BC) (Jumper et al., 2021). Warner et al. (2010) show that ImuB binds itself, ImuA, ImuC, and the β-clamp suggesting it plays a central role in the complex.

Project Goals

TLS contributes to DNA damage-induced mutagenesis resulting from damage caused by crosslinking reagents, UV, and alkylation-inducing agents (Jatsenko et al., 2017; Luján et al., 2019). However, the molecular mechanism of how the ImuABC complex coordinates DNA damage bypass remains unknown. In addition, ImuA and ImuB remain poorly studied proteins in the TLS complex, due to their insolubility when expressed *in vitro*. Thus, the goal of this study is to characterize the TLS proteins *in vitro* to determine how ImuA and ImuB associate with ImuC to promote error-prone replication through two main aims:

1) Express and purify soluble ImuA and ImuB homologs from *M. xanthus.*
2) Conduct biochemical analysis and characterization of ImuA and ImuB for DNA and protein binding sites.

MATERIALS AND METHODS

Bacterial strains, plasmids, and media

Oligonucleotides, plasmids, and bacterial strains are described in Table S1, S3, and S4. Strains were grown in Luria-Bertani (LB) broth (10 g L^{-1} NaCl, 10 g L^{-1} tryptone, and 5 g L^{-1} yeast extract). Solid LB media contained 1.5% agar with appropriate antibiotics.

Cloning

Primers were synthesized by Integrated DNA Technologies. Stop codons were introduced using Q5® Site-Directed Mutagenesis Kit (New England Biolabs). Constructs were amplified through polymerase chain reaction (PCR) with oligonucleotides outlined in Table S1 and joined with either splicing-by-overlap extension (SOE) PCR, ligation independent cloning (LIC)(Aslanidis & de Jong, n.d.; Horton et al., 1990). *M. xanthus* plasmids were synthesized by Genscript (Table S3). *M. xanthus* WT ImuB was cloned through joining the N terminal DNA fragment (ATGCGTCGCGCTTATTTACACCTTA CACGTTTCCCCGTTCAACGTCGTGTGGTTGAGAGCCCTGAGCTTGCAGGACGC CCTTTTGCTTTAGTAGAAGCAGTGCGTGGTCAGCGTCGTGTTGCGTTT) to ImuB from pET3a using SOE then LIC to clone into pMCSG7. Constructs were transformed into *E. coli* STBL3 cells. Plasmids were verified using Sanger sequencing (Genewiz).

DNA substrate preparation

DNA substrates outlined in Table S2 were synthesized with a 6-carboxyfluorescein (6-FAM) fluorophore by Integrated DNA Technologies. dsDNA was annealed by mixing equimolar concentrations of the appropriate ssDNA in MilliQ water, heating for 2 minutes

at 95℃ and then gradually cooling until the substrate was at room temperature. Substrates were stored in a -20°C freezer for short term use.

Solubility Assay

Full-length or truncations of *P. aeruginosa* or *M. xanthus* proteins were cloned using techniques stated above. Plasmids were transformed into either *E. coli* BL21, BL21 codon+, BL21 star, Rosetta, SoluBL21 or Arctic Express. Overnight cultures were sub-cultured (1:100) in 20 mL LB media with appropriate antibiotics at 37°C, 30°C for Arctic Express. In addition, SoluBL21 cells were grown in M9 media (3 g L^{-1} KH_2PO_4, 0.5 g L^{-1} NaCl, 6 g L^{-1} Na_2HPO_4, 5 g L^{-1} NaCl, 1 g L^{-1} NH_4Cl, 1 mM MgSO4, 0.1 mM $CaCl_2$, 0.3% (v/v) glycerol). Protein expression was induced at ~OD_{600} = 0.5 with varying concentrations of IPTG then grown for 3, 5, 18, or 24 hours depending on cell type. 350 µL samples were taken prior and after IPTG induction. Cells were harvested via centrifugation and resuspended in lysis buffer (50 mM Tris-HCl (pH 8.0), 1 M NaCl, 2 mM BME, 10% (w/v) sucrose, 5% (v/v) glycerol, 0.1% (v/v) Triton X-100, 0.1% (v/v) NP-40, lysozyme). Cells were lysed by sonication and lysate was clarified via centrifugation. Pre and post IPTG induction samples, cell lysates, and cell pellets were resuspended in 2X SDS load dye (100 mM Tris, pH 6.8, 3.2% (w/v) sodium dodecyl sulfate (SDS), 0.2% (w/v) bromophenol blue, 16% (v/v) glycerol, 100 mM β-mercaptoethanol). Samples were boiled at 90°C for 10 minutes and ran on a 12% SDS-PAGE (sodium dodecyl sulfate polyacrylamide gel electrophoresis) gel for 45 minutes at 200 V in 1X Tris/Glycine/SDS buffer. Gels were either stained with Coomassie blue or used for Western blot analysis.

Western Blot Analysis

Protein samples were run on an SDS-PAGE gel and electrophoretically transferred to a nitrocellulose membrane at 100 V for 32 minutes in Transfer buffer (20% (v/v) methanol, 1X Tris/Glycine/SDS). The membrane was blocked in Blocking Buffer (50 mM Tris pH 7.5, 150mM NaCl, 0.1% Tween, 5% skim milk powder) for 1 hour with rocking at room temperature. The membrane was then incubated in TBS-T (50 mM Tris pH 7.5, 150mM NaCl, 0.1% Tween) with 1:10,000 diluted mouse Monoclonal Anti-polyHistidine antibody produced (Sigma-Aldrich) for 1 hour or a T7•Tag® Antibody Horseradish Peroxidase (HRP) Conjugate (Novagen) for 30 minutes. The membrane was washed 3x for 5 minutes each with TBS-T. His_6-tagged protein blots were incubated with Anti-mouse IgG, HRP-linked Antibody (Cell-signaling) for 1 hour and washed steps repeated. Clarity Max Western ECL Substrate (Bio-rad) was applied to the membrane and imaged after 5 minutes using the ChemiDoc Imaging system (Bio-Rad Inc.).

***M. xanthus* ImuA $ImuB_{N\Delta34}$ expression and purification**

ImuA, $ImuA_{C\Delta53}$, $ImuB_{N\Delta34}$ proteins were each grown in 6 L LB at 12°C in *E. coli* Artic Express. Expression was induced at ~0.5 OD_{600} with 0.1 mM IPTG. Bacterial cells were resuspended in lysis buffer after centrifugation and lysed by sonication. Lysate was clarified by centrifugation and affinity purified by Ni-NTA (nickel-nitriloacetic acid) immobilized metal-affinity chromatography (IMAC) resin (Bio-Rad) using Ni-NTA Wash buffer (50 mM Tris-HCl (pH 8.0), 0.4 M NaCl, 10% (v/v) glycerol). 30 mM and 300 mM elution fractions containing ImuA and $ImuA_{C\Delta53}$ were further purified using heparin affinity chromatography (5 mL HiTrap Heparin HP, GE Healthcare) equilibrated with Qa buffer

(20 mM HEPES pH 8, 2mM BME, 10% glycerol, 200 mM NaCl) and eluted around 600 nM NaCl. $ImuB_{N\Delta34}$ was also subjected to nickel affinity chromatography but did not stick to the resin. The flowthrough from the resin containing $ImuB_{N\Delta34}$ was subjected to a 35% (v/v) saturated ammonium sulphate precipitation using gentle stirring at 4°C. Pellets were resuspended in Qa buffer and further purified by heparin exchange chromatography and anion exchange chromatography (5 mL HiTrapQ HP column, GE Healthcare). Both columns were equilibrated with Qa buffer, where $ImuB_{N\Delta34}$ eluted around 35% NaCl for both heparin and anion affinity chromatography. The purified proteins were concentrated using a centrifugal concentrator (Milllipore). Proteins were then quantified by absorbance at 280 nm with a Denovix DS-11 microvolume spectrophotometer and stored at -80°C until further use.

Size-exclusion chromatography coupled to multi-angle light scattering (SEC-MALS)

ImuA and $ImuB_{\Delta N34}$ were concentrated to 33 μM and 100 μM, respectively, and centrifuged to remove any aggregated protein prior to SEC-MALS. Samples were run on a Superdex 200 Increase 10/300 GL (GE Healthcare) column on an AKTA Pure FPLC system (GE Healthcare) with MALS (MiniDAWN and Optilab system (Wyatt Technology)). Data analysis was conducted using Astra software, version 7.3.1.9 (Wyatt Technology) and plotted in Prism v.9.0 (GraphPad).

Small-angle x-ray scattering (SAXS)

SAXS data were collected on the Rigakau BioSAXS 1000 at McMaster University. For SAXS studies, ImuA was buffer exchanged into SAXS buffer (20 mM HEPES pH 7.5, 200 mM NaCl). SAXS data collection was performed at 1 mg/mL. SAXS data were

analyzed using the ATSAS suite of SAXS data analysis tools (http://www.emblhamburg.de/biosaxs/software.html).

Florescence Polarization (FP)

Reaction volumes of 30 uL contained FP buffer (10 mM Tris-HCl buffer pH 8, 10 mM NaCl, 10% (v/v) glycerol and 1 mM TCEP) with 50 nM DNA and serial dilutions of ImuA or $ImuB_{\Delta N34}$ protein. Reactions were incubated at 30°C for 20 minutes, before polarization was measured by a Biotek Synergy Neo2 (company). The change in fluorescence polarization was measured and plotted as a function of protein concentration. Dissociation constants (K_D) were calculated using Prism v.9.0 (GraphPad).

Electrophoretic mobility shift assays (EMSA)

Reaction volumes of 20 µL reactions contained EMSA buffer (50 mM Tris-HCl pH 8.0, 50 mM NaCl, 1 mM DTT, 5 mM MgCl2, 4% (v/v) glycerol, 0.025 mg/mL BSA) with 10 nM DNA and serial dilutions of ImuA or $ImuB_{\Delta N34}$ protein. Reactions were incubated at 30°C for 20 minutes, after which 4 µL of 50% glycerol was added before loading on a 6% native PAGE gel (28 x 26 cm). The gel was run at 200 V for 3.5 hours at 4℃ and imaged with an Amersham Typhoon Imager (GE Healthcare).

Bacterial Adenylate Cyclase Two-Hybrid System (BAC2H)

Primers are described in Table S1. Standard cloning techniques were used to amplify ImuA, ImuB, and ImuC truncations and ligate them into vectors pUT18, pUT18C, pKT25, and pKNT25 (Euromedex). pUT18C and pKT25 compatible truncations included a stop codon in reverse primers. ImuA, ImuB and ImuC were amplified using PCR from plasmid DNA, digested with XbaI/KpnI (ThermoFisher) (ImuA, ImuB), XbaI/SmaI KpnI

(ThermoFisher) (ImuC) and ligated into appropriate vectors. Empty pUT18C and pKT25 vectors were used as a negative control while pUT18C::zip and pKT25::zip were used as a positive control. Combinations of T18 and T25 vectors were co-transformed into *E. coli* BHT101. Overnight cultures of bacteria were grown with 50 μg/ml kanamycin, 100 μg/ml ampicillin, and 0.5 mM IPTG at 37°C. 2 μL of culture was used to spot inoculate LB agar plates containing 50 μg/ml kanamycin, 100 μg/ml ampicillin, 0.1 or 0.5 mM IPTG, and 40 μg/ml 5-bromo-4-chloro-3-indolyl-β-d-galactopyranoside (X-Gal). The plates were incubated for 24 hours at 30°C.

Construction of *P. aeruginosa* strains

Upstream and downstream regions of ImuA, ImuB, ImuC genes, approximately 500 bp each, were amplified through PCR with oligonucleotides outlined in Table S1 and joined with SOE PCR. DNA fragments were cloned with standard restriction enzyme cloning into suicide vectors described in Table S3 and confirmed with Sanger sequencing. Plasmids were transformed into *E. coli* SM10. Plasmids were conjugatively transferred into PAO1 on solid LB media and plated on 5% sucrose solid LB media to initiate two-step allelic exchange. Gentamicin-sensitive colonies were selected, and mutants were confirmed with PCR and Sanger sequencing.

Growth assay

PAO1, TLS gene deletion strains, and gene deletion strains with complementation of respective ImuA, ImuB or ImuC genes, were grown overnight at 37°C in LB with shaking. Cultures were normalized to similar OD_{600} values, diluted 1:60 000 in 100 μL LB

broth, and grown at either 30°C or 37°C with shaking. OD_{600} readings were taken every 15 minutes for 24 hours at 600 nm using a Epoch 2 plate reader (Biotek).

UV mutagenesis assay

PAO1, TLS gene deletion strains, and gene deletion strains with complementation of respective ImuA, ImuB, or ImuC genes, were grown overnight at 37°C in LB with shaking. Subcultures were grown with gentamicin and 0.5 mM IPTG to OD_{600} values around 0.5 (mid-log phase). 5 mL of each culture were placed in Petri dishes and subjected to different dosages of UV irradiation using a GS Gene Linker® UV Chamber (Biorad). Aliquots were removed before and after irradiation, subjected to serial dilutions and plated on LB agar. Plates were incubated at 30°C for 48 hours to determine of viable cell counts. To determine mutation frequency, a 200 µL aliquot of irradiated cells was inoculated in 1 ml LB and grown at 30°C for 24 hours. Cultures were plated on LB agar containing 100 µg/mL rifampicin. Mutation frequencies were calculated by dividing the numbers of mutant colonies (CFU/mL) by the total number of viable cell counts.

RESULTS

P. aeruginosa TLS proteins are insoluble

Previous graduate student, Lucas Koechlin, focused on expressing and solubilizing *M. tuberculosis* ImuABC TLS proteins using different solubility tags, medias, induction temperatures, and co-expression. The proteins were insoluble- a global issue in the *imu* gene cassette. Lucas began limited testing of *P. aeruginosa* TLS proteins and successfully cloned WT ImuA and ImuB proteins (Table S3).

This thesis continued the solubilization of *P. aeruginosa* TLS proteins with emphasis placed on obtaining full-length wildtype (WT) protein. Using different cell lines and induction temperatures, WT ImuA and ImuC did not express at all, while ImuB expressed in *E. coli* BL21, SoluBL21, and Rosetta (Table 3). However, ImuB was present in inclusion bodies, confirming the insolubility of the proteins under different expression conditions (Table 3). Co-transformation of TLS proteins ImuA/ImuB, ImuB/ImuC, and ImuA/ImuB/ImuC as per the operon order in *P. aeruginosa* was also attempted – however all conditions yielded either no expression or protein that was in inclusion bodies (Table 4).

Thus, a panel of truncations of all three TLS proteins were cloned (Table 5). Truncations were based on predicted structural domains using InterPro and structural disorder using D^2P^2 (Blum et al., 2021; Oates et al., 2013). Truncations were based on disorder because regions of proteins with higher structural disorder lack secondary structure and may have issues with folding in solution (Graether, 2019). Although the RecA domain in *P. aeruginosa* ImuA has not been identified by Expasy, Pfam, or InterPro like in other

bacteria such as *M. xanthus*, ImuA does have a predicted disordered C-terminus. The cloned construct of ImuA focused on removing the C-terminal disorder to create $ImuA_{C\Delta17}$ (Figure 4A). ImuB contains an UmuC domain, along with a β-clamp binding motif ($348^{QLPLWG}352$) (Figure 4B). Thus, $ImuB_{C\Delta156}$, $ImuB_{C\Delta123}$, and $ImuB_{C\Delta118}$ truncations focused on preserving the UmuC domain and open right-hand structure while removing the predicted C-terminal disorder (Figure 4B). Warner et al. (2010) also predicted that ImuA binds after the β-clamp binding motif in *M. tuberculosis* ImuB based on yeast two-hybrid studies. Two truncations were also created to include predicted binding sites between ImuB, ImuA, and potentially ImuC: $ImuB_{N\Delta345}$, $ImuB_{N\Delta353}$ (Figure 4B). Additionally, due to the large size of ImuC, a truncation was cloned to include only the active polymerase domain spanning residues 275 – 698 in the middle of the protein (Figure 4C).

The cloned truncations were subjected to small-scale expression and solubility testing (Table 6). The polymerase domain of ImuC ($ImuC_{270-714}$) and $ImuA_{C\Delta17}$ both expressed but were insoluble (Table 6). $ImuB_{N\Delta345}$ and $ImuB_{N\Delta353}$ were soluble, but a scaled-up expression yielded 0.1 mg of protein per 6 L, which was too little to move forward with protein characterization (Table 6). The C-terminal truncations of ImuB were cloned but have not yet been tested for expression and solubility and were of lower priority as they lacked potential protein-protein interaction sites.

M. xanthus homologs of ImuA and $ImuB_{N\Delta34}$ are soluble

A bioRxiv preprint released in 2020 showed purified ImuA and ImuB TLS proteins in *M. xanthus* (Sheng et al., 2020). Given the lack of success in purifying the TLS proteins

from *P. aeruginosa* and *M. tuberculosis*, expression and purification of the *M. xanthus* homologs was attempted. These TLS proteins share higher protein sequence similarity (residues sharing similar characteristics) than identity. Between *M. xanthus* and *P. aeruginosa,* ImuA shares 20.5% sequence identity and 27.5% similarity, while ImuB shares 30% sequence identity and 40% similarity (Madeira et al., 2019). ImuC shares the highest identity and similarity between species at 50% and 64%, respectively (Madeira et al., 2019).

Sequences of the proteins of interest cloned into expression vectors were purchased from Genescript, which included WT ImuA in pET15b, an expression vector with an N-terminal His_6-tag, and $ImuB_{N\Delta34}$ in pET3a, an expression vector with a T7 tag as described by Sheng et al (2020). ImuB was cloned without the first 33 amino acids as it was misannotated in the bioRxiv pre-print. Additionally, ImuC was purchased already cloned into pET-28a(+)-TEV with a N-terminal His_6-tag independently, although this protein expression and purification was not characterized by Sheng et al. initially (2020).

Following the protocols described by Sheng et al. (2020) for purification of ImuA and $ImuB_{N\Delta34}$, all three proteins were expressed in high quantity, but were aggregated in inclusion bodies. *M. xanthus* proteins were then subjected to solubility testing as was previously done for *P. aeruginosa* proteins. When expressed individually, most conditions resulted in TLS proteins in inclusion bodies (Table 7). For example, in Figure 5, ImuA, $ImuB_{N\Delta34,}$ and ImuC were expressed and aggregated in the inclusion bodies at 18℃ in *E. coli* BL21 codon plus. However, the soluble fractions from cell lysis did not contain any TLS proteins. Thus, co-expression of *M. xanthus* proteins was attempted and was successful, by co-transforming plasmids for ImuA and $ImuB_{N\Delta34}$ into the *E. coli* Arctic

Express cell line which resulted in both proteins being soluble (Table 8). ImuC remained insoluble under a variety of expression conditions (Table 7, 8).).

Although $ImuB_{N\Delta34}$ was soluble, it did not include thirty-four N-termini residues. To see if WT ImuB could be expressed under the same conditions as $ImuB_{N\Delta34}$, ImuB was cloned into pMSCG7, an expression vector which includes an N-terminal His_6-tag. SOE PCR was used to ligate the additional N-terminal sequence to $ImuB_{N\Delta34}$ and then this product was cloned into pMCSG7 using standard LIC methods. ImuB by itself and co-expressed with ImuA or ImuC, was not expressed in most of the conditions tested (Table 7, 8). Thus, this thesis focused on purifying ImuA and $ImuB_{N\Delta34}$.

Given the solubility of co-expressed ImuA and $ImuB_{N\Delta34}$, efforts were made to increase the yield of soluble proteins. In Table 9, expression and solubility of co-expressed ImuA and $ImuB_{\Delta N34}$ were tested with different medias and IPTG (Isopropyl β-d-1-thiogalactopyranoside) concentrations at induction. Although standard LB produced soluble protein, auto induction media (AIM) and Terrific Broth (TB) were used to attempt to increase protein yield. However, growing cells in AIM, which uses carbon sources to induce protein expression, did not result in protein expression (Table 9) (Fox & Blommel, 2009). TB, which is a nutrient rich broth and used to produce high cell density for recombinant protein expression in *E. coli*, also lacked $ImuB_{\Delta N34}$ expression (Krause et al., 2010) A key finding to increase soluble protein expression required lowering IPTG concentration. Initially, inducing protein expression with 1 mM or 0.5 mM IPTG produced some soluble protein, but was once again too little to move forward with protein

characterization. The IPTG concentration was further decreased to 0.1 mM, which resulted in a yield of 1 mg for both proteins from 6 L of LB media after purification.

Purification of co-expressed ImuA and $ImuB_{N\Delta34}$ proteins was achieved through several purification steps (Figure 6). Since ImuA contained a His_6-tag, a gravity flow column with Ni-NTA affinity resin was used as the initial purification step. ImuA eluted with 30 mM and 300 mM imidazole which was confirmed via western blot and most contaminants were removed (Figure 6A). ImuA was then purified with heparin affinity chromatography, a resin used for DNA binding proteins. Some ImuA is generally lost in the flow-through, however, most ImuA elutes with high salt (600 mM NaCl) (Figure 6B). After purification, ImuA is approximately 95% pure and yields about 0.8-1mg of protein with a 260nm/280nm absorbance ratio ranging from 0.6-0.8 indicating minimal DNA contamination. $ImuB_{N\Delta34}$, lacking the His_6-tag, fails to bind the Ni-NTA column and is separated from ImuA (Figure 6A). $ImuB_{N\Delta34}$ was then salted out after the Ni-NTA column to further remove contaminants. A 35% solution of saturated ammonium sulfate was used to salt out $ImuB_{N\Delta34}$, while simultaneously removing approximately one third of the contaminants. $ImuB_{N\Delta34}$ was then subjected to heparin affinity chromatography, where it elutes around 400 mM NaCl (Figure 6C). Through Ni-NTA, salting out, and heparin affinity chromatography, little $ImuB_{N\Delta34}$ is lost, but at the expense of reduced purity. The final purification step for $ImuB_{N\Delta34}$ includes anion affinity chromatography. Some $ImuB_{N\Delta34}$ is lost in the flow-through but yields $ImuB_{N\Delta34}$ that is approximately 65% pure and yields about 0.8-1 mg of protein from 6 L of culture confirmed via western blot (Figure 6C). Like ImuA, $ImuB_{N\Delta34}$ has a low 260nm/280nm absorbance ratio ranging from 0.6-0.8

indicating little DNA contamination. Size exclusion chromatography was attempted afterwards, however 90% of the protein yield was lost, thus purification was stopped after anion exchange chromatography.

Characterising ImuA and ImuB$_{N\Delta34}$

ImuA and ImuB$_{N\Delta34}$ are trimers in solution

DNA replication machinery is composed of multiple components to form a replisome. In the Pol V TLS complex, UmuD exists as a homodimer in a functional complex (Burckhardt et al., 1988). Thus, this thesis wanted to determine the oligomeric state of ImuA and ImuB$_{N\Delta34}$ independently and in complex to gain insight into the construction of the TLS complex. SEC-MALS is an absolute technique to determine protein mass and can distinguish different protein species such as monomers, aggregates, and heterocomplexes (Some et al., 2019). It was used to determine the experimental molecular weight and oligomeric state of ImuA and ImuB$_{N\Delta34}$ in solution, looking at both the proteins individually and in complex. ImuA had an elution volume of 13 mL and ImuB$_{N\Delta34}$ had an elution volume of approximately 12 mL (Figure 7). The experimental mass determined by MALS of ImuA is ~100 kDa (Figure 7). Given that the theoretical mass of ImuA is 30 kDa, the MALS data shows that ImuA forms a trimer in solution. ImuB$_{N\Delta34}$ had an experimental mass of ~150 kDa, also 3 times its theoretical mass of 50 kDa – thus it is also a trimer in solution (Figure 7). Both results were repeated at lower protein concentrations, where the absorbance from SEC ranged from 5-15 mAU, slightly above the baseline. ImuB$_{N\Delta34}$, once again, had an experimental mass of around 150 kDa (149.8±0.4%), while ImuA had an experimental mass of around 95 kDa (94.9±0.6%)

yielding the same results (data not shown). However, the molecular weight of ImuA was calculated to be ~24.5 kDa using the volume of correlation by SAXS data, indicating that ImuA can behave as a monomer in solution as well. Preliminary testing of ImuA and $ImuB_{N\Delta34}$ in complex on SEC-MALS shows a ~190 kDa complex, which presents multiple options of how the proteins may combine and is detailed in the discussion. However, the change in absorbance was under 5 mAU, making the molecular weight of the complex unreliable (data not shown). Additionally, ImuA and $ImuB_{N\Delta34}$ did not co-purify with Ni-NTA, indicating that complex formation during chromatography may be challenging.

ImuA and $ImuB_{N\Delta34}$ bind replication fork intermediates

Since PolIII is swapped out for a TLS polymerase such as ImuC, presumably ImuA and ImuB are involved as accessory proteins to help facilitate this switch, suggesting one or both proteins may be able to bind DNA. To assess the DNA binding ability of both proteins, fluorescence polarization (FP) was used. FP studies molecular interactions between a fluorophore-labelled substrate and a binding partner, where the degree of light polarization correlates to the binding of the substrate(Checovich et al., 1995). ImuA and $ImuB_{N\Delta34}$ were tested using ssDNA, dsDNA, and DNA substrates mimicking DNA replication intermediates.

As previously stated, ImuA has a RecA domain. RecA is able to bind ssDNA with high affinity, in the event of DNA replication fork stall. However, RecA also includes a secondary dsDNA binding site that is important in the homology repair process early in the SOS response (Mazin & Kowalczykowski, 1998). Therefore, I hypothesized that ImuA will also be able to bind DNA with a preference for ssDNA. Based on my FP data, ImuA was

able to bind ssDNA, dsDNA, and DNA replication-mimicking substrates as a change in polarization signals was observed (Figure 8AD). Sheng et al. (2021) showed that ImuA is unable to bind long circular DNA through visualizing agarose EMSA's. However, we used short ssDNA strands to determine the DNA footprint and FP to measure an observable change. A random DNA sequence was chosen, as ImuA, ImuB and ImuC are involved in replication across the entire genome and therefore should not have sequence specificity. ImuA was not able to bind 15 nt ssDNA, but bound a minimum of 20 nt. For dsDNA, ImuA did not bind 20 bp but did bind 30 bp (Figure 8B). Interestingly, increasing DNA length correlated with increased affinity of ImuA for dsDNA but not for ssDNA where the DNA-binding affinity was already high (Figure 8B). ImuA had high affinity for ssDNA substrates (20, 30, 40 nt), with K_D values of 0.3-0.5 μM (0.50±0.12 μM, 0.30±0.03, 0.42±0.04 μM), in contrast to 2-3 μM (0, 3.43±0.97 μM, 2.18±0.25 μM) for dsDNA, indicating a preference for longer, ssDNA substrates (Figure 8B) (Table 10). ImuA also bound all the DNA replication-mimicking substrates with high affinity. These substrates include a 3' overhang, 5' overhang, forked, and bubble DNA which are found at a replication fork. However, ImuA had the highest affinity for the 3' overhang (K_D of 0.18±0.01 μM), which is 3.8-fold higher than the 5' overhang, forked, and bubble DNA (Figure 8) (Table 10).

A truncation of ImuA, $ImuA_{C\Delta53}$, which removed the C-terminal disordered region but included the RecA domain, was also tested for its DNA binding ability. At this time, only some ssDNA, dsDNA, and DNA replication-mimicking substrates have been tested, excluding 20 nt, 20 bp, forked and bubble DNA, due to time constraints. $ImuA_{C\Delta53}$ bound all DNA substrates tested, as expected (Figure 9A). The K_D ranges were similar to those of

WT ImuA for ssDNA (30 nt: 0.58±0.04 μM, 40 nt: 0.56±0.08 μM), the 3' overhang (0.22±0.01 μM) and the 5' overhang (0.66±0.04 μM) (Figure 9B) (Table 10). $ImuA_{C\Delta53}$ had an increased affinity for dsDNA binding compared to WT ImuA. The K_D value for 30 bp of DNA decreased from 3.43±0.97 μM to 0.58±0.14 μM when the C-terminus was removed, a 5.5-fold increase in dsDNA binding ability (Figure 9B) (Table 10). The same trend was seen with the 40 bp DNA substrate.

I hypothesized $ImuB_{N\Delta34}$ would bind DNA for 3 main reasons: 1) Although $ImuB_{N\Delta34}$ lacks the catalytic residues for polymerase activity, it still maintains polymerase structure (Pata, 2010; Timinskas & Venclovas, 2019; Warner et al., 2010); 2) ImuB also includes a UmuC domain, part of the Pol V complex responsible for bypassing damage, which also binds DNA (Blum et al., 2021); and 3) Warner et al. (2010) show that ImuB acts as a central binding hub, which potentially means it is responsible for bringing ImuC closer to DNA, and thus may bind DNA. $ImuB_{N\Delta34,}$ like ImuA, bound ssDNA, dsDNA, and DNA replication substrates as a change in polarization was observed when protein was added to the DNA (Figure 10AC). $ImuB_{N\Delta34}$ was not able to bind 20 nt ssDNA but bound a minimum of 30nt ssDNA. For dsDNA, it was observed that $ImuB_{N\Delta34}$ could not bind 15 bp but was able to bind at least 20 bp (Figure 10B). The affinity of $ImuB_{N\Delta34}$ for DNA increased as the substrate lengthened for both ssDNA and dsDNA. $ImuB_{N\Delta34}$ was able to bind ssDNA with a K_D of 2.78±0.4 μM for 30 nt. The K_D decreased 7-fold for 40 nt, indicative of tighter binding (0.41±0.02 μM) (Table 10) (Figure 10B). $ImuB_{N\Delta34}$ bound dsDNA with a K_D of 4.83±1.07 μM for 30 bp, while the K_D decreased 2.4-fold for 40 bp (2.03±0.34 μM). Like ImuA, $ImuB_{N\Delta34}$ bound to ssDNA more tightly than dsDNA (Figure

10B). However, $ImuB_{N\Delta34}$ had the highest affinity for the substrates mimicking DNA replication, where 3' overhang and forked DNA had a K_D of 0.20±0.01 μM and 0.15±0.05 μM, respectively, an 11-fold increase in binding affinity compared to the high affinity of the 40 bp dsDNA substrate (Figure 10CD) (Table 10). Both ImuA and $ImuB_{N\Delta34}$ proteins preferred ssDNA over dsDNA, with the highest affinity for the 3' overhang with a K_D of 0.18±0.01 μM and 0.20±0.01 μM, respectively. $ImuB_{N\Delta34}$ also had similar affinity for forked DNA with a K_D of 0.15±0.05 μM (Table 10).

ImuA and $ImuB_{N\Delta34}$ were able to bind DNA individually but how they interact together with DNA is unknown. To visualize how ImuA and $ImuB_{N\Delta34}$ interact on DNA together, a modified EMSA was used with 40nt ssDNA and both proteins. Both ImuA and $ImuB_{N\Delta34}$ had similar affinity for 40 nt ssDNA (0.4 μM) and could potentially fit on a 40 nt substrate as ImuA binds 20 nt and ImuB binds 30 nt minimally. Both proteins bound the DNA substrate alone producing a single shift; however, $ImuB_{N\Delta34}$ produced a higher shift than ImuA (Figure 11 lane 2,3). When ImuA and $ImuB_{N\Delta34}$ were added one after the other to the reaction, a higher shift is observed than the individual proteins alone (Figure 11). Interestingly, adding both proteins at the same time with ssDNA produces a shift similar to that of $ImuB_{N\Delta34}$ alone. The same experiment was repeated with a 40 bp dsDNA substrate, but the samples failed to migrate into the gel.

ImuA and ImuB interact through their C-terminal regions

As previously mentioned, ImuA in *M. tuberculosis* interacts with the C-terminal region of ImuB, past the little finger regulatory domain and β-clamp binding motif ($ImuB_{352-357}$), which is approximately 32% of ImuB (Warner et al., 2010). Thus, to aid in

understanding of the TLS mechanism assembly and for future crystallography experiments, more precise regions of interaction between ImuA and ImuB in *M. xanthus* were determined using BAC2H. BAC2H exploits the interaction between T18 and T25 domains of *Bordetella* adenylate cyclase toxin, fused to the proteins of interest of this study, where interaction of T18 and T25 results in cAMP synthesis. Interaction between the proteins of interest results in the joining of T18 and T25, leading to cAMP synthesis and activation of transcription of β-galactosidase (Figure 12A). β-galactosidase is then able to hydrolyse X-Gal and produces blue colonies of *E. coli* BTH101 on X-gal containing media, indicative of interaction (Battesti & Bouveret, 2012). Since ImuA is predicted to bind through the C-terminal 168 residues of ImuB from *M. tuberculosis,* truncations of ImuB were designed to delete homologous N- or C- terminal regions in the *M. xanthus* proteins. These regions included N-terminal deletions of 300 residues or less and C-terminal truncations of 160 residues or less (Table 11). Table 11 shows all interactions tested. It is important to note, eight conditions were tested for each interaction, through cloning the proteins of interest to either the N- or C- termini of T18 and T25 (4 co-transformations), and expression induced with two different IPTG concentrations each (0.1 mM and 0.5 mM), since IPTG concentration had a profound effect on expression of *M. xanthus* proteins *in vitro*. Often only one condition produced blue colonies, indicative of an interaction. For example, ImuA-T25 and T18-ImuB from *M. xanthus* interacted only with 0.1 mM IPTG (Figure 12B) (Table 11). $ImuB_{N\Delta 338}$, which encompasses the last 165 residues of ImuB including the β-clamp motif in *M. xanthus*, also interacted with WT ImuA, supporting Warner et al.'s finding (2010) that the C-terminal region is important for this interaction to occur.

However, $ImuB_{C\Delta136,}$ also interacted with WT ImuA, indicating that residues 339-367 of ImuB are important for ImuA binding (Figure 12B).

Warner et al. (2010) also hypothesized that the 44 C-terminal residues of ImuA were important to bind ImuB, but they could not confirm this as protein integrity might have been compromised due to the short length of the truncation. Thus, truncations of ImuA were also created to determine the minimal ImuA region that binds to ImuB. The N-terminal truncations of $ImuA_{N\Delta159}$ and $ImuA_{N\Delta222,}$ which removed the RecA domain completely, were able to bind the C-terminal region of $ImuB_{N\Delta338}$, showing that the C-terminus of ImuA is important for interaction with ImuB (Figure 12B). Interestingly, these truncations did not bind WT ImuB.

The C terminal region of ImuB may be required for ImuC interaction

In *M. tuberculosis* and *M. xanthus,* ImuC is only known to interact with ImuB as a binding partner in the TLS mechanism, based on current studies (Sheng et al., 2021; Warner et al., 2010). However, the regions of interaction are not known. It was hypothesized that ImuC may bind in the C-terminal region of ImuB after the β-clamp and ImuA binding site. From previous literature, WT ImuC was expected to interact with WT ImuB. However, ImuC did not interact with WT ImuB in all eight tested conditions (Figure 12C). Interestingly, ImuC did bind $ImuB_{C\Delta81}$ but not $ImuB_{C\Delta136}$ (Figure 12C).

UV-induced mutagenesis in *P. aeruginosa*

In addition to determining the molecular mechanism of TLS *in vitro,* UV-induced mutagenesis by TLS was studied *in vivo* in *P. aeruginosa*. The discovery of ImuABC complex and its involvement in mutagenesis in *M. tuberculosis* and *C. crescentus* consisted

of a robust UV mutagenesis assay used over decades (Boshoff et al., 2003; Galhardo et al., 2005). Briefly, bacterial strains deficient of TLS genes are subjected to UV damage and plated on rifampicin solid media. The assay takes advantage of rifampicin's mechanism of action. It targets the β-subunit of bacterial RNA polymerase, which is highly conserved and mutations in the *rpoB* gene can be attributed to mutagenesis (Garibyan et al., 2003; Luján et al., 2019) In *C. crescentus,* when *imuA, imuB, or imuC* genes were deleted and subjected to UV damage, fewer rifampicin resistant mutants were detected compared to WT *C. crescentus*, indicating that these genes that were part of TLS contributed to UV-induced mutagenesis (Galhardo et al., 2005). Lujan et al. (2017) then tested UV-induced mutagenesis in *P. aeruginosa* strains with ImuB and ImuC genes deleted. Initially, results showed a difference between WT PAO1 and individual genomic deletions of *imuB* or *imuC* in spontaneous (no UV) and UV-induced mutations. However, further Luria mutation fluctuation tests showed no difference in spontaneous mutagenesis between WT and deletion mutants (Luján et al., 2019). Given these conflicting results, this thesis set out to determine if more than a single gene deletion would produce different effects in spontaneous and UV-induced mutagenesis in *P. aeruginosa*. Additionally, this assay can be used to determine if *in vitro* findings have biological relevancy *in vivo*.

A set of bacterial strains of *P. aeruginosa* with individual ImuABC proteins and double gene deletions were created based on operon order: *ΔimuA ΔimuB* and *ΔimuB ΔimuC.* Strains with gene deletions were also created that incorporated a complementation vector of missing genomic genes (Table S4). To confirm that the *imuA-imuB-imuC* cassette did not disrupt cell growth, growth curves for each strain were completed. Growth curves

for all deletion mutants, including double gene deletions, were the same compared to WT PAO1, under regular growth conditions at 30°C and 37°C (Figures 13-16). Therefore, TLS gene deletion did not disrupt essential pathways. Sahil Karnani, a 4th year thesis student then studied the survival and UV-induced mutagenesis of the TLS double gene deletions (*ΔimuA ΔimuB* or *ΔimuB ΔimuC*), which was determined by the rifampicin resistance assay adapted from Galhardo (2005). Compared to WT, both double knockout strains lacking TLS genes showed similar levels of UV sensitivity and survival over increasing UV dosage (Figure 17). The UV-mutagenesis assay showed that there is no difference in spontaneous mutations between the deletion strains and WT PAO1 (0 J/m^2) (Figure 18). However, when exposed to 120 J/m^2 there was an increase in mutations, although not significant, in WT PAO1 but not in the deletion strains when compared to 0 J/m^2. (Figure 18). The difference between PAO1 and *ΔimuA ΔimuB* is significant ($p<0.05$) (Figure 18A). Strains with complementation of respective genes served as a control and restored both spontaneous and UV-induced mutation levels to wildtype.

DISCUSSION AND CONCLUSIONS

Overcoming the challenges of achieving soluble ImuA and ImuB proteins

TLS, the main mechanism of DNA damage bypass, has been highly characterized in bacterial species such as *E. coli* using the Pol V mutasome (Bruck et al., 1996; Goodman & Woodgate, 2013). However, the study of the *imu* complex, present in one third of bacteria, poses a challenge to characterization as *in vitro* expression of the proteins from species such as *M. tuberculosis* and *P. aeruginosa* thus far has only produced insoluble proteins (Sheng et al., 2021).

A variety of recombinant protein expression cell lines were used while attempting to solubilize *P. aeruginosa* proteins and truncations. The standard for high level protein expression includes the use of the cell line *E. coli* BL21 with T7 RNA polymerase and an IPTG induction system (Jeong et al., 2009). Most other cells explored in this thesis are BL21 derivatives. For example, *E. coli* Rosetta cells, a BL21 derivative, contain tRNA codons found in eukaryotes such as AGG (arginine), AGA (arginine), AUA (isoleucine), CUA leucine), CCC (proline) and GGA (glycine) which are rare in *E. coli* but present in the genome of *P. aeruginosa* (Tegel et al., 2010). In contrast, *E. coli* SoluBL21 cells have been reported to increase recombinant protein solubility for proteins that are generally insoluble through uncharacterized mutations within the BL21 cell line (Hata et al., 2013). Another cell line used to solubilize our proteins of interest, *E. coli* BL21 STAR, has more mRNA stability due to a silent mutation in the *rne131* gene inactivating the RNase E endonuclease (Makino et al., 2011). In addition, *E. coli* BL21 codon plus contains extra copies of the *argU* (encoding for arginine), *ileY* (isoleucine), and *leuW* (leucine) tRNA

genes. Without extra copies of these tRNA genes, translation of heterologous proteins is usually more limited (Rosano & Ceccarelli, 2009). Although these *E. coli* cell lines had different characteristics, none of their specialized features improved soluble *P. aeruginosa* WT or truncated ImuABC protein expression.

Given that Sheng et al. stated they were able to purify ImuA and ImuB (2020) and later ImuC from *M. xanthus* (2021), switching to these functional homologs became the basis of this thesis. The ImuABC complex is functionally homologous; however, it is not uncommon that these proteins maintain sequence diversity between species (Ippoliti et al., 2012). ImuA only shares around 10-20% sequence identity across bacterial species. For example, between *C. crescentus* and *M. tuberculosis*, there is only 13% sequence identity (Ippoliti et al., 2012). The same trend is seen with ImuB (Ippoliti et al., 2012). Overall, the highest sequence identity in ImuABC is observed between ImuC homologs, which is expected as the core polymerase structure is conserved. *C. crescentus* and *M. tuberculosis* ImuC share 37% sequence identity, while *P. aeruginosa* and *M. xanthus* ImuC share 50% sequence identity (Ippoliti et al., 2012; Madeira et al., 2019). This also applies between *P. aeruginosa* and *M. xanthus* ImuA and ImuB proteins. They have low sequence identities (Madeira et al., 2019). Although different in primary sequence identities, using soluble ImuABC homologs remains an effective way to provide primary insight into the ImuABC mechanism.

M. xanthus ImuABC and $ImuB_{N\Delta34}$ proteins underwent solubility testing like *P. aeruginosa,* as initial purification of the proteins resulted in aggregates following the protocol of Sheng et al. (2020, 2021). Both ImuA and $ImuB_{N\Delta34}$ were tested in a variety of

recombinant protein expression cell lines, but only *E. coli* Arctic Express produced soluble protein. *E. coli* Arctic Express cells contain the Cpn10 and Cpn60 chaperonins from *Oleispira antarctica,* which improves protein folding at low temperatures, and was key to producing sufficient quantities of soluble *M. xanthus* ImuA and $ImuB_{N\Delta34}$ (Hartinger et al., 2010). Given that *E. coli* Arctic Express cells are grown at 12°C, this improved the ability to achieve soluble protein yield. Generally, insolubility of recombinant proteins is correlated with higher induction temperatures due to rapid protein accumulation (Gutiérrez-González et al., 2019; San-Miguel et al., 2013). Additionally, soluble protein expression was further improved by lowering IPTG concentrations when inducing protein expression (Table 9). Previous research has also shown that IPTG concentration plays a major role in obtaining soluble proteins from *E. coli* Arctic Express cells. As an example, human Prethrombin-2 was initially insoluble when expressed in different cell lines (Silaban et al., 2019). However, testing a variety of IPTG concentrations produced soluble protein expression, where even a 0.025 mM difference in IPTG concentration resulted in insoluble protein (Silaban et al., 2019). The same effect was seen with ImuA and $ImuB_{N\Delta34,}$ where 0.1 mM IPTG was the optimal concentration to produce the highest yield of protein. IPTG is a gratuitous inducer, meaning it is not metabolized, and high concentrations of IPTG can increase insolubility due to increased expression rate (Donovan et al., 1996; Rizkia et al., 2015). The high expression rate could have contributed to ImuABC protein aggregation. Finally, individually ImuA and $ImuB_{N\Delta34}$ did not yield soluble protein. This changed when co-expressing both proteins together. Co-expression increases solubility of binding partners and multiprotein complexes, which can stabilize each other *in vivo* (Anderson et al., 2010;

Sørensen & Mortensen, 2005). Overall, with the help of chaperonins, low induction temperatures, and optimal IPTG concentrations, ImuA and $ImuB_{N\Delta34}$ were successfully expressed together as soluble proteins.

The purification of ImuA and $ImuB_{N\Delta34}$ entailed several steps (Figure 6). Ni-NTA IMAC resin was used as the initial purification step since ImuA was expressed with a His_6-tag. The transition metal Ni^{2+} on the resin can form coordination bonds with electron donor groups on the histidine, effectively separating the tagged protein from the cellular lysate (Bornhorst & Falke, 2000). This step is versatile, cheap, accessible, and can result in a 95% purity (Bornhorst & Falke, 2000; Janknecht et al., 1991). Ni-NTA allowed for over 90% purity of ImuA and separation from co-expressed $ImuB_{N\Delta34.}$ Ammonium sulphate precipitation was able to remove one third of contaminants from $ImuB_{N\Delta34}$ before proceeding to heparin affinity chromatography. The use of heparin was introduced as these negatively charged polysaccharides attract DNA-binding proteins present during DNA replication (Bolten et al., 2018). Not surprisingly, both ImuA and $ImuB_{N\Delta34,}$ as part of a DNA damage bypass pathway, bound to heparin with minimal protein loss, leaving ImuA approximately 95% pure (Figure 6B). $ImuB_{N\Delta34}$ required further purification with anion exchange chromatography, resulting in approximately 65% purity (Figure 6C). Additional purification attempts with size exclusion chromatography resulted in significant protein loss, likely due to protein aggregate formation, as most of the protein eluted in the void volume. Thus, $ImuB_{N\Delta34}$ purification was stopped after the three described purification steps, to retain enough protein for biochemical analysis.

The Role of an ImuB trimer in TLS

It was determined through SEC-MALS that *in vitro,* $ImuB_{N\Delta34}$ can form a trimer in solution. At multiple concentrations, a monomer was never observed (Figure 7). Based on the ImuB truncation, the N-terminal 34 amino acids are not essential to form the trimer. These results are further supported by Warner et al. who showed that ImuB was able to self-interact *in vivo* through the C-terminal domain (2010). What role, though, would an ImuB trimer play in forming the TLS mutasome? Given that ImuB lacks the catalytic triad necessary for polymerase activity and can interact with ImuA, ImuC, and the β-clamp as observed by yeast two-hybrid screens, ImuB may be the central binding hub in the ImuABC complex (Warner et al., 2010). The potential to form a trimer could allow for simultaneous binding of multiple components (ImuA, ImuC, β-clamp) in the complex. This phenomenon is also observed in Pol V and the Pol III DNA replication mutasome where PolIII, a clamp loader, and the β-clamp, form the larger complex (Burckhardt et al., 1988; O'Donnell, 2006; Wegrzyn et al., 2016). Therefore, $ImuB_{N\Delta34}$ trimers may be a functional state in forming the ImuABC complex. Each ImuB monomer could bind to another ImuB monomer and would also be responsible for binding one other protein simultaneously – either ImuA, ImuC or the β-clamp, creating a five protein TLS complex, with the β-clamp acting as the tether to the DNA (Figure 19). ImuB is likely to also play a tethering role of ImuC to the DNA unlike PolIII or UmuC, both of which directly bind to the β-clamp and then DNA (Bailey et al., 2006; Oakley, 2019; Patoli et al., 2013). This complex may also be stabilized on the DNA by additional interactions between ImuA, ImuB and DNA, as discussed below.

The switch from DNA replication to TLS in bacteria containing the Pol V mutasome is not directly mediated by the polymerase UmuC, but rather UmuD'$_2$ which can bind PolIII (Patoli et al., 2013; Sutton et al., 1999). Given ImuB's central role in the ImuABC complex and its ability to bind the β-clamp, it is highly likely that ImuB is also responsible for the PolIII to ImuABC switch.

Oligomeric state may impact ImuA function

SEC-MALS has also shown that ImuA behaves as a trimer in solution and has one conserved PM in the middle of the protein (Figure 7) (Sheng et al., 2021). ImuA possesses homology to RecA, a protein that also has two of the same PMs and uses them to form a polymer chain during the SOS response (del Val et al., 2019; Leite et al., 2016). Sheng et al. (2021) predicted that ImuA binds to RecA through this motif, thus inhibiting further RecA polymerization to promote the transition from error-free template switching to TLS. By stopping RecA polymerization, it would allow for ImuB to bind ImuA and the β-clamp, beginning formation of the TLS polymerase complex. Although SEC-MALS shows that ImuA behaves as a trimer in solution because of the PM, it is not clear if this is biologically relevant. It is possible that ImuA transitions between different oligomeric states, the most likely being that of a trimer to monomer for 3 possible reasons. 1) Preliminary data. SEC-MALS data suggests that an ImuA-ImuB complex consists of a trimer of ImuB and one ImuA. SAXS data also indicated that ImuA has a molecular weight consist with a monomer in solution. 2) Warner et al. (2010) did not observe self-interaction of ImuA *in vivo;* 3) The hypothesis by Sheng et al. (2021) that ImuA halts the RecA polymerization by binding to RecA is a logical mechanism to switch to TLS. With these reasons, it is possible that ImuA

forms a trimer on its own, oligomerizing through the PM, which then could dissociate to monomers when bound to RecA. After this, ImuA could recruit the ImuB trimer with ImuC to the lesion and β-clamp (Figure 19). While an ImuA trimer has not been observed *in vivo,* this thesis has shown that IPTG induction concentration plays an important role in ImuA expression, both *in vitro* and *in vivo*. Future studies should retest ImuA self-interactions *in vivo* with different IPTG concentrations to see if an ImuA trimer can form. Additionally, Warner et al. (2010) show that each protein is required for TLS to occur *in vivo*, but it remains to be seen if ImuA simply loads ImuB and ImuC onto the β-clamp for replication bypass, as proposed by Sheng et al., (2021), or if ImuA remains bound to the ImuB trimer as replication past the damage occurs. Further characterization is needed to confirm either an active or passive role for ImuA.

ImuA DNA binding may help initiate TLS

In addition to self-oligomerization, both ImuA and $ImuB_{N\Delta34}$ were able to bind a variety of DNA substrates: ssDNA, dsDNA, and substrates mimicking replication fork intermediates. Not surprisingly, ImuA bound ssDNA with high affinity, regardless of substrate length (Table 10). This was expected, as ImuA has a RecA domain where RecA binds to and accumulates on ssDNA during the SOS response (Leite et al., 2016; Podlesek & Žgur Bertok, 2020). RecA also binds dsDNA with a lower affinity than ssDNA, through its secondary binding site used for the homology search process in homologous recombination (Mazin & Kowalczykowski, 1998). This same trend is seen in ImuA, but it is unknown whether ImuA contains different DNA binding sites for ssDNA or dsDNA.

However, the biological relevance for ImuA binding dsDNA remains unknown as its role has only been identified in TLS.

These results are also somewhat contradictory to Sheng et al. (2021), as they show that ImuA cannot bind 6000 nt ssDNA or 3000 bp dsDNA, although the ssDNA and dsDNA substrates used in this thesis were significantly shorter, suggesting that length may be a factor in whether ImuA can bind longer DNA substrates in the absence of other proteins. Given the hypothesis that ImuA inhibits RecA polymerization (Sheng et al., 2021), it is likely that RecA may be needed to bind ImuA to longer DNA substrates.

Additionally, ImuA had high affinity for substrates representing what occurs at a replication fork. These include 3’ overhangs and 5’ overhangs that mimic the leading and lagging strands from DNA replication, respectively, as does the forked DNA substrate. The DNA bubble is also present when DNA replication occurs bidirectionally. The highest affinity of ImuA was for a 3’ overhang, which is not surprising as the polymerase complex reads DNA in a 3’-5’ direction but synthesizes DNA in a 5’-3’ direction. After the 3’overhang, ssDNA was bound with the second highest affinity, which was also expected if it does indeed inhibit RecA polymerization on ssDNA. Additionally, ImuA had a lower affinity for the other DNA replication fork substrates (5’ overhang, forked, and bubble DNA) probably due to less than ideal binding conditions such as DNA directionality, blunt ends, or steric hinderance, respectively.

ImuA can also bind dsDNA, but with lower affinity than the other DNA substrates tested. As described above, the ImuA homolog RecA also binds dsDNA for homologous recombination, although the biological significance of this function for ImuA is unknown

(Mazin & Kowalczykowski, 1998). However, the C-terminal region of ImuA may regulate which DNA substrate to bind. $ImuA_{C\Delta53}$ had a ssDNA binding capacity similar to WT. However, a 5.5-fold increase in 30 bp dsDNA binding ability was observed compared to WT ImuA (Table 10). Since the removal of the C-terminus increased affinity of dsDNA but did not change ssDNA affinity, the ImuA C-terminus may either provide steric hinderance to inhibit dsDNA binding or contain a regulatory region to control for dsDNA binding. Overall, ImuA prefers ssDNA where it is able to bind RecA on the accumulated ssDNA for TLS activation. If ImuA plays an active role in TLS bypassing the damage, the dsDNA binding activity could be used to stabilize the newly synthesized dsDNA.

$ImuB_{N\Delta34}$ DNA binding may stabilize the TLS complex

$ImuB_{N\Delta34}$ was also predicted to bind DNA, given that it is the central binding hub of the TLS complex. Like ImuA, $ImuB_{N\Delta34}$ prefers ssDNA to dsDNA. However, in contrast to ImuA, there is an increase in affinity as the ssDNA substrate lengthens. The lower affinity for 30 nt ssDNA could be attributed to the large size of the trimer (150 kDa) having difficulty fitting onto the DNA and forming a stable interaction. This concept is solidified as the 40 nt ssDNA has a 7-fold increase in affinity to 30 nt, and a similar binding to that of ImuA for 40 nt ssDNA (Table 10).

Additionally, $ImuB_{N\Delta34}$ binds DNA replication fork substrates with high affinity, with the exception of bubble DNA. Both 3' overhang and forked DNA showed similar K_D's of 0.20±0.01 μM and 0.15±0.05 μM, respectively, which fits with the inactive polymerase being involved as the central hub in TLS DNA damage bypass. The low affinity for bubble DNA, comparable to $ImuB_{N\Delta34}$ affinity for dsDNA, can be attributed to the size of the

bubble, where the trimer likely does not fit on the smaller substrate. Given that $ImuB_{N\Delta34}$ prefers the same substrates as ImuA, ImuB likely binds the ssDNA between ImuA and the β-clamp, and tethers ImuC to bypass the damage.

Building a model of ImuA and ImuB working together during TLS

To visualize how these proteins work together on DNA, a modified EMSA was used with a 40 nt ssDNA (Figure 11). Both ImuA and $ImuB_{N\Delta34}$ individually produced single shifts, indicating that one binding event occurred. Based on SEC-MALS data, it's hypothesized that $ImuB_{N\Delta34}$ binds DNA as a trimer, although future SEC-MALS experiments of $ImuB_{N\Delta34}$ with DNA are needed to confirm this. The same would be expected for ImuA, but although ImuA was a trimer by SEC-MALS, it is possible that it dissociates when performing biochemical functions such as binding to DNA. The observed EMSA shift of $ImuB_{N\Delta34}$ (MW of trimer, 150kDa) is much higher than ImuA. If ImuA was a trimer (MW, 100 kDa), a higher shift on the EMSA, similar to $ImuB_{N\Delta34}$ would be expected given that the protein-DNA complexes have similar masses. Therefore, it's hypothesized that ImuA binds DNA as a monomer, further suggesting that monomeric ImuA binds ssDNA and RecA (Sheng et al. 2021).

When both proteins are added to the DNA binding reaction, one after another (ImuA then $ImuB_{N\Delta34}$ or $ImuB_{N\Delta34}$ then ImuA) and then visualized by EMSA, a higher shift is seen than with the individual proteins. This is the result of two possibilities: 1) both proteins binding to DNA to produce a higher shift or 2) a direct protein-protein interaction of ImuA-$ImuB_{N\Delta34}$, where only one of the proteins binds DNA. Further experiments are needed to determine the true result. Direct protein-protein interactions can be tested through

in vitro interaction assays such as biolayer interferometry or microscale thermophoresis. Interestingly, when adding both proteins at the same time to the reaction, $ImuB_{N\Delta34}$ outcompetes ImuA, since a shift is seen at the same level as $ImuB_{N\Delta34}$ binding DNA alone. Since the proteins were incubated for a shorter amount of time on the DNA when added simultaneously compared to adding one and then the other, it is possible that a longer incubation time is needed to observe the shift. However, based on these results where proteins added one after another produce a higher shift, it's likely that when one protein binds to the DNA, it recruits the other protein. In TLS, it would mean that ImuA likely binds to RecA and ssDNA initially to inhibit RecA polymerization on ssDNA. Then the trimer of ImuB is recruited to the damage site through ImuA and either interacts with ssDNA, ImuA, and the β-clamp to tether ImuC to the DNA (Figure 19).

To further determine which interactions are critical to form the ImuABC complex, BAC2H was used. Using a lower IPTG concentration was critical in observing interactions, similar to the importance of IPTG concentrations for *in vitro* protein expression. Both $ImuB_{C\Delta136}$ and $ImuB_{N\Delta338}$ were able to bind WT ImuA (Figure 12B). The region of overlap between these two constructs involves residues 339-367 in ImuB, which is located at the beginning of the C-terminal region and includes the β-clamp binding motif. Therefore, the region of interaction for ImuB and ImuA most likely occurs between ImuB residues 343-367, as residues 339-343 make up the β-clamp binding motif. Reciprocally, the last 81 residues of ImuA are important for ImuB binding. Removing the RecA domain ($ImuA_{N\Delta222}$), prevented binding of $ImuA_{N\Delta222}$ to WT ImuB. This result is likely due to issues with ImuB expression, as seen earlier *in vitro*. However, $ImuA_{N\Delta222}$, which excludes

the PM motif, retained binding to $ImuB_{N\Delta 338}$, indicating that there is no overlap between the ImuB and potential RecA binding sites. These results suggest that ImuA could simultaneously bind RecA while recruiting ImuB to itself on ssDNA.

These results shows that the beginning of the uncharacterized C-terminal region of ImuB, which resembles no known protein domains, contains an ImuA binding site. It is likely that the remainder of the C-terminal region contains a binding site for ImuC as all the binding sites for ImuA, the β-clamp, and self-oligomerization are in this region. This hypothesis is supported by the BAC2H result that WT ImuC was able to interact with $ImuB_{C\Delta 81}$. This result suggests that ImuB has a binding site near residues 367-422 for ImuC. However, a WT ImuB and ImuC interaction was not observed, likely due to issues with WT ImuB expression under these conditions. Further BAC2H research can be completed to determine the region of ImuB necessary for interaction with ImuC to better define the proposed model of the TLS mechanism.

Solidifying the role of ImuABC in UV-induced mutagenesis

The study of the ImuABC complex began with *in vivo* characterization of the UV-induced mutagenesis (Boshoff et al., 2003; Galhardo et al., 2005). The TLS ImuABC homolog, Pol V, was also discovered due to its profound effect on UV-induced mutations in the 1970's (Kato & Shinoura, 1977). Using this UV-mutagenesis assay with TLS homologs in the opportunistic pathogen *P. aeruginosa* allows for the application of *in vitro* findings such as interaction sites to be tested *in vivo*.

Initially, growth of *P. aeruginosa* WT and deletion strains was tested at two temperatures, 30°C and 37°C, to confirm *imuA, imuB, and imuC* are not essential genes for

growth. Two temperatures were tested: 30°C, a lower temperature, which was shown to increase activity of ImuC, and the optimal growth temperature of 37°C (Jatsenko et al., 2017). There were no changes seen in growth between temperatures, which is expected as TLS is not an essential pathway under normal growth conditions, and the SOS response is not triggered by the change in temperature. Survival after UV irradiation and the UV-induced mutagenesis assay were carried out at 30°C as ImuC has been shown to be more active in response to DNA damage at this temperature possibly due to slower growth conditions (Jatsenko et al., 2017). It was expected that the cell survival of double deletion strains would decrease after UV irradiation, due to a lack of TLS to bypass DNA damage. This trend was seen with gene knockouts of *imuA, imuB, and imuC* in other bacterium such as *C. crescentus* and *Mycobacterium smegmatis* (Boshoff et al., 2003; Galhardo et al., 2005). However, this is not the case in *P. aeruginosa,* where survival remains the same with or without *imuA, imuB,* and *imuC* after increasing UV dosages. This could be attributed to the smaller UV-induced mutator phenotype where the effect of UV-mutagenesis in the ImuABC in *P. aeruginosa* is not as pronounced as in other species (Luján et al., 2019).

Based on the UV-mutagenesis assay, no difference was observed in spontaneous mutations between WT or the double deletion strains, where Lujan et al. had mixed results (2017). Given that TLS acts as a late-stage SOS response mechanism, it would not be activated during regular growth and limited stress. However, the UV-induced mutagenesis assay was completed with a dose (120 J/m^2) that would ensure enough stress to activate the SOS response. At this UV dose, there was approximately 15% cell survival, which still

allowed for enough rifampicin-resistant mutants to develop and be quantified. Between the absence and presence of UV-induced stress, WT PAO1 exhibited increased mutation rates, although not significant. In contrast, mutation rates in the *ΔimuA ΔimuB* and *ΔimuB ΔimuC* deletions stay the same when exposed to UV damage compared to no UV damage. These results show that ImuABC could play a minor role in UV-induced mutagenesis in *P. aeruginosa* since the phenotype is not as pronounced as in other bacterial species, complementing the work carried out in other species. Testing other DNA damaging agents that also trigger the SOS response and a greater mutagenesis phenotype could also provide greater insight on TLS and the types of DNA damage it can bypass in the opportunistic pathogen *P. aeruginosa*.

Conclusions

The ImuABC TLS complex has remained insoluble for decades, preventing biochemical analysis and determination of mechanism, similar to what has been described for the functionally homologous Pol V complex. Overall, the key findings of this research show that *in vitro*: 1) ImuA and $ImuB_{N\Delta34}$ can be expressed as soluble proteins using the *E. coli* Arctic Express cell line; 2) Both proteins act as trimers in solution with ImuA also capable of forming a monomer, as determined by SAXS; 3) ImuA and $ImuB_{N\Delta34}$ are able to preferentially bind ssDNA and 4) The C-terminal region of ImuB interacts with ImuC and the C-terminal region of ImuA. These findings, combined with previously published data from Sheng et. al (2021) support a model for TLS, where DNA replication proceeds normally until a DNA lesion is encountered and PolIII stalls at the site of damage. This triggers the accumulation of ssDNA, RecA polymerization, and induction of the SOS

response genes, including the *imuA-imuB-imuC* gene cassette. ImuA likely initiates TLS by binding to and inhibiting RecA polymerization (Sheng et al., 2021). This recruits a trimer of ImuB to the lesion, which acts as the central binding hub between ImuA, the β-clamp, and ImuC. As ImuB-ImuC binds to the DNA, RecA polymers may dissociate (Sheng et al. 2021). However, based on EMSA data presented in this thesis, it remains unclear if ImuA also dissociates by being outcompeted by ImuB or remains bound to ImuB during the bypass of damage. Given that there is no interaction between ImuC and the β-clamp, it's likely that ImuB acts as the main tether for all proteins involved and is responsible for the polymerase switch. Once ImuC is able to bind at the DNA lesion, it replicates past the damage, before dissociating so that error-free replication by PolIII can resume. Future studies will benefit from investigating the mechanisms that guide the physical switches between TLS and PolIII during replication.

REFERENCES

Aguilera, A., & Gómez-González, B. (2008). Genome instability: A mechanistic view of its causes and consequences. *Nature Reviews Genetics*, *9*(3), 204–217. https://doi.org/10.1038/nrg2268

Anderson, M., Huh, J. H., Ngo, T., Lee, A., Hernandez, G., Pang, J., Perkins, J., & Dutnall, R. N. (2010). Co-expression as a convenient method for the production and purification of core histones in bacteria. *Protein Expression and Purification*, *72*(2), 194–204. https://doi.org/10.1016/j.pep.2010.03.013

Aslanidis, C., & de Jong, P. J. (n.d.). Ligation-independent cloning of PCR products (LIC-PCR). In *Nucleic Acids Research* (Vol. 18, Issue 20). https://academic.oup.com/nar/article/18/20/6069/1141286

Bailey, S., Wing, R. A., & Steitz, T. A. (2006). The Structure of T. aquaticus DNA Polymerase III Is Distinct from Eukaryotic Replicative DNA Polymerases. *Cell*, *126*(5), 893–904. https://doi.org/10.1016/j.cell.2006.07.027

Battesti, A., & Bouveret, E. (2012). The bacterial two-hybrid system based on adenylate cyclase reconstitution in Escherichia coli. *Methods*, *58*(4), 325–334. https://doi.org/10.1016/J.YMETH.2012.07.018

Bębenek, A., & Ziuzia-Graczyk, I. (2018). Fidelity of DNA replication—a matter of proofreading. *Current Genetics*, *64*(5), 985–996. https://doi.org/10.1007/s00294-018-0820-1

Blum, M., Chang, H. Y., Chuguransky, S., Grego, T., Kandasaamy, S., Mitchell, A., Nuka, G., Paysan-Lafosse, T., Qureshi, M., Raj, S., Richardson, L., Salazar, G. A., Williams, L., Bork, P., Bridge, A., Gough, J., Haft, D. H., Letunic, I., Marchler-Bauer, A., … Finn, R. D. (2021). The InterPro protein families and domains database: 20 years on. *Nucleic Acids Research*, *49*(D1), D344–D354. https://doi.org/10.1093/nar/gkaa977

Bolten, S. N., Rinas, U., & Scheper, T. (2018). Heparin: role in protein purification and substitution with animal-component free material. In *Applied Microbiology and Biotechnology* (Vol. 102, Issue 20, pp. 8647–8660). Springer Verlag. https://doi.org/10.1007/s00253-018-9263-3

Bornhorst, J. A., & Falke, J. J. (2000). Purification of Proteins Using Polyhistidine Affinity Tags. *Methods Enzymol.*, *326*, 245–254.

Boshoff, H. I. M., Reed, M. B., Iii, C. E. B., & Mizrahi, V. (2003). DnaE2 Polymerase Contributes to In Vivo Survival and the Emergence of Drug Resistance in

Mycobacterium tuberculosis. *Cell*, *113*, 183–193. http://genolist.pasteur.fr/Tuberculist

Boudsocq, F., Kokoska, R. J., Plosky, B. B., Vaisman, A., Ling, H., Kunkel, T. A., Yang, W., & Woodgate, R. (2004). Investigating the role of the little finger domain of Y-family DNA polymerases in low fidelity synthesis and translesion replication. *Journal of Biological Chemistry*, *279*(31), 32932–32940. https://doi.org/10.1074/jbc.M405249200

Bradbury, B. J., & Pucci, M. J. (2008). Recent advances in bacterial topoisomerase inhibitors. In *Current Opinion in Pharmacology* (Vol. 8, Issue 5, pp. 574–581). https://doi.org/10.1016/j.coph.2008.04.009

Bruck, I., Woodgate, R., McEuntee, K., & Goodman, M. F. (1996). Purification of a soluble UmuD'C complex from Escherichia coli: Cooperative binding of UmuD'C to single-stranded DNA. *Journal of Biological Chemistry*, *271*(18), 10767–10774. https://doi.org/10.1074/jbc.271.18.10767

Burckhardt, S. E., Woodgate, R., Scheuermann, R. H., & Echols, H. (1988). UmuD mutagenesis protein of Escherichia coli: Overproduction, purification, and cleavage by RecA (SOS response/LexA cleavage/fidelity of DNA replication/protein self-cleavage). *Proc. Natl. Acad. Sci. USA*, *85*, 1811–1815.

Checovich, W. J., Bolger, R. E., & Burke, T. (1995). Fluorescence polarization-a new tool for cell and molecular biology. *Nature*, *375*.

del Val, E., Nasser, W., Abaibou, H., & Reverchon, S. (2019). RecA and DNA recombination: A review of molecular mechanisms. In *Biochemical Society Transactions* (Vol. 47, Issue 5, pp. 1511–1531). Portland Press Ltd. https://doi.org/10.1042/BST20190558

Donovan, R. S., Robinson, C. W., & Glick, B. R. (1996). Review: Optimizing inducer and culture conditions for expression of foreign proteins under the control of the lac promoter. *Journal of Industrial Microbiology*, *16*, 145–154.

Erill, I., Campoy, S., Mazon, G., & Barbé, J. (2006). Dispersal and regulation of an adaptive mutagenesis cassette in the bacteria domain. *Nucleic Acids Research*, *34*(1), 66–77. https://doi.org/10.1093/nar/gkj412

Filée, J., Forterre, P., Sen-Lin, T., & Laurent, J. (2002). Evolution of DNA polymerase families: Evidences for multiple gene exchange between cellular and viral proteins. *Journal of Molecular Evolution*, *54*(6), 763–773. https://doi.org/10.1007/s00239-001-0078-x

Fox, B. G., & Blommel, P. G. (2009). Autoinduction of protein expression. In *Current Protocols in Protein Science* (Issue SUPPL. 56). https://doi.org/10.1002/0471140864.ps0523s56

Freidberg, E., Walker, G., Siede, W., Wood, R., Schultz, R., & Ellenburger, T. (2005). *DNA Repair and Mutagenesis*.

Fuchs, R. P., & Fujii, S. (2013). Translesion DNA synthesis and mutagenesis in prokaryotes. *Cold Spring Harbor Perspectives in Biology*, *5*(12). https://doi.org/10.1101/cshperspect.a012682

Galhardo, R. S., Rocha, R. P., Marques, M. v., & Menck, C. F. M. (2005). An SOS-regulated operon involved in damage-inducible mutagenesis in Caulobacter crescentus. *Nucleic Acids Research*, *33*(8), 2603–2614. https://doi.org/10.1093/nar/gki551

Garibyan, L., Huang, T., Kim, M., Wolff, E., Nguyen, A., Nguyen, T., Diep, A., Hu, K., Iverson, A., Yang, H., & Miller, J. H. (2003). Use of the rpoB gene to determine the specificity of base substitution mutations on the Escherichia coli chromosome. *DNA Repair*, *2*(5), 593–608. https://doi.org/10.1016/S1568-7864(03)00024-7

Gáspári, Z. (2020). *Structural Bioinformatics Methods and Protocols Methods*. http://www.springer.com/series/7651

Goodman, M., & Woodgate, R. (2013). Translesion DNA Polymerases. *Cold Spring Harbor Pespectives in Biology*.

Graether, S. P. (2019). Troubleshooting guide to expressing intrinsically disordered proteins for use in NMR experiments. In *Frontiers in Molecular Biosciences* (Vol. 5, Issue JAN). Frontiers Media S.A. https://doi.org/10.3389/fmolb.2018.00118

Gruber, A. J., Erdem, A. L., Sabat, G., Karata, K., Jaszczur, M. M., Vo, D. D., Olsen, T. M., Woodgate, R., Goodman, M. F., & Cox, M. M. (2015). A RecA Protein Surface Required for Activation of DNA Polymerase V. *PLoS Genetics*, *11*(3). https://doi.org/10.1371/journal.pgen.1005066

Gutiérrez-González, M., Farías, C., Tello, S., Pérez-Etcheverry, D., Romero, A., Zúñiga, R., Ribeiro, C. H., Lorenzo-Ferreiro, C., & Molina, M. C. (2019). Optimization of culture conditions for the expression of three different insoluble proteins in Escherichia coli. *Scientific Reports*, *9*(1). https://doi.org/10.1038/s41598-019-53200-7

Hartinger, D., Heinl, S., Schwartz, H. E., Grabherr, R., Schatzmayr, G., Haltrich, D., & Moll, W.-D. (2010). Enhancement of solubility in Escherichia coli and purification

of an aminotransferase from Sphingopyxis sp. MTA144 for deamination of hydrolyzed fumonisin B 1. *Microb Cell Fact*. http://www.microbialcellfactories.com/content/9/1/62

Hata, S., Kitamura, F., & Sorimachi, H. (2013). Efficient expression and purification of recombinant human μ-calpain using an Escherichia coli expression system. *Genes to Cells*, *18*(9), 753–763. https://doi.org/10.1111/gtc.12071

Hawver, L. A., Gillooly, C. A., & Beuning, P. J. (2011). Characterization of Escherichia coli UmuC active-site loops identifies variants that confer UV hypersensitivity. *Journal of Bacteriology*, *193*(19), 5400–5411. https://doi.org/10.1128/JB.05301-11

Hedglin, M., Kumar, R., & Benkovic, S. J. (2013). Replication clamps and clamp loaders. *Cold Spring Harbor Perspectives in Biology*, *5*(4), 1–19. https://doi.org/10.1101/cshperspect.a010165

Heltzel, J. M. H., Maul, R. W., Wolff, D. W., & Sutton, M. D. (2012). Escherichia coli DNA polymerase IV (Pol IV), but Not Pol II, dynamically switches with a stalled Pol III* replicase. *Journal of Bacteriology*, *194*(14), 3589–3600. https://doi.org/10.1128/JB.00520-12

Horton, R., Cai, Z., Ho, S., & Pease, L. (1990). Gene Splicing by Overlap Extension: Tailor-Made Genes Using the Polymerase Chain Reaction. *BioTechniques*, *8*(5), 528–535.

Ippoliti, P. J., DeLateur, N. A., Jones, K. M., & Beuning, P. J. (2012). Multiple strategies for translesion synthesis in bacteria. *Cells*, *1*(4), 799–831. https://doi.org/10.3390/cells1040799

Janknecht, R., de Martynofft, G., Loutt, J., Hipskind, R. A., Nordheim, A., & Stunnenbergt, H. G. (1991). Rapid and efficient purification of native histidine-tagged protein expressed by recombinant vaccinia virus (Ni2-chelate affinity chromatography/serum response factor/in vitro transcription). *Proc. Nadl. Acad. Sci. USA*, *88*, 8972–8976.

Jaszczur, M., Bertram, J. G., Robinson, A., van Oijen, A. M., Woodgate, R., Cox, M. M., & Goodman, M. F. (2016). Mutations for Worse or Better: Low-Fidelity DNA Synthesis by SOS DNA Polymerase V Is a Tightly Regulated Double-Edged Sword. *Biochemistry*, *55*(16), 2309–2318. https://doi.org/10.1021/acs.biochem.6b00117

Jaszczur, M. M., Vo, D. D., Stanciauskas, R., Bertram, J. G., Sikand, A., Cox, M. M., Woodgate, R., Mak, C. H., Pinaud, F., & Goodman, M. F. (2019). Conformational regulation of Escherichia coli DNA polymerase V by RecA and ATP. *PLoS Genetics*, *15*(2). https://doi.org/10.1371/journal.pgen.1007956

Jatsenko, T., Sidorenko, J., Saumaa, S., & Kivisaar, M. (2017). DNA polymerases ImuC and DinB are involved in DNA alkylation damage tolerance in Pseudomonas aeruginosa and Pseudomonas putida. *PLoS ONE*, *12*(1). https://doi.org/10.1371/JOURNAL.PONE.0170719

Jeong, H., Barbe, V., Lee, C. H., Vallenet, D., Yu, D. S., Choi, S. H., Couloux, A., Lee, S. W., Yoon, S. H., Cattolico, L., Hur, C. G., Park, H. S., Ségurens, B., Kim, S. C., Oh, T. K., Lenski, R. E., Studier, F. W., Daegelen, P., & Kim, J. F. (2009). Genome Sequences of Escherichia coli B strains REL606 and BL21(DE3). *Journal of Molecular Biology*, *394*(4), 644–652. https://doi.org/10.1016/j.jmb.2009.09.052

Jiang, Q., Karata, K., Woodgate, R., Cox, M. M., & Goodman, M. F. (2009). The active form of DNA polymerase v is UmuD′ 2 C-RecA-ATP. *Nature*, *460*(7253), 359–363. https://doi.org/10.1038/nature08178

Joseph, A. M., & Badrinarayanan, A. (2020). Visualizing mutagenic repair: novel insights into bacterial translesion synthesis. *FEMS Microbiology Reviews*, *44*(5), 572–582. https://doi.org/10.1093/femsre/fuaa023

Jumper, J., Evans, R., Pritzel, A., Green, T., Figurnov, M., Ronneberger, O., Tunyasuvunakool, K., Bates, R., Žídek, A., Potapenko, A., Bridgland, A., Meyer, C., Kohl, S. A. A., Ballard, A. J., Cowie, A., Romera-Paredes, B., Nikolov, S., Jain, R., Adler, J., … Hassabis, D. (2021). Highly accurate protein structure prediction with AlphaFold. *Nature*, *596*(7873), 583–589. https://doi.org/10.1038/s41586-021-03819-2

Kanehisa, M., Furumichi, M., Sato, Y., Ishiguro-Watanabe, M., & Tanabe, M. (2021). KEGG: Integrating viruses and cellular organisms. *Nucleic Acids Research*, *49*(D1), D545–D551. https://doi.org/10.1093/nar/gkaa970

Karata, K., Vaisman, A., Goodman, M. F., & Woodgate, R. (2012). Simple and efficient purification of Escherichia coli DNA polymerase V: Cofactor requirements for optimal activity and processivity in vitro. *DNA Repair*, *11*(4), 431–440. https://doi.org/10.1016/j.dnarep.2012.01.012

Katayama, T., Ozaki, S., Keyamura, K., & Fujimitsu, K. (2010). Regulation of the replication cycle: Conserved and diverse regulatory systems for DnaA and oriC. In *Nature Reviews Microbiology* (Vol. 8, Issue 3, pp. 163–170). https://doi.org/10.1038/nrmicro2314

Kato, T., & Shinoura, Y. (1977). Isolation and Characterization of Mutants of Escherichia coli Deficient in Induction of Mutations by Ultraviolet Light. *Molecular and General Genetics MGG Volume*, *156*, 121–131.

Knobel, P. A., & Marti, T. M. (2011). Translesion DNA synthesis in the context of cancer research. *Cancer Cell International*, *11*. https://doi.org/10.1186/1475-2867-11-39

Krause, M., Ukkonen, K., Haataja, T., Ruottinen, M., Glumoff, T., Neubauer, A., Neubauer, P., & Vasala, A. (2010). A novel fed-batch based cultivation method provides high cell-density and improves yield of soluble recombinant proteins in shaken cultures. *Microbial Cell Factories*. http://www.microbialcellfactories.com/content/9/1/11

Lamers, M. H., Georgescu, R. E., Lee, S. G., O'Donnell, M., & Kuriyan, J. (2006). Crystal Structure of the Catalytic α Subunit of E. coli Replicative DNA Polymerase III. *Cell*, *126*(5), 881–892. https://doi.org/10.1016/j.cell.2006.07.028

Leite, W. C., Galvão, C. W., Saab, S. C., Iulek, J., Etto, R. M., Steffens, M. B. R., Chitteni-Pattu, S., Stanage, T., Keck, J. L., & Cox, M. M. (2016). Structural and functional studies of H. seropedicae RecA Protein - Insights into the polymerization of RecA protein as nucleoprotein filament. *PLoS ONE*, *11*(7). https://doi.org/10.1371/journal.pone.0159871

Lemontt, J. F. (1971). MUTANTS OF YEAST DEFECTIVE IN MUTATION INDUCED BY ULTRAVIOLET LIGHT. *Genetics*, *68*(1), 21–33.

Lih-Ling, L., & Little, J. (1988). Isolation and Characterization of Noncleavable (Ind-) Mutants of the LexA Repressor of Escherichia coli K-12. *JOURNAL OF BACTERIOLOGY*, *170*(5), 2163–2173.

Lindahl, T., & Barnes, D. E. (2000). Repair of endogenous DNA damage. *Cold Spring Harbor Symposia on Quantitative Biology*, *65*, 127–133. https://doi.org/10.1101/sqb.2000.65.127

Luján, A. M., Moyano, A. J., Martino, R. A., Feliziani, S., Urretavizcaya, M., & Smania, A. M. (2019). ImuB and ImuC contribute to UV-induced mutagenesis as part of the SOS regulon in Pseudomonas aeruginosa. *Environmental and Molecular Mutagenesis*, *60*(7), 594–601. https://doi.org/10.1002/em.22290

Madeira, F., Park, Y. M., Lee, J., Buso, N., Gur, T., Madhusoodanan, N., Basutkar, P., Tivey, A. R. N., Potter, S. C., Finn, R. D., & Lopez, R. (2019). The EMBL-EBI search and sequence analysis tools APIs in 2019. *Nucleic Acids Research*, *47*(W1), W636–W641. https://doi.org/10.1093/nar/gkz268

Makino, T., Skretas, G., & Georgiou, G. (2011). Strain engineering for improved expression of recombinant proteins in bacteria. *Microbial Cell Factories*, *10*. https://doi.org/10.1186/1475-2859-10-32

Mazin, A. v, & Kowalczykowski, S. C. (1998). The function of the secondary DNA-binding site of RecA protein during DNA strand exchange. In *The EMBO Journal* (Vol. 17, Issue 4).

McCulloch, S. D., & Kunkel, T. A. (2008). The fidelity of DNA synthesis by eukaryotic replicative and translesion synthesis polymerases. *Cell Research*, *18*(1), 148–161. https://doi.org/10.1038/cr.2008.4

Mckenzie, G. J., Harris, R. S., Lee, P. L., & Rosenberg, S. M. (2000). The SOS response regulates adaptive mutation. *Proc Natl Acad Sci U S A*, *97*(12), 6646–6651. www.pnas.orgcgidoi10.1073pnas.120161797

Mertz, T. M., Harcy, V., & Roberts, S. A. (2017). Risks at the DNA replication fork: Effects upon carcinogenesis and tumor heterogeneity. In *Genes* (Vol. 8, Issue 1). MDPI AG. https://doi.org/10.3390/genes8010046

Nelson, J., Lawrence, C., & Hinkle, D. (1998). Deoxycytidyl transferase activity of yeast REV1 protein. *Nature*, *382*, 729–731.

Oakley, A. J. (2019). A structural view of bacterial DNA replication. *Protein Science*, *28*(6), 990–1004. https://doi.org/10.1002/pro.3615

Oates, M. E., Romero, P., Ishida, T., Ghalwash, M., Mizianty, M. J., Xue, B., Dosztányi, Z., Uversky, V. N., Obradovic, Z., Kurgan, L., Dunker, A. K., & Gough, J. (2013). D2P2: Database of disordered protein predictions. *Nucleic Acids Research*, *41*(D1). https://doi.org/10.1093/nar/gks1226

O'Donnell, M. (2006). Replisome architecture and dynamics in Escherichia coli. In *Journal of Biological Chemistry* (Vol. 281, Issue 16, pp. 10653–10656). https://doi.org/10.1074/jbc.R500028200

Pata, J. D. (2010). Structural diversity of the Y-family DNA polymerases. In *Biochimica et Biophysica Acta - Proteins and Proteomics* (Vol. 1804, Issue 5, pp. 1124–1135). https://doi.org/10.1016/j.bbapap.2010.01.020

Patoli, A. A., Winter, J. A., & Bunting, K. A. (2013). The UmuC subunit of the E. coli DNA polymerase v shows a unique interaction with the β-clamp processivity factor. *BMC Structural Biology*, *13*(1). https://doi.org/10.1186/1472-6807-13-12

Pei, J., Kim, B. H., & Grishin, N. v. (2008). PROMALS3D: A tool for multiple protein sequence and structure alignments. *Nucleic Acids Research*, *36*(7), 2295–2300. https://doi.org/10.1093/nar/gkn072

Peng, R., Chen, J. H., Feng, W. W., Zhang, Z., Yin, J., Li, Z. S., & Li, Y. Z. (2017). Error-prone DnaE2 balances the genome mutation rates in Myxococcus xanthus DK1622. *Frontiers in Microbiology*, *8*(FEB). https://doi.org/10.3389/fmicb.2017.00122

Podlesek, Z., & Žgur Bertok, D. (2020). The DNA Damage Inducible SOS Response Is a Key Player in the Generation of Bacterial Persister Cells and Population Wide Tolerance. *Frontiers in Microbiology*, *11*. https://doi.org/10.3389/fmicb.2020.01785

Rangarajan, S., Woodgate, R., & Goodman, M. F. (1999). A phenotype for enigmatic DNA polymerase II: A pivotal role forpol II in replication restart in UV-irradiatedEscherichia coli. *Genetics*, *96*, 9224–9229. www.pnas.org.

Rietsch, A., Vallet-Gely, I., Dove, S. L., & Mekalanos, J. J. (2005). *ExsE, a secreted regulator of type III secretion genes in Pseudomonas aeruginosa*. www.pnas.orgcgidoi10.1073pnas.0503005102

Rizkia, P. R., Silaban, S., Hasan, K., Kamara, D. S., Subroto, T., Soemitro, S., & Maksum, I. P. (2015). Effect of Isopropyl-β-D-thiogalactopyranoside Concentration on Prethrombin-2 Recombinan Gene Expression in Escherichia Coli ER2566. *Procedia Chemistry*, *17*, 118–124. https://doi.org/10.1016/j.proche.2015.12.121

Robinson, A., Causer, R. J., & Dixon, N. E. (2012). Architecture and Conservation of the Bacterial DNA Replication Machinery, an Underexploited Drug Target. In *Current Drug Targets* (Vol. 13).

Rosano, G. L., & Ceccarelli, E. A. (2009). Rare codon content affects the solubility of recombinant proteins in a codon bias-adjusted Escherichia coli strain. *Microbial Cell Factories*, *8*. https://doi.org/10.1186/1475-2859-8-41

San-Miguel, T., Pérez-Bermúdez, P., & Gavidia, I. (2013). Production of soluble eukaryotic recombinant proteins in E. coli is favoured in early log-phase cultures induced at low temperature. *SpringerPlus*. http://www.springerplus.com/content/2/1/89

Sheng, D., Wang, Y., Jiang, Z., Liu, D., & Li, Y. (2020). ImuA participates in SOS mutagenesis by interacting with RecA1 and ImuB 1 in Myxococcus xanthus. *BioRxiv*. https://doi.org/10.1101/2020.12.14.422803

Sheng, D., Wang, Y., Jiang, Z., Liu, D., & Li, Y. (2021). ImuA Facilitates SOS Mutagenesis by Inhibiting RecA-Mediated Activity in Myxococcus xanthus. *Applied and Environmental Microbiology*, *87*(18). https://doi.org/10.1128/AEM

Silaban, S., Gaffar, S., Simorangkir, M., Maksum, I. P., & Subroto, T. (2019). Effect of IPTG Concentration on Recombinant Human Prethrombin-2 Expression in Escherichia coli BL21(DE3) ArcticExpress. *IOP Conference Series: Earth and Environmental Science*, *217*(1). https://doi.org/10.1088/1755-1315/217/1/012039

Silverman, J. M., Agnello, D. M., Zheng, H., Andrews, B. T., Li, M., Catalano, C. E., Gonen, T., & Mougous, J. D. (2013). Haemolysin Coregulated Protein Is an Exported Receptor and Chaperone of Type VI Secretion Substrates. *Molecular Cell*, *51*(5), 584–593. https://doi.org/10.1016/j.molcel.2013.07.025

Some, D., Amartely, H., Tsadok, A., & Lebendiker, M. (2019). Characterization of proteins by size-exclusion chromatography coupled to multi-angle light scattering (Sec-mals). *Journal of Visualized Experiments*, *2019*(148). https://doi.org/10.3791/59615

Sommer, S., Bailone, A., & Devoret, R. (1993). The appearance of the UmuD'C protein complex in Escherichia co//switches repair from homologous recombination to SOS mutagenesis. *Molecular Microbiology*, *10*(5), 963–971.

Sørensen, H. P., & Mortensen, K. K. (2005). Soluble expression of recombinant proteins in the cytoplasm of Escherichia coli. *Microbial Cell Factories*, *4*. https://doi.org/10.1186/1475-2859-4-1

Stover, C. K., Pham[2], X. Q., Erwin, A. L., Mizoguchi, S. D., Warrener, P., Hickey, M. J., Brinkman[3], F. S. L., Hufnagle, W. O., Kowalik, D. J., Lagrou, M., Garber, R. L., Goltry, L., Tolentino, E., Westbrock-Wadman, S., Yuan, Y., Brody, L. L., Coulter, S. N., Folger, K. R., Kas[2], A., … Olson[2], M. v. (2000). Complete genome sequence of Pseudomonas aeruginosa PAO1, an opportunistic pathogen. In *NATURE* (Vol. 406). www.nature.com

Sutton, M. D., Opperman, T., & Walker, G. C. (1999). The Escherichia coli SOS mutagenesis proteins UmuD and UmuD interact physically with the replicative DNA polymerase. *Proc Natl Acad Sci U S A*, *96*(22), 12373–12378. www.pnas.org

Taft-Benz, S. A., & Schaaper, R. M. (2004). The θ Subunit of Escherichia coli DNA Polymerase III: A Role in Stabilizing the ε Proofreading Subunit. *Journal of Bacteriology*, *186*(9), 2774–2780. https://doi.org/10.1128/JB.186.9.2774-2780.2004

Tang, M., Bruck, I., Eritja, R., Turner, J., Frank, E. G., Woodgate, R., O'donnell, M., Goodman, M. F., & Lehman, R. (1998). Biochemical basis of SOS-induced mutagenesis in Escherichia coli: Reconstitution of in vitro lesion bypass dependent on the UmuD2□C mutagenic complex and RecA protein. *Proc. Natl. Acad. Sci. USA*, *95*, 20892–22725. www.pnas.org.

Tang, M., Shen, X., Frank, E. G., O'donnell, M., Woodgate, R., Goodman, M. F., & Lehman, R. (1999). UmuD2C is an error-prone DNA polymerase, Escherichia coli pol V. *Proc. Natl. Acad. Sci. USA*, *96*, 8919–8924. www.pnas.org.

Tegel, H., Tourle, S., Ottosson, J., & Persson, A. (2010). Increased levels of recombinant human proteins with the Escherichia coli strain Rosetta(DE3). *Protein Expression and Purification*, *69*(2), 159–167. https://doi.org/10.1016/j.pep.2009.08.017

Timinskas, K., & Venclovas, Č. (2019). New insights into the structures and interactions of bacterial Y-family DNA polymerases. *Nucleic Acids Research*, *47*(9), 4383–4405. https://doi.org/10.1093/nar/gkz198

Warner, D. F., Ndwandwe, D. E., Abrahams, G. L., Kana, B. D., Machowski, E. E., Venclovas, Č., & Mizrahi, V. (2010). Essential roles for imuA′- and imuB-encoded accessory factors in DnaE2-dependent mutagenesis in Mycobacterium tuberculosis. *Proceedings of the National Academy of Sciences of the United States of America*, *107*(29), 13093–13098. https://doi.org/10.1073/pnas.1002614107

Waters, L. S., Minesinger, B. K., Wiltrout, M. E., D'Souza, S., Woodruff, R. v., & Walker, G. C. (2009a). Eukaryotic Translesion Polymerases and Their Roles and Regulation in DNA Damage Tolerance. *Microbiology and Molecular Biology Reviews*, *73*(1), 134–154. https://doi.org/10.1128/mmbr.00034-08

Wegrzyn, K. E., Gross, M., Uciechowska, U., & Konieczny, I. (2016). Replisome assembly at bacterial chromosomes and iteron plasmids. In *Frontiers in Molecular Biosciences* (Vol. 3, Issue AUG). Frontiers Media S.A. https://doi.org/10.3389/fmolb.2016.00039

TABLES AND FIGURES

Table 1. DNA polymerase families, domains, and functions. Table adapted from Filée et al., 2002.

Polymerase Family	Domain	Function
A	Bacteria, Eukarya	Mitochondrial DNA replication DNA repair/tolerance 3'-5' exonuclease activity
B	Bacteria, Eukarya, Archaea	Chromosomal DNA replication DNA repair/tolerance 3'-5' exonuclease activity
C	Bacteria	Chromosomal DNA replication 3'-5' exonuclease activity
D	Archaea	Chromosomal DNA replication 3'-5' exonuclease activity
X	Bacteria, Eukarya, Archaea	DNA repair/tolerance, TLS
Y	Bacteria, Eukarya, Archaea	DNA repair/tolerance Main TLS polymerases

Table 2. TLS polymerases across all domains. Table adapted from Goodman & Woodgate, 2013.

Organism	TLS Polymerases	Description
Bacteria	Pol II Pol IV (DinB) Pol V/ImuABC	LexA regulated Pol V/ImuABC primary TLS mechanism
Eukarya *Homo sapiens*	REV1 REV3 Pol η Pol ι Pol κ	REV1 catalytic subunit of Pol ι REV3 scaffold for η, ι, κ Multiple DNA bypass functions
Yeast *S. cerevisae*	Rev1p	Incorporates dCMP in abasic sites
Archaea *Sulfolobus solfataricus*	Dpo4	Ortholog of Pol V

Table 3. Expression and solubility testing of TLS proteins in *P. aeruginosa.* Protein expression was induced with 0.5 mM IPTG in LB media with different *E. coli* cell lines. N: not expressed, E: expressed, S: soluble.

Protein	**Cell line**	**Expression condition**		
		18 h at 18 °C	*5 h at 30 °C*	*3 h at 37 °C*
pMCSG10::*imuA*	BL21	N	N	N
	SoluBL21	N	N	N
	Rosetta	N	N	N
pMCSG7::*imuB*	BL21	E	E	E
	SoluBL21	N	E	E
	Rosetta	E	E	E
pMCSG10::*imuB*	BL21	E	E	E
	SoluBL21	N	N	N
	Rosetta	E	E	E
pMCSG7::*imuC*	BL21	N	N	N
	SoluBL21	N	N	N
	Rosetta	N	N	N

Table 4. Solubility testing of *P. aeruginosa* TLS protein co-expression. Proteins were co-transformed in different *E. coli* cell lines and expression was induced with 1 mM IPTG in 20 mL of LB media. I: insoluble, N: not expressed, S: soluble.

Proteins	**Cell line**	**Expression condition**	
		18 h at 16 °C	*3 h at 37 °C*
ImuA, ImuB	BL21 codon +	N	ImuB-I, ImuA-N
	Rosetta	N	N
ImuB, ImuC	BL21 codon +	ImuB-I, ImuC-N	I
	BL21 star	I	I
	Rosetta	N	I
ImuA, ImuB, ImuC	BL21 codon +	N	ImuA-N, ImuB-I, ImuC-I,
	BL21 star	ImuA-N, ImuB-I, ImuC-I,	ImuA-N, ImuB-I, ImuC-I,
	Rosetta	N	N

Table 5. *P. aeruginosa* TLS proteins and truncations cloned. C-terminal truncations were cloned with Q5 SDM. N-terminal truncations were cloned using LIC. Constructs were confirmed via Sanger sequencing.

Protein Construct (aa)	Cloning Method	Plasmid	Description
$ImuA_{C\Delta17}$	SDM	pMCSG10	C terminal truncation removing disorder
$ImuB_{C\Delta156}$	SDM	pMCSG7	C terminal truncation removing disorder
$ImuB_{C\Delta123}$	SDM	pMCSG7	C terminal truncation removing disorder and the β-clamp binding motif
$ImuB_{C\Delta118}$	SDM	pMCSG7	C terminal truncation removing disorder but including β-clamp binding motif
$ImuB_{N\Delta345}$	LIC	pMCSG7	N terminal truncation removing the β-clamp binding motif
$ImuB_{N\Delta353}$	LIC	pMCSG7	N terminal truncation including β-clamp binding motif
ImuC	LIC	pMCSG7	WT
$ImuC_{270\text{-}714}$	LIC	pMCSG7	DNA Polymerase III domain

Table 6. Expression and solubility testing of TLS protein truncations. Protein expression was induced with 0.5mM IPTG in LB media with different *E. coli* cell lines. N: not expressed, E: expressed, S: soluble.

Protein	Cell line	Expression condition		
		18 h at 18 °C	*5 h at 30 °C*	*3 h at 37 °C*
pMCSG7::$imuA_{C\Delta17}$	Arctic Express	24 h at 12 °C - I		
pMCSG7::$imuB_{N\Delta345}$	BL21	S	S	S
	SoluBL21	S	S	S
	Rosetta	S	S	S
pMCSG7::$imuB_{N\Delta353}$	BL21	S	S	S
	SoluBL21	S	S	S
	Rosetta	S	S	S
pMCSG7::$imuC_{270\text{-}714}$	BL21	E	E	E
	SoluBL21	N	E	E
	Rosetta	E	E	E

Table 7. Solubility testing of *M. xanthus* TLS proteins. Protein expression was induced with 0.5 mM IPTG in 20 mL of LB media with different *E. coli* cell lines. Protein expression was also induced at 0.1 mM IPTG for ImuB. I: insoluble, N: not expressed, S: soluble.

Protein	**Cell line**	**Expression condition**		
		18 h at 12 °C	*18 h at 16 °C*	*3 h at 37 °C*
ImuA	Artic Express	I	-	-
	BL21 codon +	-	I	I
	SoluBL21	-	N	N
$ImuB_{N\Delta34}$	Artic Express	I	-	-
	BL21 codon +	-	I	I
	SoluBL21	-	I	I
ImuB	Artic Express	N	-	-
	BL21 codon +	-	N	N
	SoluBL21	-	N	-
ImuC	Artic Express	I	-	-
	BL21 codon +	-	I	I
	SoluBL21	-	N	N

Table 8. Solubility testing of *M. xanthus* TLS proteins when co-expressed. Protein expression was induced with 1 mM IPTG in 20 mL of LB media with different *E. coli* cell lines. Protein expression was also induced at 0.1 mM IPTG for ImuA ImuB. I: insoluble, N: not expressed, S: soluble.

Protein	**Cell line**	**Expression condition**		
		24 h at 12 °C	*18 h at 16 °C*	*3 h at 37 °C*
ImuA ImuB$_{N\Delta34}$	Artic Express	**S**	-	-
	BL21 codon +	-	N	ImuA-I, ImuB$_{N\Delta34}$-N
	BL21 star	-	ImuA-**S,** ImuB$_{N\Delta34}$-N	ImuA-I, ImuB$_{N\Delta34}$-N
	Rosetta	-	ImuA-**S**, ImuB$_{N\Delta34}$-N	ImuA-I, ImuB$_{N\Delta34}$-N
ImuA ImuB	Arctic Express	ImuA-**S,** ImuB$_{N\Delta34}$-N	-	-
	BL21 codon +	-	N	ImuA-**S,** ImuB$_{N\Delta34}$-N
ImuB$_{N\Delta34}$ ImuC	Artic Express	-	-	-
	BL21 codon +	-	N	-
	BL21 star	-	I	I
	Rosetta	-	N	N
ImuA ImuB$_{N\Delta34}$ ImuC	Artic Express	ImuA-**S**, ImuB$_{N\Delta34}$-**S,** ImuC-I	-	-
	BL21 codon +	-	N	N
	BL21 star	-	ImuA-I, ImuB$_{N\Delta34}$-N, ImuC-I	ImuA-I, ImuB$_{N\Delta34}$-N, ImuC-I
	Rosetta	-	ImuA-N, ImuB$_{N\Delta34}$-N, ImuC-I	N

Table 9. *M. xanthus* ImuA and ImuB$_{N\Delta34}$ protein expression optimization. N: not expressed, SS: slightly soluble, S: soluble.

Media used	**0.1 mM IPTG**	**0.5 mM IPTG**
LB	**S**	SS
AIM	N	N
TB	ImuA-**S** ImuB$_{N\Delta34}$ -N	-

Table 10. K_D values for ImuA, $ImuA_{C\Delta53}$ and $ImuB_{N\Delta34}$ binding different DNA substrates. K_D was calculated using three independent FP measurements (± SEM) in Prism v.9.0 (GraphPad). – indicates experiment has not been completed.

DNA substrate	ImuA	$ImuA_{C\Delta53}$	$ImuB_{N\Delta34}$
20 nt	0.50 (±0.12)	-	0.00
30 nt	0.30 (±0.03)	0.58 (±0.04)	2.78 (±0.41)
40 nt	0.42 (±0.04)	0.56 (±0.08)	0.41 (±0.02)
20 bp	0.00	-	4.41 (±1.09)
30 bp	3.43 (±0.97)	0.58 (±0.14)	4.83 (±1.07)
40 bp	2.18 (±0.25)	1.24 (±0.33)	2.03 (±0.34)
3’ overhang	0.18 (±0.01)	0.22 (±0.01)	0.20 (±0.01)
5’ overhang	0.71 (±0.04)	0.66 (±0.04)	0.66 (±0.07)
forked	0.71 (±0.07)	-	0.15 (±0.05)
bubble	0.77 (±0.09)	-	2.07 (±0.13)

Table 11. BAC2H testing of interactions between ImuB and ImuA or ImuC. Interactions induced with 0.1 or 0.5 mM IPTG and indicated by Y. ImuA and ImuC were fused to T25 on either pKT25 (indicated by C) or pKNT25 (indicated by N). ImuB was fused to T25 on either pUT18 (indicated by N) or pUT18C (indicated by C).

ImuC N	ImuC C		ImuA N	ImuA C	ImuA CΔ68 N	ImuA CΔ68 C	ImuA NΔ159 N	ImuA NΔ159 C	ImuA NΔ222 N	ImuA NΔ222 C
n	n	ImuB C	**Y**	n	n	n	n	n	n	n
n	n	ImuB N	n	n	n	n	n	n	n	n
n	n	$ImuB_{N\Delta300}$ C	**Y**	n	n	n	n	n	n	n
n	n	$ImuB_{N\Delta300}$ N	**Y**	n	n	n	n	n	n	**Y**
n	n	$ImuB_{N\Delta320}$ C	**Y**	n	n	n	n	n	n	**Y**
n	n	$ImuB_{N\Delta320}$ N	n	n	n	n	n	n	n	n
n	n	$ImuB_{N\Delta338}$ C	**Y**	n	n	n	n	n	n	n
n	n	$ImuB_{N\Delta338}$ N	**Y**	n	n	n	n	**Y**	n	**Y**
n	n	$ImuB_{C\Delta160}$ C	n	n	n	n	n	n	n	n
n	n	$ImuB_{C\Delta160}$ N	n	n	n	n	n	n	n	n
n	n	$ImuB_{C\Delta136}$ C	**Y**	**Y**	n	n	n	n	n	n
n	n	$ImuB_{C\Delta136}$ N	n	n	n	n	n	n	n	n
Y	n	$ImuB_{C\Delta81}$ C	n	n	n	n	n	n	n	n
n	n	$ImuB_{C\Delta81}$ N	n	n	n	n	n	n	n	n

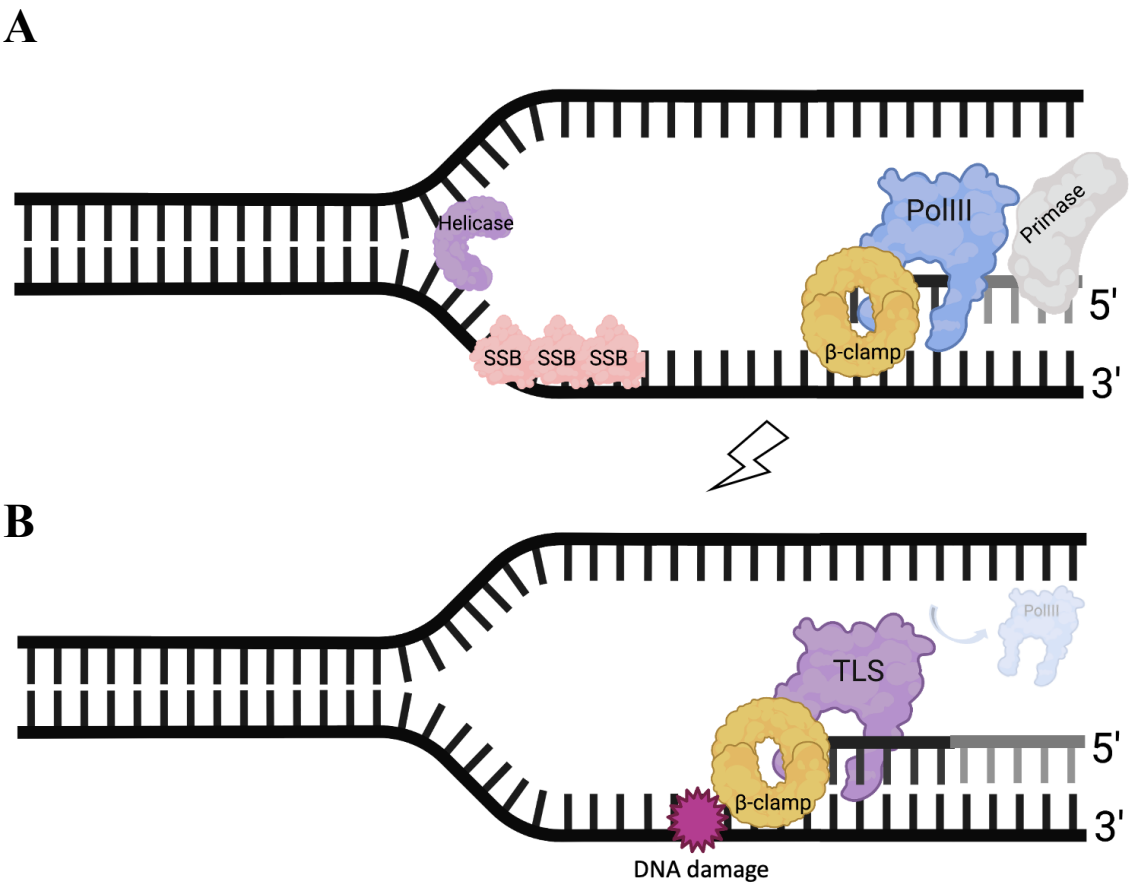

Figure 1. DNA replication in bacteria. A. DNA replication uses Pol III to synthesize DNA in a 5'-3' direction (Oakley, 2019; O'Donnell, 2006). **B.** DNA damage bypass during replication stall. Upon PolIII encountering unrepaired DNA damage, the replication fork becomes stalled. TLS polymerase switches for PolIII to bypass the damage (Freidberg et al., 2005; Waters et al., 2009). Created using Biorender.com**.**

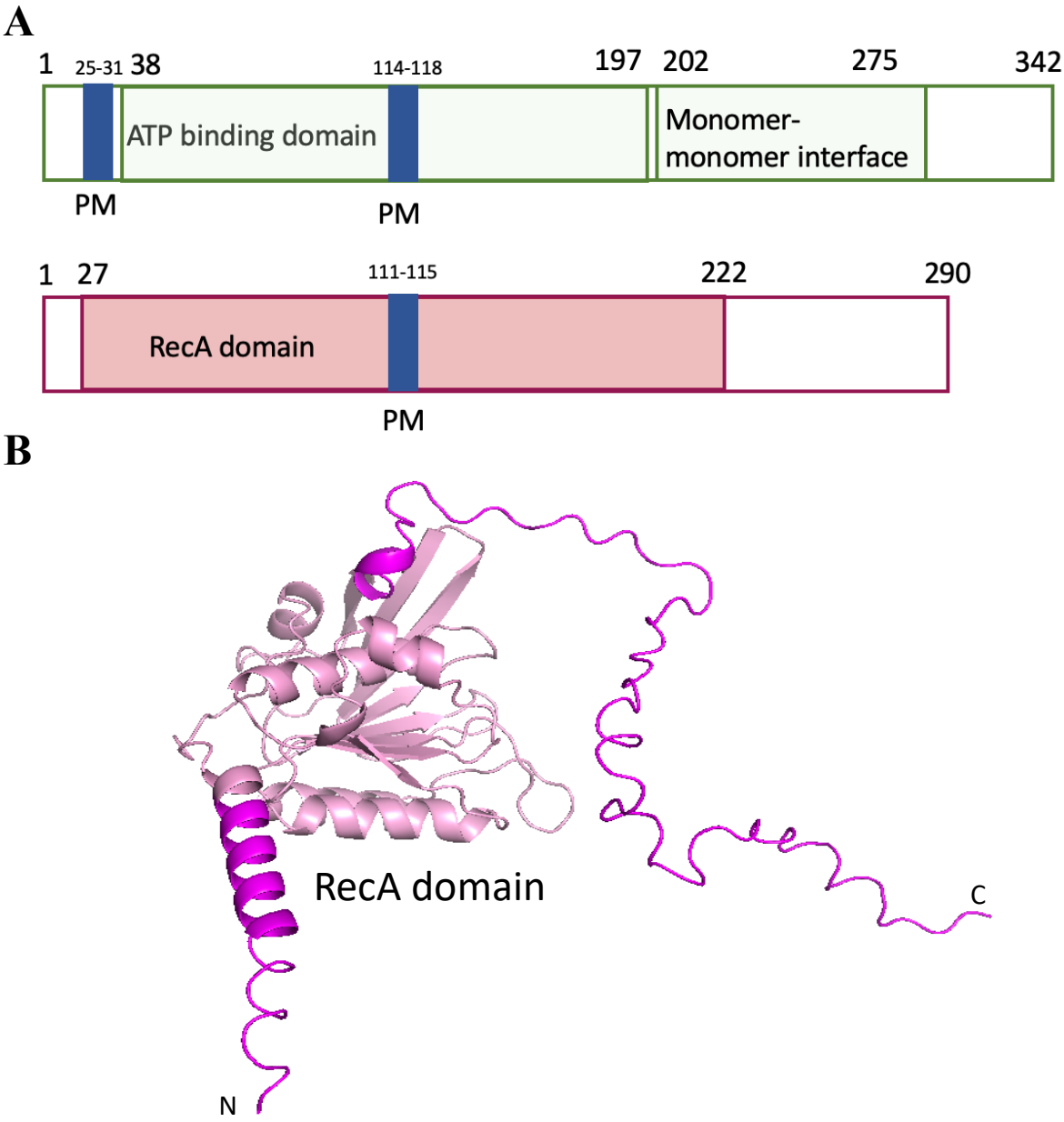

Figure 2. *M. xanthus* ImuA structure predictions. A. Secondary structure prediction of RecA, green, and ImuA, pink, using InterPro (https://www.ebi.ac.uk/interpro/). ATP binding domain (IPR020588), monomer-monomer interface (IPR020587), RecA domain (IPR013765). PM domains indicated in blue: RecA: $25^{GSVMTLG}31$ and $114^{EELLV}118$; ImuA: $111^{ERLLI}115$ (Sheng et al., 2021). **B.** ImuA structure prediction using Alphafold. RecA domain in light pink. N and C-termini marked by N and C, respectively. Created using Pymol.

.

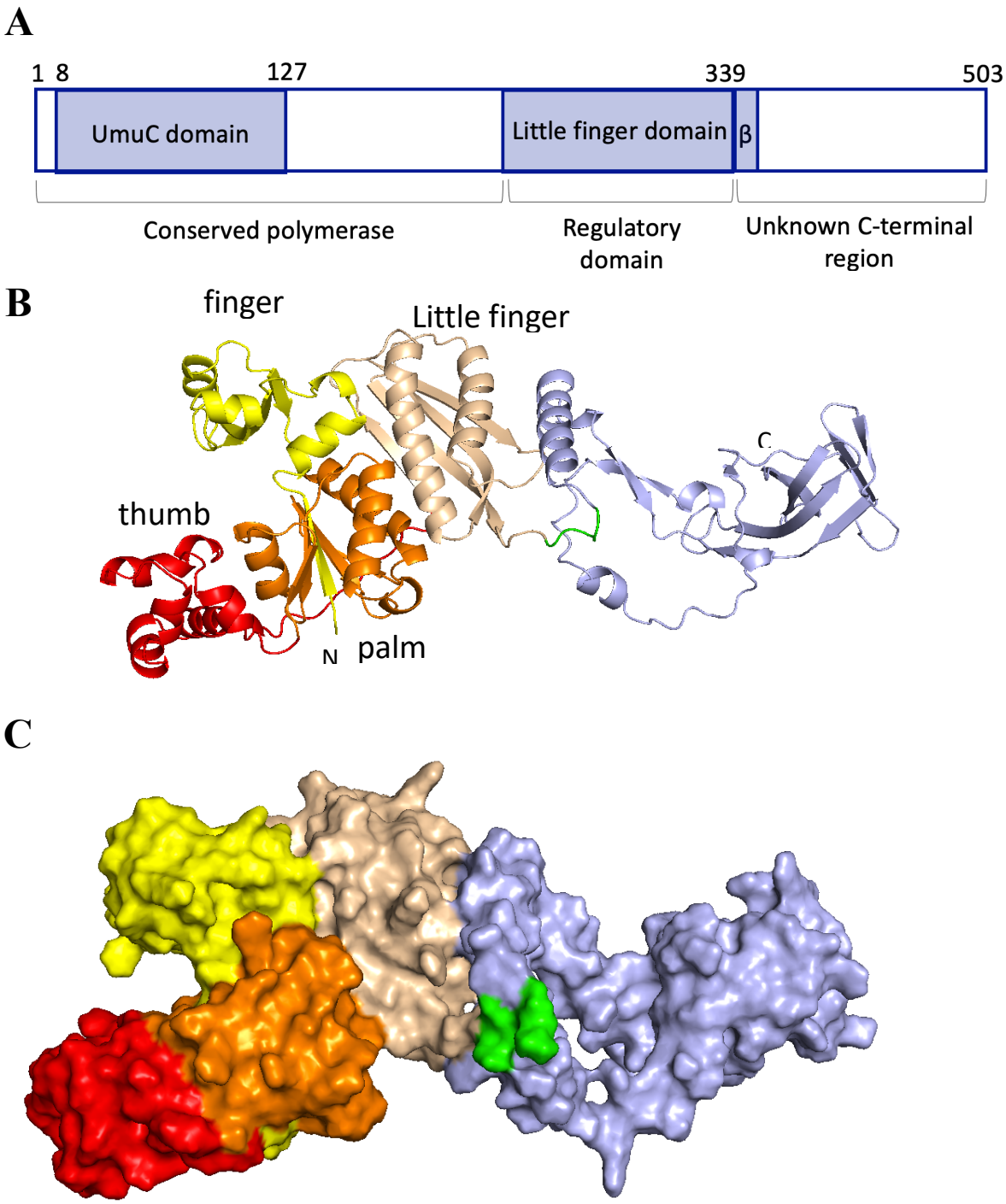

Figure 3. *M. xanthus* ImuB structure prediction. A. Secondary structure prediction of ImuB using InterPro (https://www.ebi.ac.uk/interpro/). UmuC domain (IPR001126), little finger domain (IPR01796). β indicates β-clamp binding motif. Created using Biorender.com **B.** Predicted structure of ImuB using Alphafold, with polymerase structural domains noted. **C.** Predicted structure of ImuB surface model. Finger domain in yellow, palm domain in orange, thumb domain in red, β-clamp–binding motif in green, C terminal region in purple. N and C-termini marked by N and C, respectively. Created using Pymol.

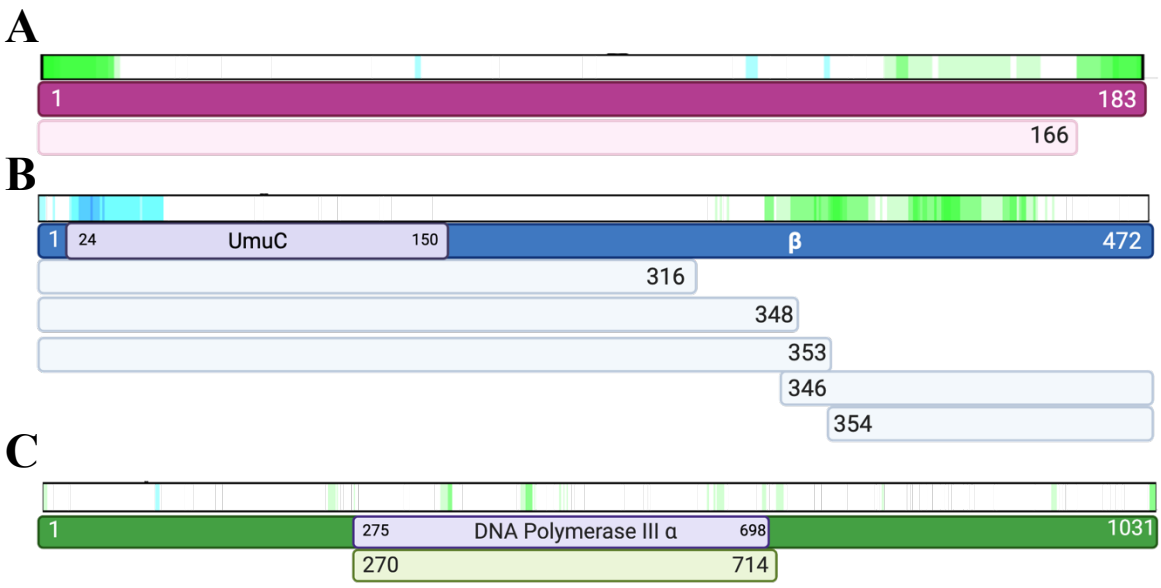

Figure 4. Predicted disorder of TLS proteins in *P. aeruginosa* and associated truncations designed for protein expression A. ImuA disorder prediction (top) and cloned construct (bottom) **B.** ImuB disorder prediction (top) and cloned constructs (bottom). β-sliding clamp binding motif, 349-353 aa, indicated by β. UmuC domain, (IPR001126) **C.** ImuC disorder prediction (top) and cloned construct (bottom). DNA Polymerase III alpha domain (IPR011708, IPR040982). For the disorder prediction: white – predicted structured protein; green and blue – predicted disordered protein. Disorder prediction analysis by D^2P^2. Secondary structure prediction using InterPro. Created using Biorender.com.

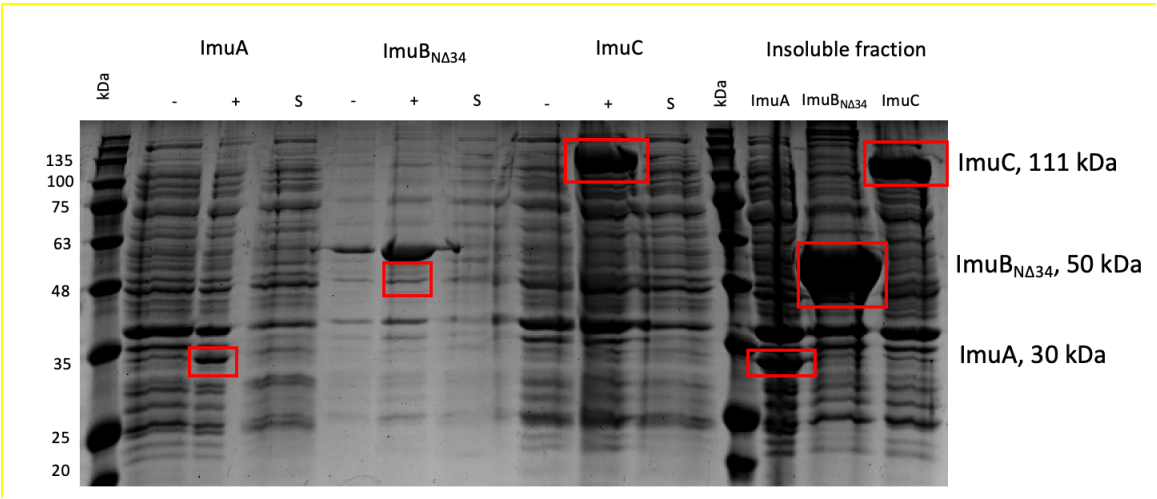

Figure 5. *M. xanthus* ImuABC proteins are insoluble in *E. coli* BL21 codon plus at 16 °C. (-): prior to IPTG induction, (+): after IPTG induction, S: soluble fraction. The 12% (w/v) SDS-PAGE gels were visualized using 0.1% (w/v) Coomassie stain.

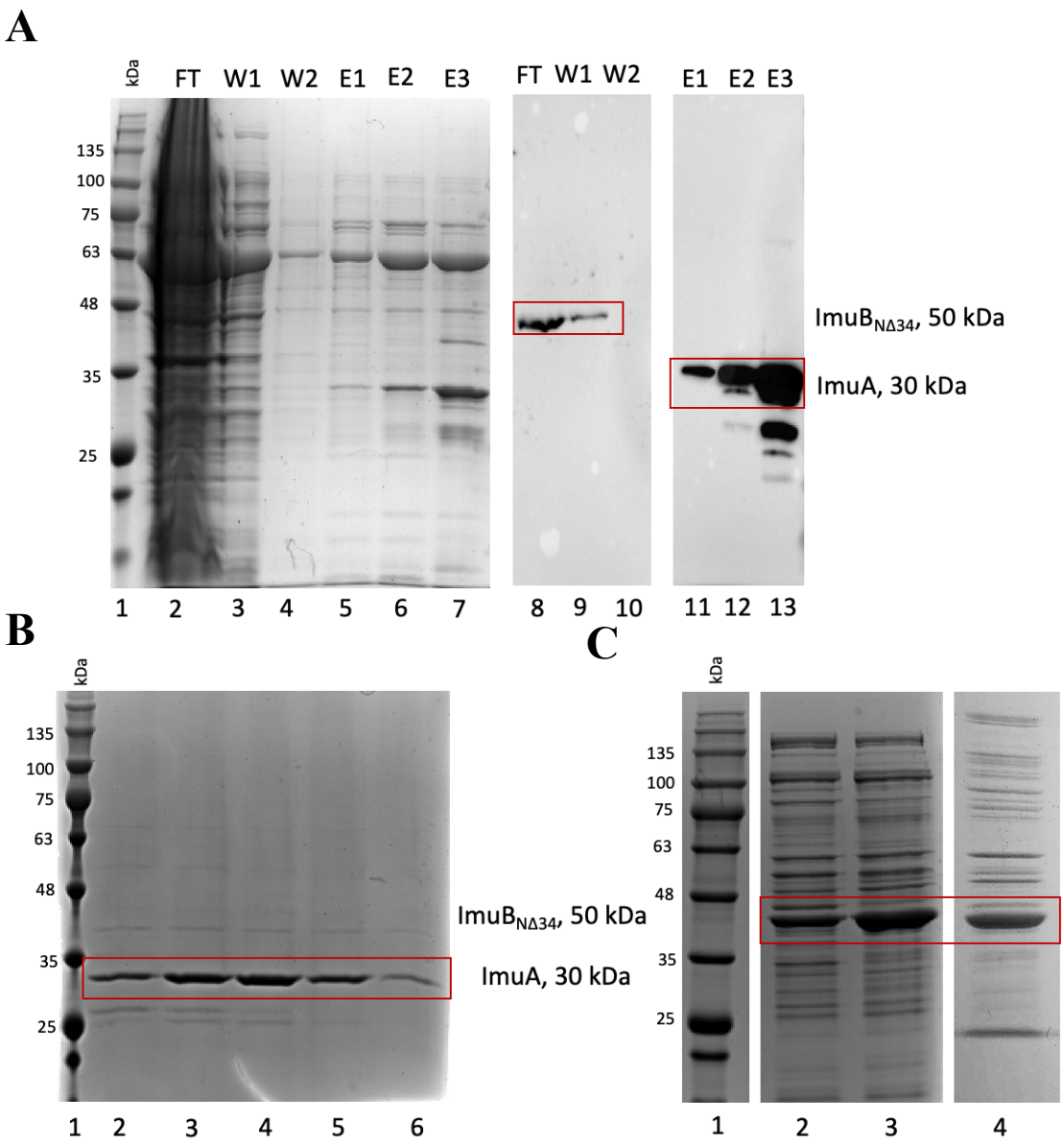

Figure 6. Purification of ImuA and ImuB$_{N\Delta34}$ from *E. coli* Artic Express A. Ni-NTA chromatography visualized on SDS-page gel (lanes 1-7) and confirmed via western blot (lanes 8-13). Lanes: 1: BluElf prestained protein ladder, 2,8: flowthrough, 3-4,9-10: washes, 5-7,11-13: elutions. **B.** Heparin affinity chromatography purification of ImuA. Lanes: 1: BluElf prestained protein ladder, 2-6: elution fractions over gradient of 550 mM NaCl to 650 mM NaCl. **C.** ImuB$_{N\Delta34}$ purification. Lanes: 1: BluElf prestained protein ladder, 2-3: Eluted fractions from heparin affinity chromatography (400 mM NaCl), 4: Eluted fractions from anion affinity chromatography (300 mM NaCl). The 12% (w/v) SDS-PAGE gels were visualized using 0.1% (w/v) Coomassie stain. Note: Gels have been cropped.

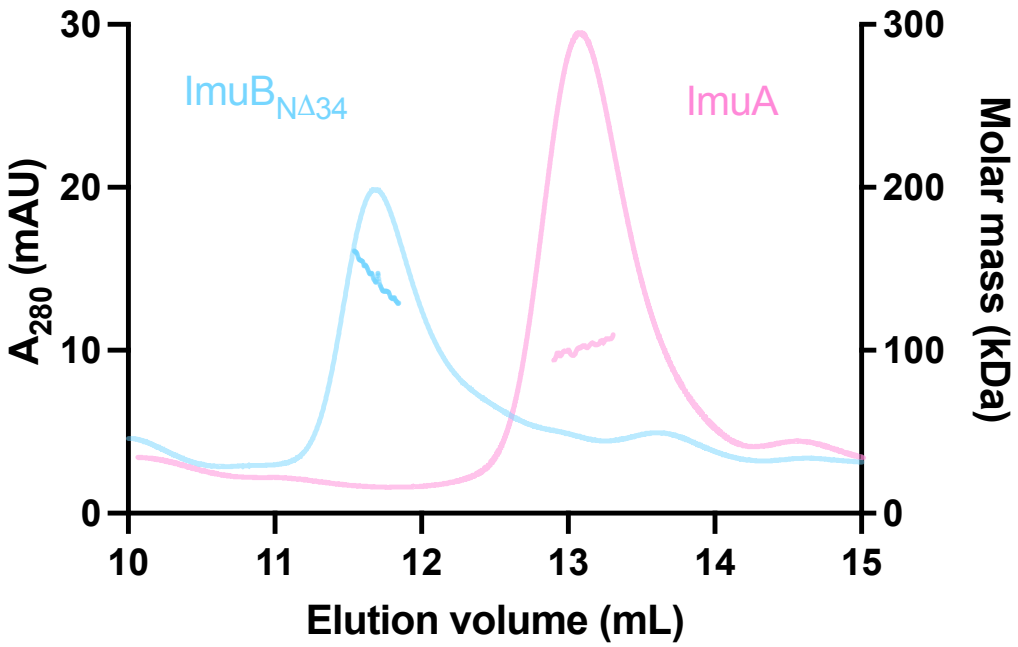

Figure 7. ImuA and ImuB$_{N\Delta34}$ are trimers in solution determined by SEC-MALS. Chromatogram and molar mass of ImuB$_{\Delta N34}$ (blue) and ImuA (pink). Elution of ImuB$_{N\Delta34}$ and ImuA seen at 11.75 mL and 13 mL, respectively. Experimental mass ImuB$_{N\Delta34}$ is 140.3 kDa (±1.904%). Theoretical mass: 50 kDa. Experimental mass ImuA is 100.9 kDa (±0.234%). Theoretical mass: 30 kDa. Data analysis was conducted using Astra software, version 7.3.1.9 (Wyatt Technology) and plotted in Prism v.9.0 (GraphPad).

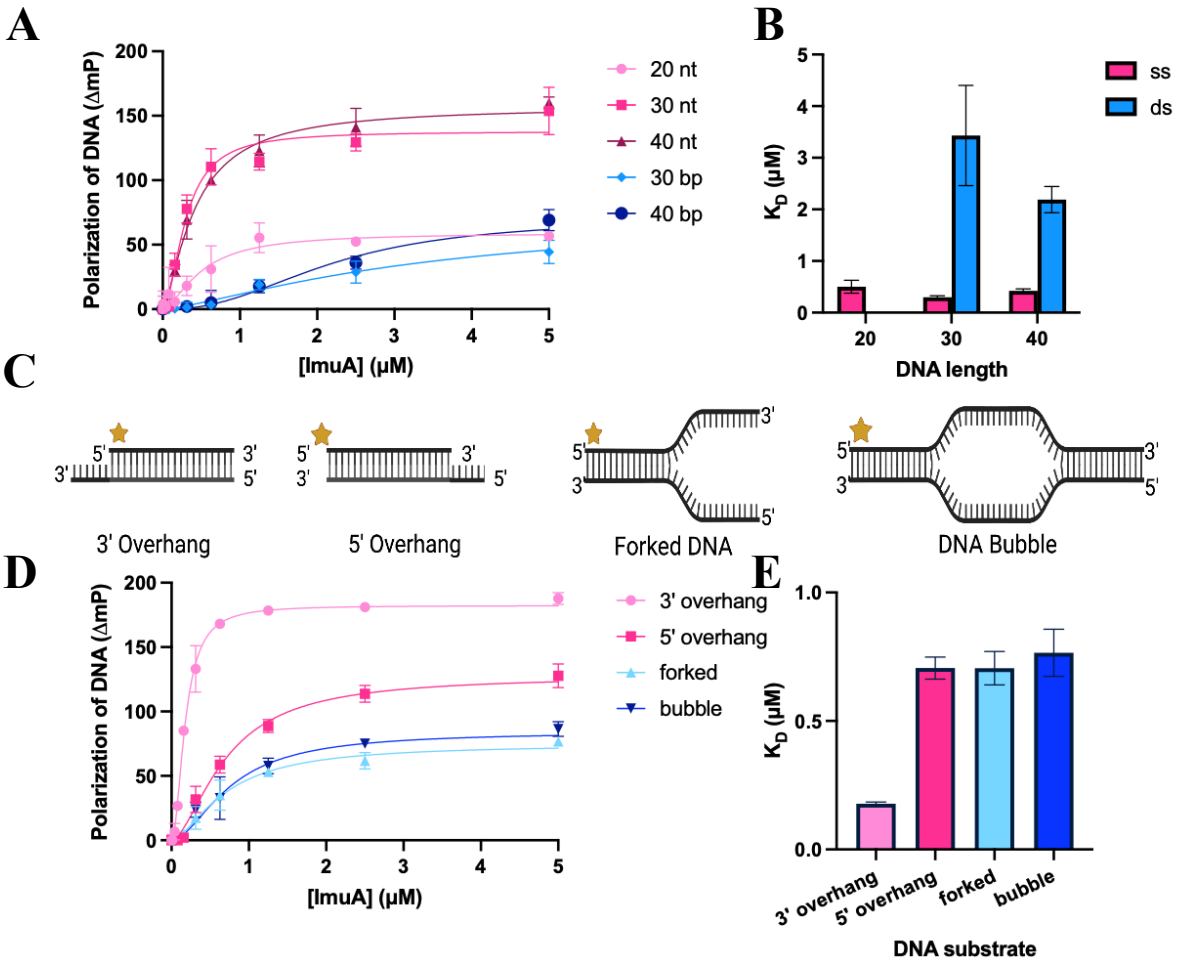

Figure 8. DNA binding of ImuA by FP. A. DNA binding curves of ImuA to different single or double stranded oligonucleotides. **B.** K_D values of ImuA binding to ssDNA or dsDNA. **C**. Schematic of DNA substrates mimicking DNA replication intermediates. Star indicates location 6-FAM label. Created using Biorender.com **D.** DNA binding curves of ImuA to DNA substrates mimicking DNA replication intermediates. **E.** K_D values of ImuA binding to DNA replication intermediates. Binding curves were constructed from three independent measurements (± SEM).

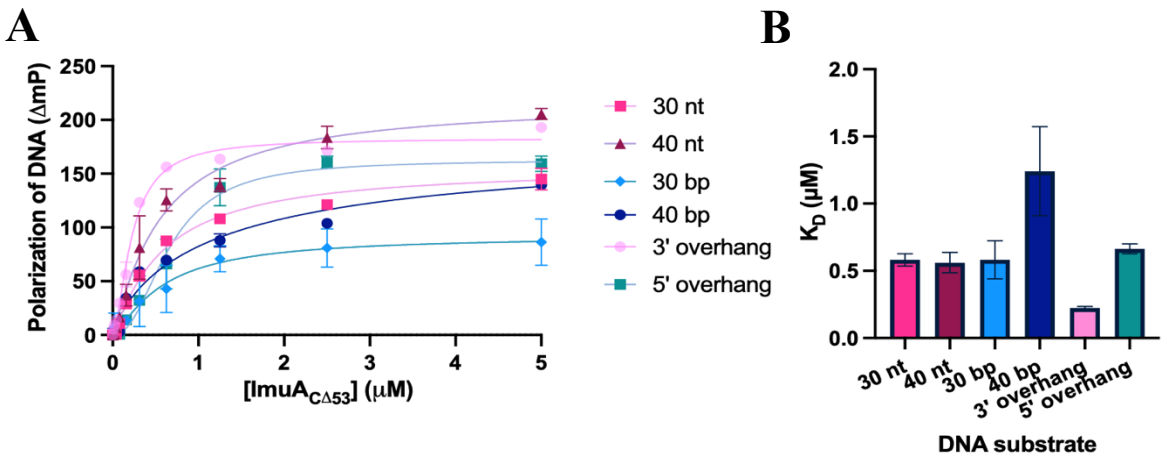

Figure 9. DNA binding of ImuA$_{CΔ53}$ by FP. A. DNA binding curves of ImuA$_{CΔ53}$ to different ssDNA, dsDNA oligonucleotides or DNA substrates mimicking DNA replication intermediates **B.** K_D values of ImuA$_{CΔ53}$ binding to ssDNA, dsDNA and DNA replication intermediates. Binding curves were constructed from three independent measurements (± SEM).

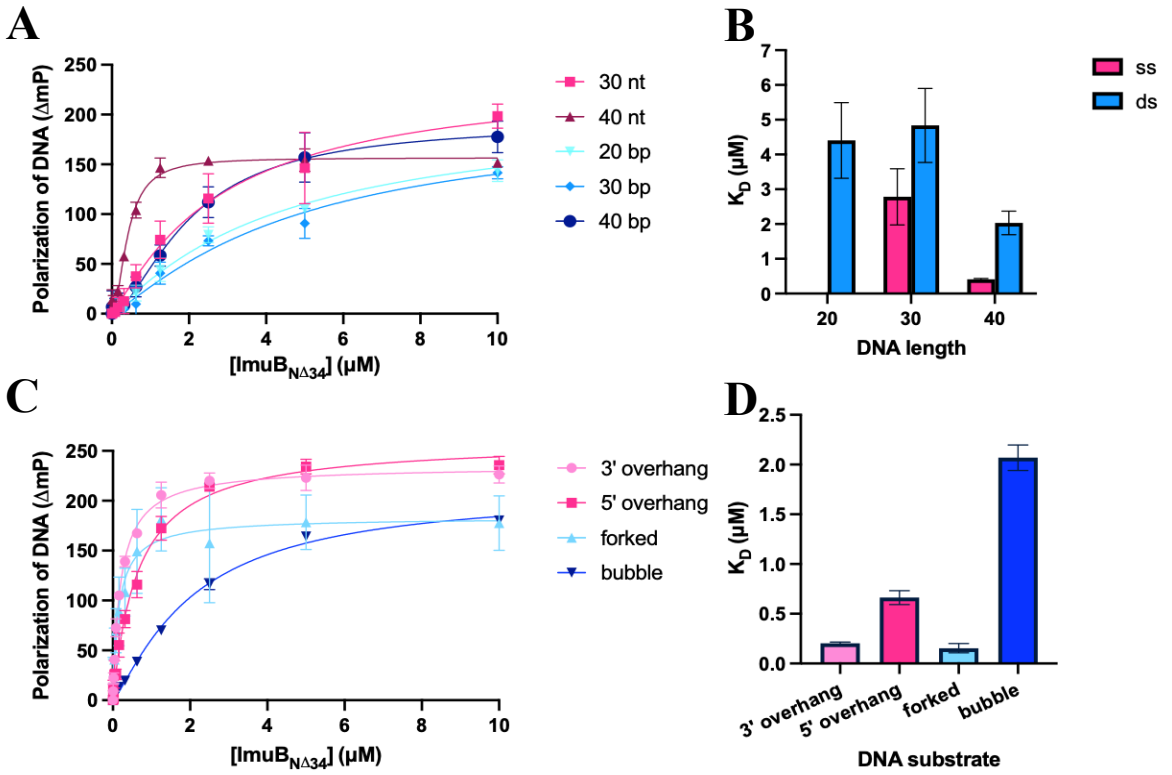

Figure 10. DNA binding of ImuB$_{NΔ34}$ by FP. A. DNA binding curves of ImuB$_{NΔ34}$ to different single or double stranded oligonucleotides. **B.** K_D values of ImuB$_{NΔ34}$ binding to ssDNA or dsDNA. **C**. DNA binding curves of ImuB$_{NΔ34}$ to DNA substrates mimicking DNA replication intermediates. **D**. K_D values of ImuB$_{NΔ34}$ binding to DNA replication intermediates. Binding curves were constructed from three independent measurements (± SEM).

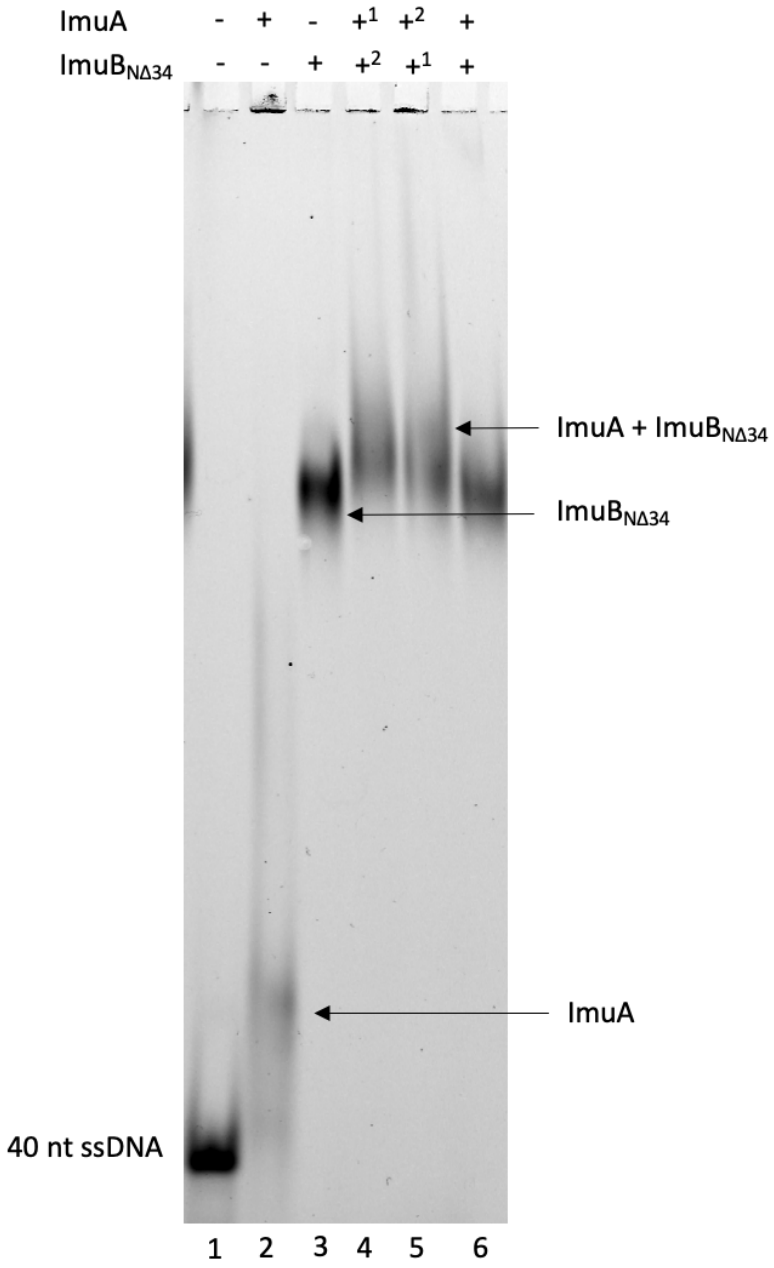

Figure 11. Complex formation of ImuA, ImuB$_{N\Delta34}$, and ssDNA. 40 nt ssDNA 6-FAM-labelled DNA substrate was pre-incubated either with nothing, one, or both proteins. ($+^1$) indicates which protein was added first, ($+^2$) indicates which protein was added second, (+) in lane 6 indicates proteins were added at the same time. Reactions were visualized on a 6% native polyacrylamide gel. Representative gel from three independent experiments.

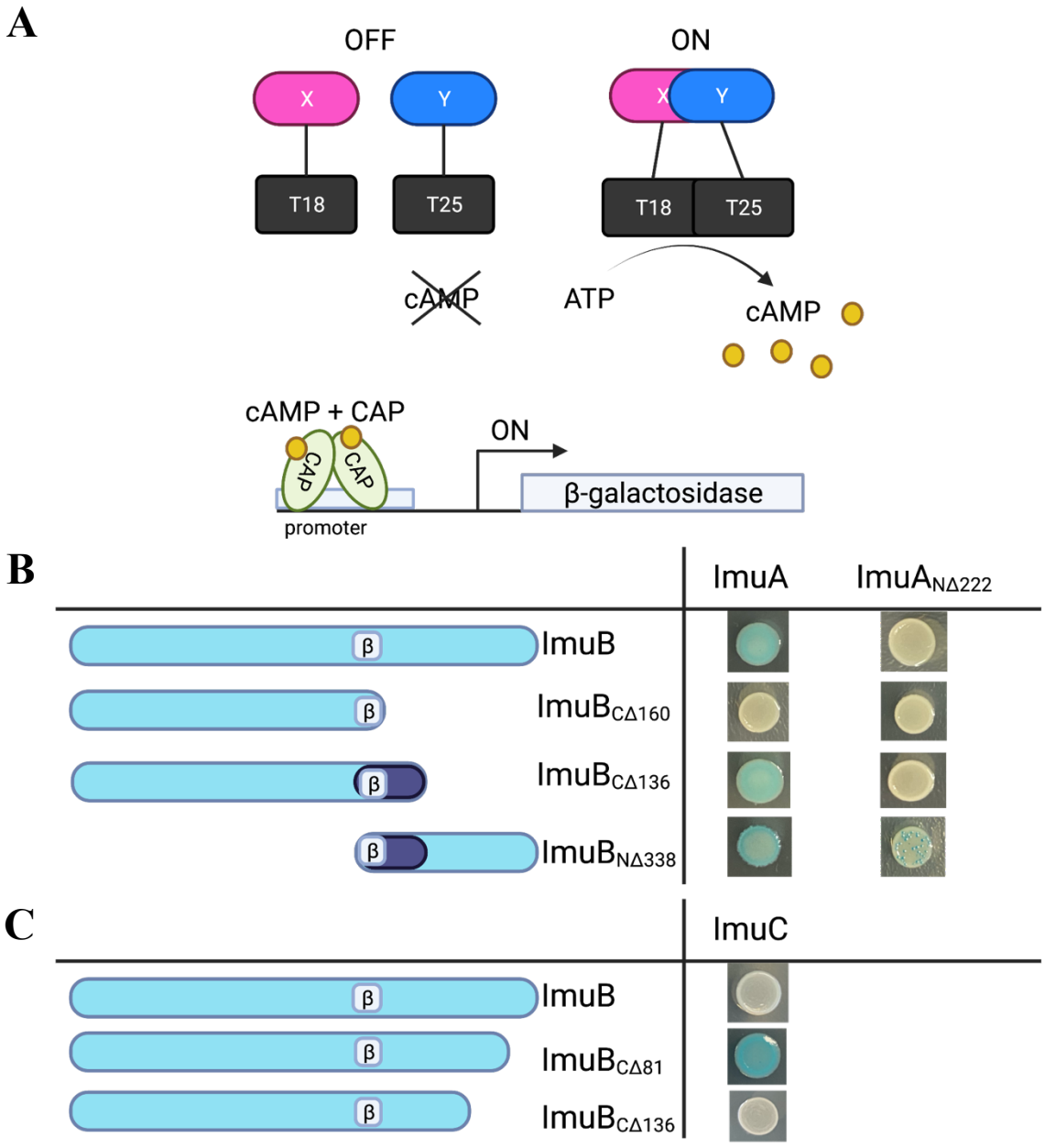

Figure 12. Identifying key Interactions between ImuA and ImuB using BAC2H. A. Schematic of BAC2H. If two proteins interact, the joining of T18 and T25 domains of *Bordetella* adenylate cyclase toxin results in cAMP synthesis, causing β-galactosidase to hydrolyze X-Gal and produce blue colonies of *E. coli* BTH101 on solid media (Battesti & Bouveret, 2012). **B.** ImuA and ImuB protein interactions. Purple area indicates region of interaction in ImuB. **C.** ImuC and ImuB protein interactions. β indicates β-clamp binding motif. Created using Biorender.com

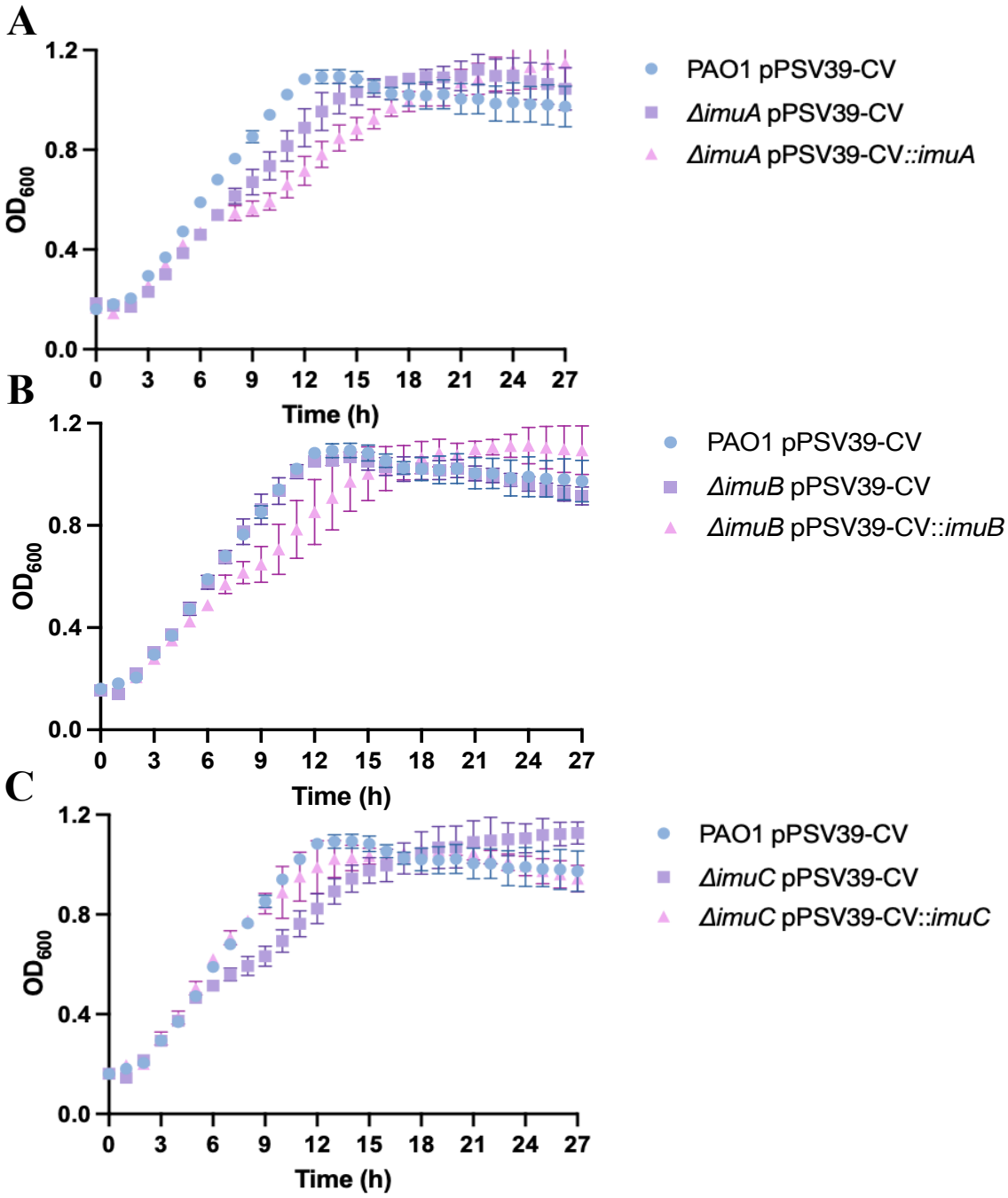

Figure 13. Individual gene deletions of ImuABC proteins do not affect *P. aeruginosa* growth at 30°C. Growth of PAO1 and **A.** *ΔimuA* **B.** *ΔimuB* **C.** *ΔimuC* gene deletions with complementation of respective genes. Data are presented as mean± standard deviation in n=3 replicates.

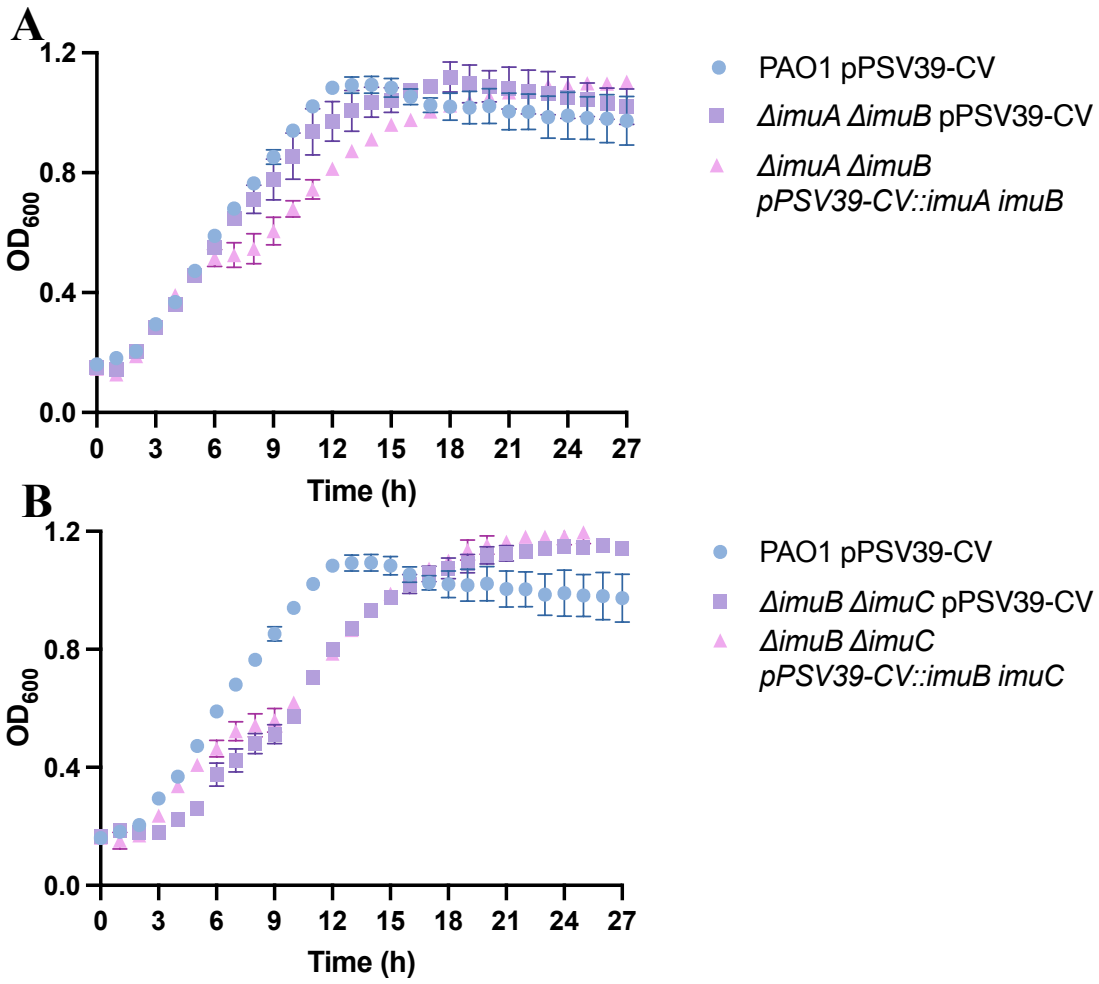

Figure 14. Double gene deletions of ImuABC proteins do not affect *P. aeruginosa* growth at 30°C. Growth of PAO1 and **A.** *ΔimuA ΔimuB* **B**. *ΔimuB ΔimuC* gene deletions with complementation of respective genes. Data are presented as mean± standard deviation in n=3 replicates.

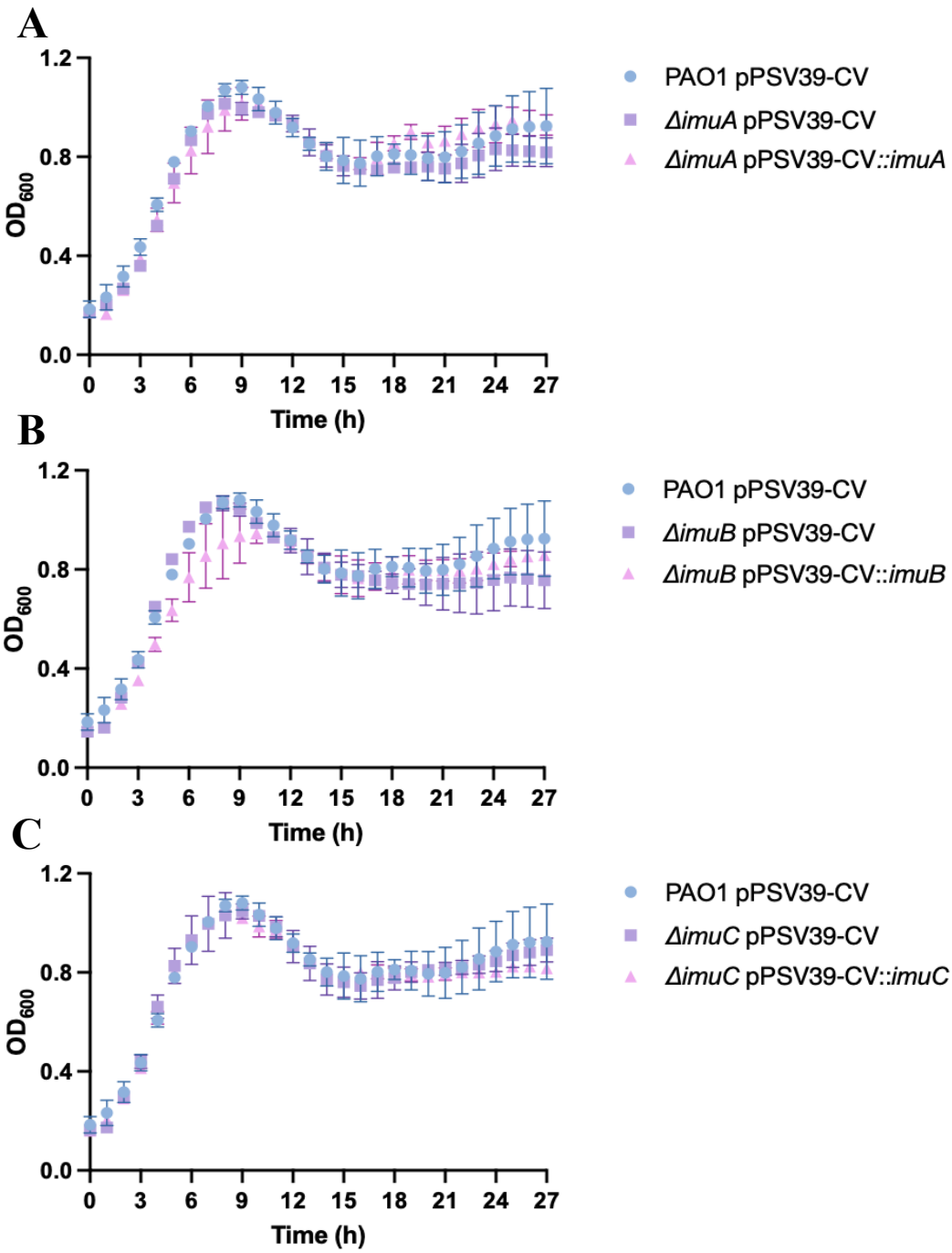

Figure 15. Individual gene deletions of ImuABC proteins do not affect *P. aeruginosa* growth at 37°C. Growth of PAO1 and **A.** *ΔimuA* **B.** *ΔimuB* **C**. *ΔimuC* gene deletions with complementation of respective genes. Data are presented as mean± standard deviation in n=3 replicates.

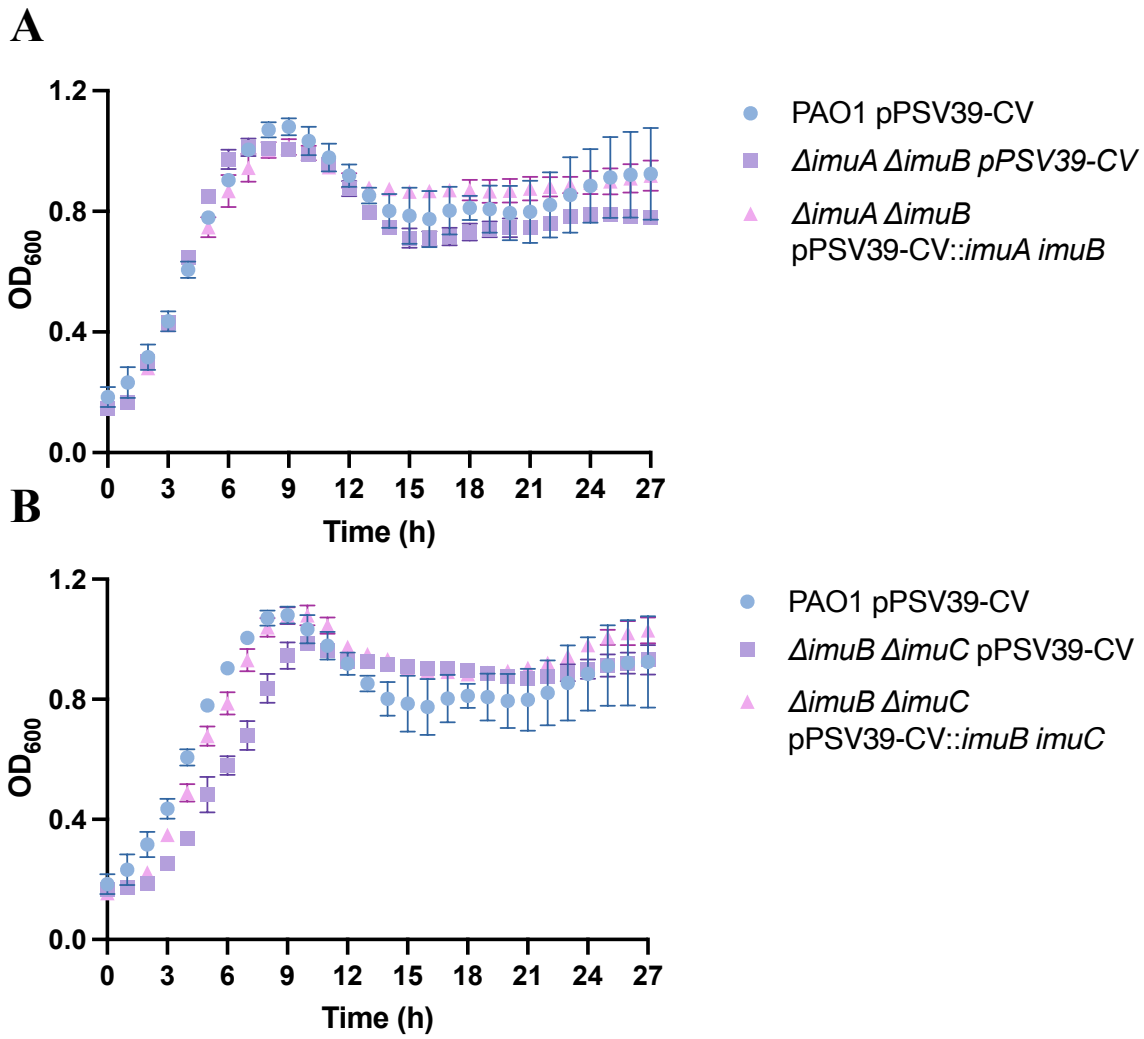

Figure 16. Double gene deletions of ImuABC proteins do not affect *P. aeruginosa* growth at 37 °C. Growth of PAO1 and **A**. *ΔimuA ΔimuB* **B.** *ΔimuB ΔimuC* gene deletions with complementation of respective genes. Data are presented as mean± standard deviation in n=3 replicates.

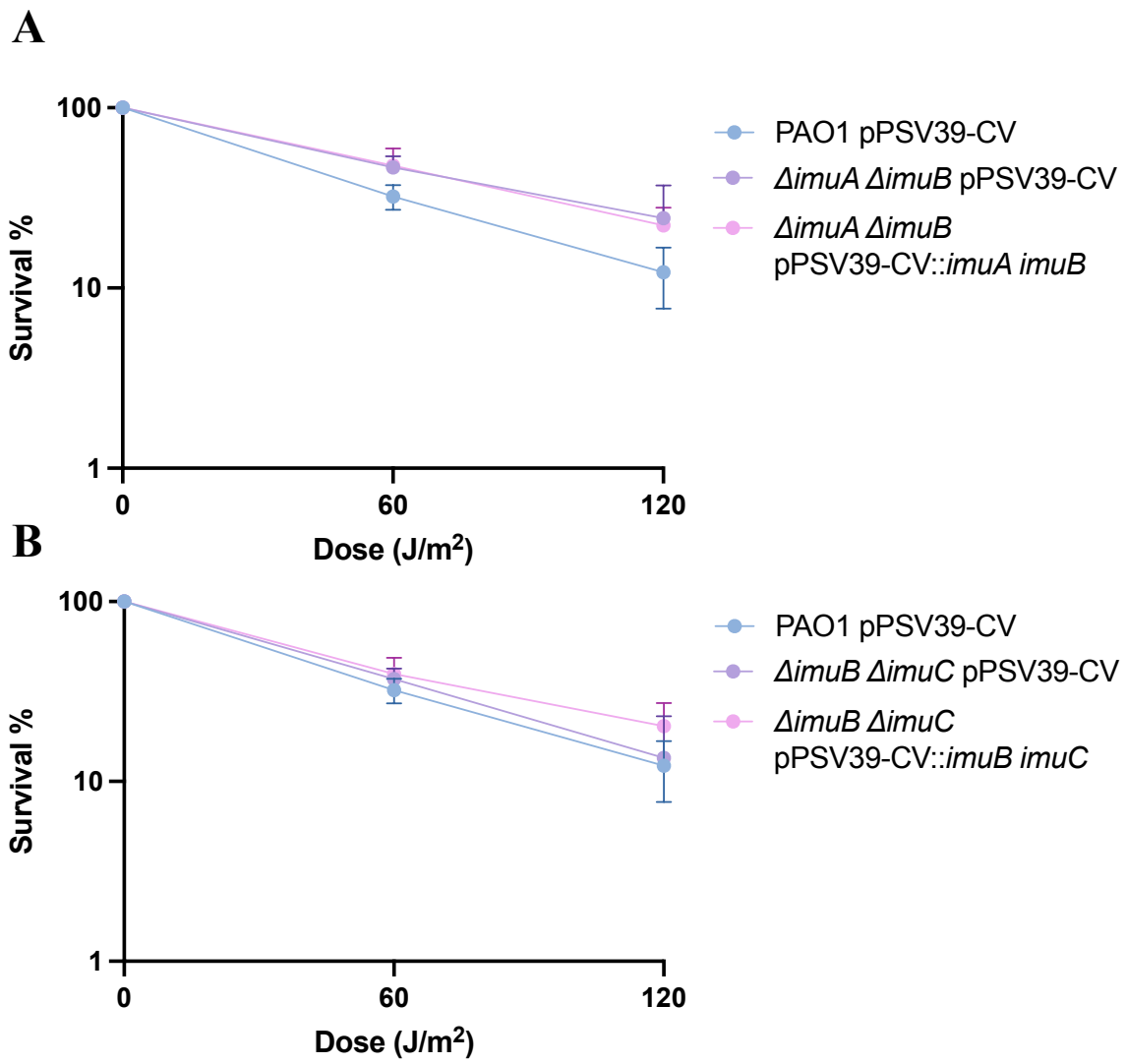

Figure 17. ImuABC are not involved UV irradiation survival in *P. aeruginosa*. Survival of **A.** *ΔimuA ΔimuB* **B**. *ΔimuB ΔimuC* gene deletions with complementation of respective genes. Data are presented as mean± SEM n=4+ separate experiments**.**

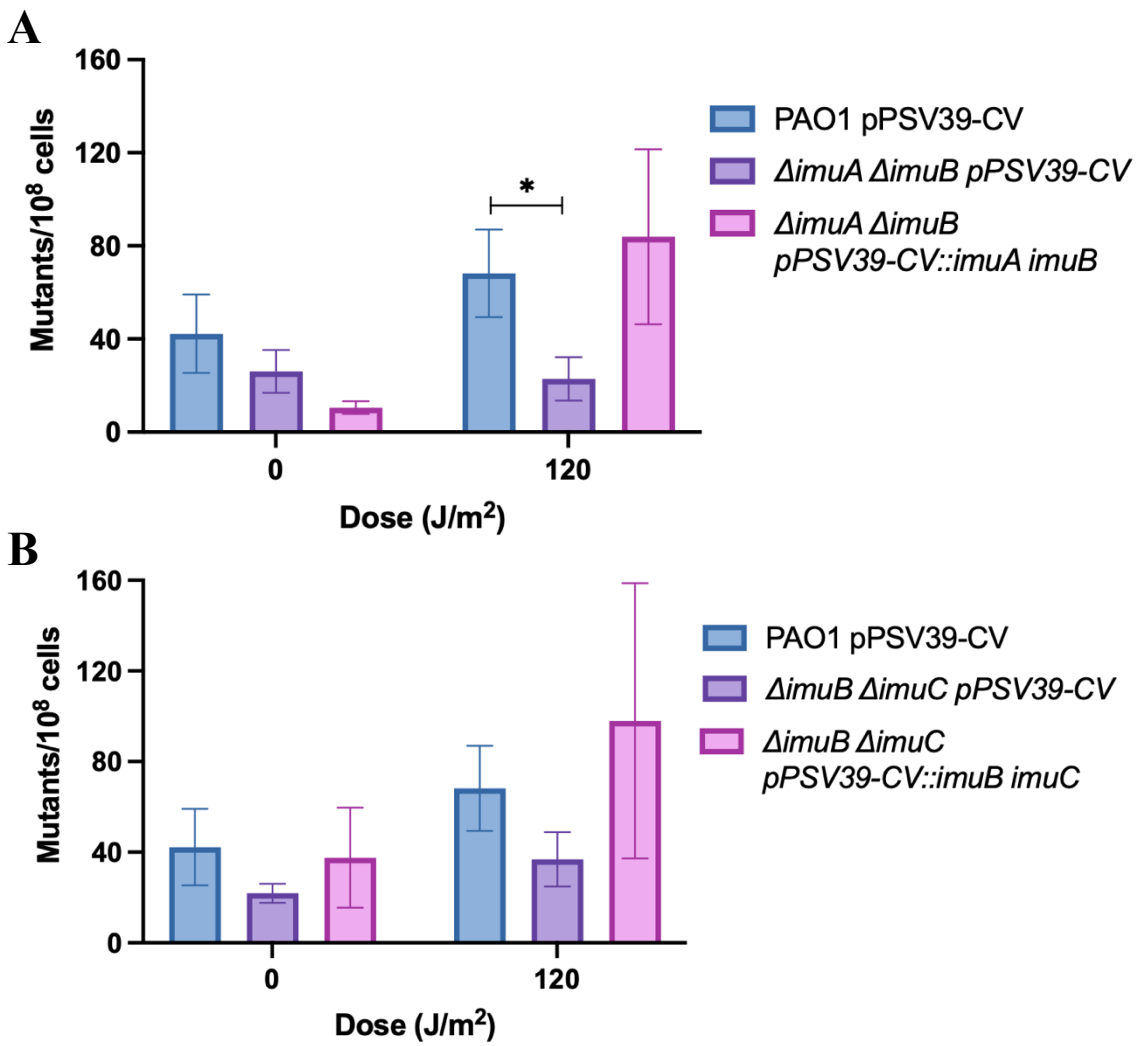

Figure 18. UV-induced mutagenesis in *P. aeruginosa* involves ImuABC. Mutagenesis results of **A.** *ΔimuA ΔimuB* **B.** *ΔimuB ΔimuC* gene deletions with complementation of respective genes. Data are presented as mean±SEM in n=4+ separate experiments. * represents $p<0.05$.

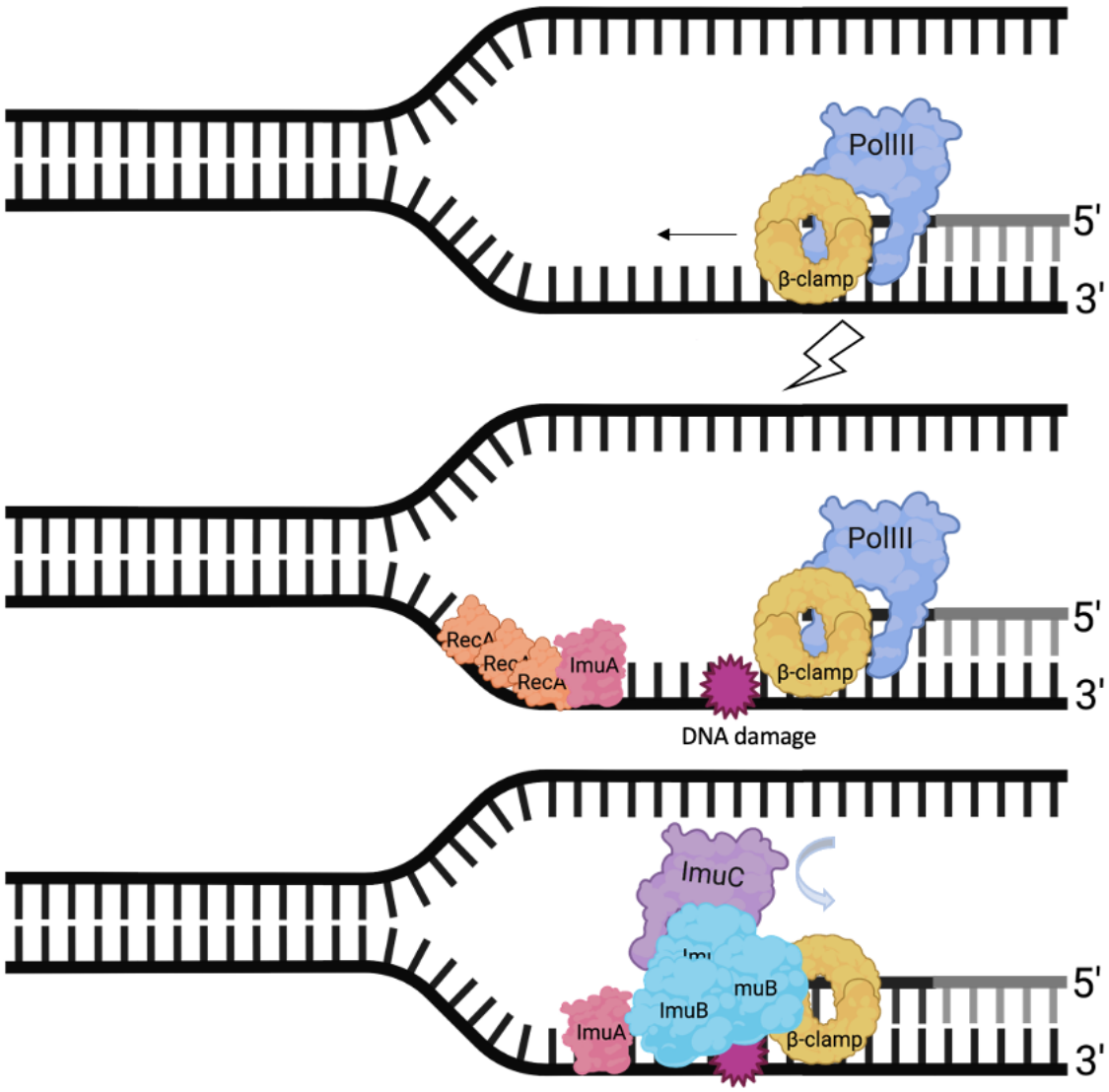

Figure 19. Hypothetical mechanism of ImuABC switching during DNA replication. DNA replication occurs with PolIII until a DNA lesion is encountered and the replication fork stalls. The accumulation of ssDNA activates the SOS response and transcription of the *imuA-imuB/imuC* gene cassette. ImuA binds to RecA and ssDNA, inhibiting error free pathways such as template switching. ImuB, acting as a trimer, is then able to bind to the ImuA, the β-clamp, and ImuC to tether ImuC closer to DNA. DNA damage bypass is then able to occur.

SUPPLEMENTAL

Table S1. Oligonucleotides used in this study. Underlined sequences indicate restriction enzyme recognition sites.

Oligonucleotide	Sequence (5'-3')	Restriction Enzyme
P. aeruginosa		
*imuA*_upstream_P1	TGT TAA GCT AAA GCT TGC CAG CGC TTC GTT GCG ATA AAG	HindIII
*imuA*_upstream_P2	TTC AGC ATG CTT GCG GCT CGA GTT CGG CAC GGC GGA CTG GCC	-
*imuA*_downstream_P1	AAC TCG AGC CGC AAG CAT GCT GAA GCC TGG CAA TGA GGC GGC C	-
*imuA*_downstream_P2	TGT TAA GCT ATC TAG ATG CAG CGC TGT CTC GTC CTC G	XbaI
*imuB*_upstream_P1	TGT TAA GCT AAA GCT TCA CTG CTA CCC GGC GGC G	HindIII
*imuB*_upstream_P2	TTC AGC ATG CTT GCG GCT CGA GTT CCA GAG CAT GGC CGC CTC	
*imuB*_downstream_P1	AAC TCG AGC CGC AAG CAT GCT GAA GCA TGA GCG CCT ACG CCG	
*imuB*_downstream_P2	TGT TAA GCT ATC TAG AAC GTC GCC GCA GGC CAC G	XbaI
*imuC*_upstream_P1	TGT TAA GCT AAA GCT TTG GAG CAT CAC GGG CGC GC	HindIII
*imuC*_upstream_P2	TTC AGC ATG CTT GCG GCT CGA GTT TGC AGC CAC AGC GGC CCC	-
*imuC*_downstream_P1	AAC TCG AGC CGC AAG CAT GCT GAA CAT TGA GAC AAA GAA AAA GGC AGC TCG	-
imuC_downstream_P2	TGT TAA GCT ATC TAG AAG GTG AAG TCG ACG AAC CGA AAG	XbaI
*imuA*_comp_P1	TCA ATC AGT ATC TAG ATC ATT GCC AGG CGC TGG CTG G	SacI
*imuA*_comp_P2	TGT TAA GCT AGA GCT CAC GGG AGG AAA GAG TGC CGG CCG GCG CTT CC	XbaI
*imuB*_comp_P1	TGT TAA GCT AGA GCT CAC GGG AGG AAA GAA TGC TCT GGG CTT GCA TTC TCC	SacI
*imuB*_comp_P2	TCA ATC AGT ATC TAG ATC ATG CGA ACC AGC CAT GCA GC	XbaI
*imuC*_comp_P1	TGT TAA GCT AGA GCT CAC GGG AGG AAA GAG TGG CTG CAT GGC TGG TTC G	SacI
*imuC*_comp_P2	TCA ATC AGT ATC TAG ATC AAT GGA AAT CCC GGC TGC GG	XbaI

*imuA*_F	TAC TTC CAA TCC AAT GCA ATG CCG GCC GGC GCT TCC C	
*imuA*_R	TTA TCC ACT TCC AAT G TTA TCA TCA TTG CCA GGC GCT GGC TG	
*imuB*_F	TAC TTC CAA TCC AAT GCA ATG CTC TGG GCT TGC ATT C	
*imuB*_R	TTA TCC ACT TCC AAT G TTA TCA TCA TGC GAA CCA GCC ATG	
*imuC*_F	TAC TTC CAA TCC AAT GCA ATG GCT GCA TGG CTG GTT C	
*imuC*_R	TTA TCC ACT TCC AAT G TTA TCA TCA ATG GAA ATC CCG GCT	
$imuA_{C\Delta 17}$_F	C ATC CTC AAG TAG CGG GGC GGC CTC GCG C	
$imuA_{C\Delta 17}$_R	CGC AGG CGT GGG GGG CGG	
$imuB_{C\Delta 156}$_F	T CTC GAA CAG TAG CAA CTG CCC GCC CC	
$imuB_{C\Delta 156}$_R	CGG CCG CGG GTC AGT TCG	
$imuB_{C\Delta 124}$_F	C GAG CGC CCA TAG CAG TAT CTC G	
$imuB_{C\Delta 124}$_R	TCG AAC AGT TCG CGG TGC	
$imuB_{C\Delta 118}$_F	G TAT CTC GGC TGA GAA CAG TTG CGG G	
$imuB_{C\Delta 118}$_F	TGC TGT GGG CGCT CGT CG	
$imuB_{N\Delta 345}$_F	TAC TTC CAA TCC AAT GAA ATG GAG CGC CCA CAG CAG TAT C	
$imuB_{N\Delta 353}$_F	TAC TTC CAA TCC AAT GAA ATG TGG GAA CAG TTG CGG GAA CG	
$imuC_{270\text{-}714}$_F	TAC TTC CAA TCC AAT GAA ATG CAC GAC CCG GCG TCA TGG C	
$imuC_{270\text{-}714}$_R	TTA TCC ACT TCC AAT G TTA TCA GCC TTT GAT CTG CTC GAA G	
M. xanthus		
*imuB*_Nterm_P1	TAC TTC CAA TCC AAT GAA ATG CGT CGC GCT TAT TTA CAC CTT AC	
*imuB*_Nterm_P2	CGA CGC TGA CCA CGC ACT GCT TC	
*imuB*_pet3a_P3	CGT GGT CAG CGT CGT GTT GCG TTT G	
*imuB*_pet3a_P4	TTA TCC ACT TCC AAT GTT ATC ATC GAA CAG GCC TTG CAG GTA AAA AC	
$imuA_{C\Delta 53}$_F	T GGC CGC CTC tag GAT GTT GCG G	
$imuA_{C\Delta 53}$_R	CCA CCC TCA AGG CCC AAG TC	
*imuA*_T25_F	TC AAT CAG TAT CTA GAG ATG TCA GCG GCA GAA CAA AGG GTA	XbaI
$imuA_{N\Delta 159}$_T25_F	TC AAT CAG TAT CTA GAG CGC CTT GCT GAA GCG CGT AAG	XbaI

imuA$_{N\Delta 223}$_T25_F	TC AAT CAG TAT CTA GAG TCT GCG CTG TAC CCG GCC TTG	XbaI
imuA$_{C\Delta 68}$_T25_R	TGT TAA GCT AGG TAC CCG TTA CCA CGG CAG TTC GGC TCT C	KpnI
imuA$_{C\Delta 68}$_T25_N_R	TGT TAA GCT AGG TAC CCG CCA CGG CAG TTC GGC TCT CG	KpnI
*imuA*_T25_R	TGT TAA GCT AGG TAC CCG TTA GTG TGC CGG CAG CGC CG	KpnI
*imuA*_T25_N_R	TGT TAA GCT AGG TAC CCG GTG TGC CGG CAG CGC CGC	KpnI
*imuB*_T18_F	TC AAT CAG TAT CTA GAG ATG CGT CGC GCT TAT TTA CAC CTT	XbaI
imuB$_{N\Delta 300}$_T18C_F	TC AAT CAG TAT CTA GAG CGT GCG AAA CTG CTG CAC GAA	XbaI
imuB$_{N\Delta 320}$_T18_F	TC AAT CAG TAT CTA GAG CCG GTT GCG GAA GTG AGC G	XbaI
imuB$_{N\Delta 338}$_T18_F	TC AAT CAG TAT CTA GAG CAA CTG GCG CTG GGT GAT GC	XbaI
*imuB*_T18_R	TGT TAA GCT AGG TAC CCG TTA ATC GAA CAG GCC TTG CAG GTA	KpnI
*imuB*_T18_N_R	TGT TAA GCT AGG TAC CCG ATC GAA CAG GCC TTG CAG GTA AAA	KpnI
imuB$_{C\Delta 160}$_T18_N_R	TGT TAA GCT AGG TAC CCG ACC CAG CGC CAG TTG CTG G	KpnI
imuB$_{C\Delta 160}$_T18_R	TGT TAA GCT AGG TAC CCG TTA ACC CAG CGC CAG TTG CTG G	KpnI
imuB$_{C\Delta 136}$_T18_N_R	TGT TAA GCT AGG TAC CCG GCT CGC TTC ACC CAG GGT G	KpnI
imuB$_{C\Delta 136}$_T18_R	TGT TAA GCT AGG TAC CCG TTA GCT CGC TTC ACC CAG GGT G	KpnI
imuB$_{C\Delta 81}$_T18_N_R	TGT TAA GCT AGG TAC CCG CAG ACG GCT CGG ACG TTC AC	KpnI
imuB$_{C\Delta 81}$_T18_R	TGT TAA GCT AGG TAC CCG TTA CAG ACG GCT CGG ACG TTC	KpnI
*imuC*_T25_F	TC AAT CAG TAT CTA GAG ATG GAT TAT GCT GAA CTA GTA TGT	XbaI
*imuC*_T25_R	TG TTA AGC TAC CCG GGC TTA ACC CGG CAG TGT ACC A	SmaI
*imuC*_T25_N_R	TG TTA AGC TAC CCG GGC ACC CGG CAG TGT ACC AC	SmaI

Table S2. DNA substrates used in this study.

Substrate	Sequence (5'-3', followed by 3'-5')
forked	6-FAM/AGC AGG AGG TGG CGT CGG GTG GAC GGG TGG ATT GAA ATT TAG GCT GGC ACG GTC G AGG TCT CGA CTA ACT CTA GTC GTT GTT CCA CCC GTC CAC CCG ACG CCA CCT CCT G
helicase	6-FAM/AGC CCT GCT GCC GAC CAA CGA AGG T TTT TTT TTT TTT TTT TTT TTC GGG ACG ACG
3' overhang	6-FAM/AGC CCT GCT GCC GAC CAA CGA AGG T ACC TTC GTT GGT CGG CAG CAG GGC TTTTTTTTTTTTTTTTTT
5' overhang	6-FAM/AGC CCT GCT GCC GAC CAA CGA AGG T TTT TTT TTT TTT TTT TTT TTA CCT TCG TTG GTC GGC AGC AGG GC

Table S3. Plasmids used in this study. s

Plasmids	Description	Source
P. aeruginosa		
pMCSG7	expression vector containing N-His_6-tag and Amp^R	Addgene
pMCSG10	expression vector containing His_6-GST-TEV and Amp^R	Addgene
pMCSG10::*imuA*	expression vector containing *imuA**	This study
pMCSG7::*imuB*	expression vector containing *imuB**	This study
pMCSG10::*imuB*	expression vector containing *imuB**	This study
pMCSG7::*imuC*	expression vector containing *imuC*	This study
pMCSG10::$imuA_{C\Delta 17}$	Expression vector with *imuA* C-terminal truncation	This study
pMCSG7::$imuB_{C\Delta 156}$	Expression vector with *imuB* C-terminal truncation	This study
pMCSG7::$imuB_{C\Delta 124}$	Expression vector with *imuB* C-terminal truncation excluding β-clamp motif	This study
pMCSG7::$imuB_{C\Delta 118}$	Expression vector with *imuB* C-terminal truncation including β-clamp motif	This study
pMCSG7::$imuB_{N\Delta 345}$	Expression vector with *imuB* N-terminal truncation excluding β-clamp motif	This study
pMCSG7::$imuB_{N\Delta 353}$	Expression vector with *imuB* N-terminal truncation including β-clamp motif	This study

pMCSG7::*imuC*$_{270\text{-}714}$	Expression vector with *imuC* DNA Polymerase III domain	This study
pEXG2	Allelic exchange vector containing *sacB* and Gm^R	(Rietsch et al., 2005)
pEXG2::ΔPA0671	pEXG2 containing DNA fragment for *imuA* deletion	This study
pEXG2:: ΔPA0670	pEXG2 containing DNA fragment for *imuB* deletion	This study
pEXG2::ΔPA0669	pEXG2 containing DNA fragment for *imuC* deletion	This study
pEXG2::ΔPA0671 ΔPA0670	pEXG2 containing DNA fragment for *imuA imuB* deletion	This study
pEXG2::ΔPA0670 ΔPA0669	pEXG2 containing DNA fragment for *imuB imuC* deletion	This study
pEXG2::ΔPA0671 ΔPA0670 ΔPA0669	pEXG2 containing DNA fragment for *imuA imuB imuC* deletion	This study
pPSV39-CV	Complementation/expression vector with lacI, lacUV5 promoter, C-terminal VSV-G tag, GmR	(Silverman et al., 2013).
pPSV39-CV::*imuA*	Complementation vector containing *imuA*	This study
pPSV39-CV::*imuB*	Complementation vector containing *imuB*	This study
pPSV39-CV::*imuC*	Complementation vector containing *imuC*	This study
pPSV39-CV::*imuA imuB*	Complementation vector containing *imuA imuB*	This study
pPSV39-CV::*imuB imuC*	Complementation vector containing *imuB imuC*	This study
pPSV39-CV::*imuA imuB imuC*	Complementation vector containing *imuA imuB imuC*	This study
M. xanthus		
pET-15b*::imuA*	Expression vector containing *imuA,* His_6-tag and Amp^R	Genscript
pET-15b*::imuA*$_{C\Delta 53}$	Expression vector containing *imuA*$_{\Delta C53,}$ His_6-tag and Amp^R	This study
pET-3a::*imuB*$_{N\Delta 34}$	Expression vector containing *imuB*$_{\Delta N34,}$ T7 tag, and Amp^R	Genscript
pMCSG7::*imuB*	Expression vector containing *imuB,* T7 tag, and Amp^R	This study
pET-28a(+)-TEV::*imuC*	Expression vector containing *imuC,* His_6-tag, and Kan^R	Genscript
pKT25::zip	BAC2H positive control, leucine zipper, Kan^R	Euromedex
pKT25	T25 fragment of adenylate cyclase, C-terminus, Kan^R	Euromedex

pKNT25	T25 fragment of adenylate cyclase, N-terminus, Kan^R	Euromedex
pUT18C::zip	BAC2H positive control, leucine zipper, Amp^R	Euromedex
pUT18	T18 fragment of adenylate cyclase, N-terminus, Amp^R	Euromedex
pUT18C	T18 fragment of adenylate cyclase, C-terminus, Amp^R	Euromedex
pKT25::*imuA*	*M. xanthus* WT *imuA* in pKT25, Kan^R	This study
pKNT25::*imuA*	*M. xanthus* WT *imuA* in pKNT25, Kan^R	This study
pKT25::$imuA_{C\Delta 68}$	*M. xanthus* $imuA_{C\Delta 68}$ in pKT25, Kan^R	This study
pKNT25::$imuA_{C\Delta 68}$	*M. xanthus* $imuA_{C\Delta 68}$ in pKNT25, Kan^R	This study
pKT25::$imuA_{N\Delta 159}$	*M. xanthus* $imuA_{N\Delta 159}$ in pKT25, Kan^R	This study
pKNT25::$imuA_{N\Delta 159}$	*M. xanthus* $imuA_{N\Delta 159}$ in pKNT25, Kan^R	This study
pKT25::$imuA_{N\Delta 222}$	*M. xanthus* $imuA_{N\Delta 222}$ in pKT25, Kan^R	This study
pKNT25::$imuA_{N\Delta 222}$	*M. xanthus* $imuA_{N\Delta 222}$ in pKNT25, Kan^R	This study
pKT25::*imuC*	*M. xanthus* WT *imuC* in pKT25, Kan^R	This study
pKNT25::*imuC*	*M. xanthus* WT *imuC* in pKNT25, Kan^R	This study
pUT18::*imuB*	*M. xanthus* WT *imuB* in pUT18, Amp^R	This study
pUT18C::*imuB*	*M. xanthus* WT *imuB* in pUT18C, Amp^R	This study
pUT18::$imuB_{C\Delta 160}$	*M. xanthus* $imuB_{C\Delta 160}$ in pUT18, Amp^R	This study
pUT18C::$imuB_{C\Delta 160}$	*M. xanthus* $imuB_{C\Delta 160}$ in pUT18C, Amp^R	This study
pUT18::$imuB_{C\Delta 136}$	*M. xanthus* $imuB_{C\Delta 136}$ in pUT18, Amp^R	This study
pUT18C::$imuB_{C\Delta 136}$	*M. xanthus* $imuB_{C\Delta 136}$ in pUT18C, Amp^R	This study
pUT18::$imuB_{C\Delta 81}$	*M. xanthus* $imuB_{C\Delta 81}$ in pUT18, Amp^R	This study
pUT18C::$imuB_{C\Delta 81}$	*M. xanthus* $imuB_{C\Delta 81}$ in pUT18C, Amp^R	This study
pUT18::$imuB_{N\Delta 300}$	*M. xanthus* $imuB_{N\Delta 300}$ in pUT18, Amp^R	This study
pUT18C::$imuB_{N\Delta 300}$	*M. xanthus* $imuB_{N\Delta 300}$ in pUT18C, Amp^R	This study
pUT18::$imuB_{N\Delta 320}$	*M. xanthus* $imuB_{N\Delta 320}$ in pUT18, Amp^R	This study
pUT18C::$imuB_{N\Delta 320}$	*M. xanthus* $imuB_{N\Delta 320}$ in pUT18C, Amp^R	This study
pUT18::$imuB_{N\Delta 338}$	*M. xanthus* $imuB_{N\Delta 338}$ in pUT18, Amp^R	This study
pUT18C::$imuB_{N\Delta 338}$	*M. xanthus* $imuB_{N\Delta 338}$ in pUT18C, Amp^R	This study

Table S4. Bacterial strains used in this study.

Strains	Description	Source
E. coli SM10 λpir	*thi-1 thr leu tonA lac Y supE recA*::RP4-2-Tc::Mu, pir, Km^R Allelic exchange strain	Biomedal
E. coli BHT101	F^-, cya-99, araD139, galE15, galK16, rpsL1, hsdR2, mcrA1, mcrB1, Str^R Bacterial two-hybrid strain	Euromedex

E. coli STBL3	F^- mcrB mrrhsdS20(rB-, mB-) recA13 supE44 ara-14 galK2 lacY1 proA2 rpsL20 xyl-5 λ-leumtl-1, Str^R Cloning strain	Invitrogen
E. coli Artic Express	F^- ompT hsdS(rB – mB –) dcm+ Tetr gal endA Hte [cpn10 cpn60] $Gent^R$ Protein expression at lower temperatures	Agilent
E. coli BL21	F^- ompT hsdSB (rB–, mB–) gal dcm Protein expression	Agilent
E. coli BL21 codon+	F^- ompT gal dcm lon hsdSB(rB− mB−) λ(DE3) pLysS, Cm^R Protein expression, extra tRNA genes	Agilent
E. coli BL21 star	F^- ompT hsdSB (rB–, mB–) gal dcm rne131Protein expression with enhanced mRNA stability	Invitrogen
E. coli SoluBL21	F^- ompT hsdSB (rB - mB -) gal dcm Protein expression from insoluble proteins	Genlantis
E. coli Rosetta	F^- ompT hsdSB(rB- mB-) gal dcm pRARE, Cam^R Eukaryotic protein expression for rare codons	Novagen
PAO1	Wildtype *Pseudomanonas aureginosa*	(Stover et al., 2000)
ΔPA0671	*imuA* deletion strain with empty pPSV39	This study
ΔPA0670	*imuB* deletion strain with empty pPSV39	This study
ΔPA0669	*imuC* deletion strain with empty pPSV39	This study
ΔPA0671 ΔPA0670	*imuA imuB* deletion strain with empty pPSV39	This study
ΔPA0670 ΔPA0669	*imuB imuC* deletion strain with empty pPSV39	This study
ΔPA0671 pPSV39-CV::*imuA*	*imuA* deletion strain with *imuA* expression vector	This study
ΔPA0670 pPSV39-CV::*imuB*	*imuB* deletion strain with *imuB* expression vector cic	This study
ΔPA0669 pPSV39-CV::*imuC*	*imuC* deletion strain with *imuC* expression vector	This study
ΔPA0671 ΔPA0670 pPSV39-CV::*imuA imuB*	*imuA* deletion strain with *imuA imuB* expression vector	This study
ΔPA0670 ΔPA0669 pPSV39-CV::*imuB imuC*	*imuA* deletion strain with *imuB imuC* expression vector	This study
PAO1 pPSV39-CV	Wildtype PAO1 with empty pPSV39	This study

SAB01	*E. coli* BH101 with pKT25::zip pUT18C::zip positive BAC2H control	This study
SAB02	*E. coli* BH101 with pKT25 and pUT18C negative BAC2H control	This study
SAB03	*E. coli* BH101 with pKNT25 and pUT18C negative BAC2H control	This study
SAB04	*E. coli* BH101 with pKT25 and pUT18 negative BAC2H control	This study
SAB05	*E. coli* BH101 with pKNT25 and pUT18 negative BAC2H control	This study
SAB06	*E. coli* BH101 with pKT25::*imuA* pUT18C::*imuB*	This study
SAB07	*E. coli* BH101 with pKNT25::*imuA* pUT18C::*imuB*	This study
SAB08	*E. coli* BH101 with pKT25::*imuA* pUT18::*imuB*	This study
SAB09	*E. coli* BH101 with pKNT25::*imuA* pUT18::*imuB*	This study
SAB10	*E. coli* BH101 with pKT25::*imuC* pUT18C::*imuB*	This study
SAB11	*E. coli* BH101 with pKNT25::*imuC* pUT18C::*imuB*	This study
SAB12	*E. coli* BH101 with pKT25::*imuC* pUT18::*imuB*	This study
SAB13	*E. coli* BH101 with pKNT25::*imuC* pUT18::*imuB*	This study
SAB14	*E. coli* BH101 with pKT25::*imuC* pUT18C::$imuB_{N\Delta 300}$	This study
SAB15	*E. coli* BH101 with pKT25::*imuC* pUT18::$imuB_{N\Delta 300}$	This study
SAB15	*E. coli* BH101 with pKT25::*imuC* pUT18C::$imuB_{N\Delta 321}$	This study
SAB16	*E. coli* BH101 with pKT25::*imuC* pUT18::$imuB_{N\Delta 321}$	This study
SAB17	*E. coli* BH101 with pKT25::*imuC* pUT18C::$imuB_{N\Delta 338}$	This study
SAB18	*E. coli* BH101 with pKT25::*imuC* pUT18::$imuB_{N\Delta 338}$	This study
SAB19	*E. coli* BH101 with pKNT25::*imuC* pUT18C::$imuB_{N\Delta 300}$	This study
SAB20	*E. coli* BH101 with pKNT25::*imuC* pUT18::$imuB_{N\Delta 300}$	This study
SAB21	*E. coli* BH101 with pKNT25::*imuC*	This study

	pUT18C::*imuB*$_{N\Delta 321}$	
SAB22	*E. coli* BH101 with pKNT25::*imuC* pUT18::*imuB*$_{N\Delta 321}$	This study
SAB23	*E. coli* BH101 with pKNT25::*imuC* pUT18C::*imuB*$_{N\Delta 338}$	This study
SAB24	*E. coli* BH101 with pKNT25::*imuC* pUT18::*imuB*$_{N\Delta 338}$	This study
SAB25	*E. coli* BH101 with pKT25::*imuC* pUT18C::*imuB*$_{C\Delta 160}$	This study
SAB26	*E. coli* BH101 with pKT25::*imuC* pUT18::*imuB*$_{C\Delta 160}$	This study
SAB27	*E. coli* BH101 with pKT25::*imuC* pUT18C::*imuB*$_{C\Delta 136}$	This study
SAB28	*E. coli* BH101 with pKT25::*imuC* pUT18::*imuB*$_{C\Delta 136}$	This study
SAB29	*E. coli* BH101 with pKT25::*imuC* pUT18C::*imuB*$_{C\Delta 81}$	This study
SAB30	*E. coli* BH101 with pKT25::*imuC* pUT18::*imuB*$_{C\Delta 81}$	This study
SAB31	*E. coli* BH101 with pKNT25::*imuC* pUT18C::*imuB*$_{C\Delta 160}$	This study
SAB32	*E. coli* BH101 with pKNT25::*imuC* pUT18::*imuB*$_{C\Delta 160}$	This study
SAB33	*E. coli* BH101 with pKNT25::*imuC* pUT18C::*imuB*$_{C\Delta 136}$	This study
SAB33	*E. coli* BH101 with pKNT25::*imuC* pUT18::*imuB*$_{C\Delta 136}$	This study
SAB34	*E. coli* BH101 with pKNT25::*imuC* pUT18C::*imuB*$_{C\Delta 81}$	This study
SAB35	*E. coli* BH101 with pKNT25::*imuC* pUT18::*imuB*$_{C\Delta 81}$	This study
SAB36	*E. coli* BH101 with pKT25::*imuA* pUT18C::*imuB*$_{N\Delta 300}$	This study
SAB37	*E. coli* BH101 with pKT25::*imuA* pUT18::*imuB*$_{N\Delta 300}$	This study
SAB38	*E. coli* BH101 with pKT25::*imuA* pUT18C::*imuB*$_{N\Delta 321}$	This study
SAB39	*E. coli* BH101 with pKT25::*imuA* pUT18::*imuB*$_{N\Delta 321}$	This study
SAB40	*E. coli* BH101 with pKT25::*imuA* pUT18C::*imuB*$_{N\Delta 338}$	This study
SAB41	*E. coli* BH101 with pKT25::*imuA* pUT18::*imuB*$_{N\Delta 338}$	This study

SAB42	*E. coli* BH101 with pKNT25::*imuA* pUT18C::*imuB*$_{N\Delta 300}$	This study
SAB43	*E. coli* BH101 with pKNT25::*imuA* pUT18::*imuB*$_{N\Delta 300}$	This study
SAB44	*E. coli* BH101 with pKNT25::*imuA* pUT18C::*imuB*$_{N\Delta 321}$	This study
SAB45	*E. coli* BH101 with pKNT25::*imuA* pUT18::*imuB*$_{N\Delta 321}$	This study
SAB46	*E. coli* BH101 with pKNT25::*imuA* pUT18C::*imuB*$_{N\Delta 338}$	This study
SAB47	*E. coli* BH101 with pKNT25::*imuA* pUT18::*imuB*$_{N\Delta 338}$	This study
SAB48	*E. coli* BH101 with pKT25::*imuA* pUT18C::*imuB*$_{C\Delta 160}$	This study
SAB49	*E. coli* BH101 with pKT25::*imuA* pUT18::*imuB*$_{C\Delta 160}$	This study
SAB50	*E. coli* BH101 with pKT25::*imuA* pUT18C::*imuB*$_{C\Delta 136}$	This study
SAB51	*E. coli* BH101 with pKT25::*imuA* pUT18::*imuB*$_{C\Delta 136}$	This study
SAB52	*E. coli* BH101 with pKT25::*imuA* pUT18C::*imuB*$_{C\Delta 81}$	This study
SAB53	*E. coli* BH101 with pKT25::*imuA* pUT18::*imuB*$_{C\Delta 81}$	This study
SAB54	*E. coli* BH101 with pKNT25::*imuA* pUT18C::*imuB*$_{C\Delta 160}$	This study
SAB55	*E. coli* BH101 with pKNT25::*imuA* pUT18::*imuB*$_{C\Delta 160}$	This study
SAB56	*E. coli* BH101 with pKNT25::*imuA* pUT18C::*imuB*$_{C\Delta 136}$	This study
SAB57	*E. coli* BH101 with pKNT25::*imuA* pUT18::*imuB*$_{C\Delta 136}$	This study
SAB58	*E. coli* BH101 with pKNT25::*imuA* pUT18C::*imuB*$_{C\Delta 81}$	This study
SAB59	*E. coli* BH101 with pKNT25::*imuA* pUT18::*imuB*$_{C\Delta 81}$	This study
SAB60	*E. coli* BH101 with pKT25::*imuA*$_{C\Delta 68}$ pUT18C::*imuB*$_{N\Delta 300}$	This study
SAB61	*E. coli* BH101 with pKT25::*imuA*$_{C\Delta 68}$ pUT18::*imuB*$_{N\Delta 300}$	This study
SAB62	*E. coli* BH101 with pKT25::*imuA*$_{C\Delta 68}$ pUT18C::*imuB*$_{N\Delta 321}$	This study
SAB63	*E. coli* BH101 with pKT25::*imuA*$_{C\Delta 68}$ pUT18::*imuB*$_{N\Delta 321}$	This study

SAB64	*E. coli* BH101 with pKT25::*imuA*$_{C\Delta 68}$ pUT18C::*imuB*$_{N\Delta 338}$	This study
SAB65	*E. coli* BH101 with pKT25::*imuA*$_{C\Delta 68}$ pUT18::*imuB*$_{N\Delta 338}$	This study
SAB66	*E. coli* BH101 with pKNT25::*imuA*$_{C\Delta 68}$ pUT18C::*imuB*$_{N\Delta 300}$	This study
SAB67	*E. coli* BH101 with pKNT25::*imuA*$_{C\Delta 68}$ pUT18::*imuB*$_{N\Delta 300}$	This study
SAB68	*E. coli* BH101 with pKNT25::*imuA*$_{C\Delta 68}$ pUT18C::*imuB*$_{N\Delta 321}$	This study
SAB69	*E. coli* BH101 with pKNT25::*imuA*$_{C\Delta 68}$ pUT18::*imuB*$_{N\Delta 321}$	This study
SAB70	*E. coli* BH101 with pKNT25::*imuA*$_{C\Delta 68}$ pUT18C::*imuB*$_{N\Delta 338}$	This study
SAB71	*E. coli* BH101 with pKNT25::*imuA*$_{C\Delta 68}$ pUT18::*imuB*$_{N\Delta 338}$	This study
SAB72	*E. coli* BH101 with pKT25::*imuA*$_{C\Delta 68}$ pUT18C::*imuB*$_{C\Delta 160}$	This study
SAB73	*E. coli* BH101 with pKT25::*imuA*$_{C\Delta 68}$ pUT18::*imuB*$_{C\Delta 160}$	This study
SAB74	*E. coli* BH101 with pKT25::*imuA*$_{C\Delta 68}$ pUT18C::*imuB*$_{C\Delta 136}$	This study
SAB75	*E. coli* BH101 with pKT25::*imuA*$_{C\Delta 68}$ pUT18::*imuB*$_{C\Delta 136}$	This study
SAB76	*E. coli* BH101 with pKT25::*imuA*$_{C\Delta 68}$ pUT18C::*imuB*$_{C\Delta 81}$	This study
SAB77	*E. coli* BH101 with pKT25::*imuA*$_{C\Delta 68}$ pUT18::*imuB*$_{C\Delta 81}$	This study
SAB78	*E. coli* BH101 with pKNT25::*imuA*$_{C\Delta 68}$ pUT18C::*imuB*$_{C\Delta 160}$	This study
SAB79	*E. coli* BH101 with pKNT25::*imuA*$_{C\Delta 68}$ pUT18::*imuB*$_{C\Delta 160}$	This study
SAB80	*E. coli* BH101 with pKNT25::*imuA*$_{C\Delta 68}$ pUT18C::*imuB*$_{C\Delta 136}$	This study
SAB81	*E. coli* BH101 with pKNT25::*imuA*$_{C\Delta 68}$ pUT18::*imuB*$_{C\Delta 136}$	This study
SAB82	*E. coli* BH101 with pKNT25::*imuA*$_{C\Delta 68}$ pUT18C::*imuB*$_{C\Delta 81}$	This study
SAB83	*E. coli* BH101 with pKNT25::*imuA*$_{C\Delta 68}$ pUT18::*imuB*$_{C\Delta 81}$	This study
SAB84	*E. coli* BH101 with pKT25::*imuA*$_{C\Delta 68}$ pUT18C::*imuB*	This study

SAB85	*E. coli* BH101 with pKNT25::*imuA*$_{C\Delta 68}$ pUT18C::*imuB*	This study
SAB86	*E. coli* BH101 with pKT25::*imuA*$_{C\Delta 68}$ pUT18::*imuB*	This study
SAB87	*E. coli* BH101 with pKNT25::*imuA*$_{C\Delta 68}$ pUT18::*imuB*	This study
SAB88	*E. coli* BH101 with pKT25::*imuA*$_{N\Delta 159}$ pUT18C::*imuB*$_{N\Delta 300}$	This study
SAB89	*E. coli* BH101 with pKT25::*imuA*$_{N\Delta 159}$ pUT18::*imuB*$_{N\Delta 300}$	This study
SAB90	*E. coli* BH101 with pKT25::*imuA*$_{N\Delta 159}$ pUT18C::*imuB*$_{N\Delta 321}$	This study
SAB91	*E. coli* BH101 with pKT25::*imuA*$_{N\Delta 159}$ pUT18::*imuB*$_{N\Delta 321}$	This study
SAB92	*E. coli* BH101 with pKT25::*imuA*$_{N\Delta 159}$ pUT18C::*imuB*$_{N\Delta 338}$	This study
SAB93	*E. coli* BH101 with pKT25::*imuA*$_{N\Delta 159}$ pUT18::*imuB*$_{N\Delta 338}$	This study
SAB94	*E. coli* BH101 with pKNT25::*imuA*$_{N\Delta 159}$ pUT18C::*imuB*$_{N\Delta 300}$	This study
SAB95	*E. coli* BH101 with pKNT25::*imuA*$_{N\Delta 159}$ pUT18::*imuB*$_{N\Delta 300}$	This study
SAB96	*E. coli* BH101 with pKNT25::*imuA*$_{N\Delta 159}$ pUT18C::*imuB*$_{N\Delta 321}$	This study
SAB97	*E. coli* BH101 with pKNT25::*imuA*$_{N\Delta 159}$ pUT18::*imuB*$_{N\Delta 321}$	This study
SAB98	*E. coli* BH101 with pKNT25::*imuA*$_{N\Delta 159}$ pUT18C::*imuB*$_{N\Delta 338}$	This study
SAB99	*E. coli* BH101 with pKNT25::*imuA*$_{N\Delta 159}$ pUT18::*imuB*$_{N\Delta 338}$	This study
SAB100	*E. coli* BH101 with pKT25::*imuA*$_{N\Delta 159}$ pUT18C::*imuB*$_{C\Delta 160}$	This study
SAB101	*E. coli* BH101 with pKT25::*imuA*$_{N\Delta 159}$ pUT18::*imuB*$_{C\Delta 160}$	This study
SAB102	*E. coli* BH101 with pKT25::*imuA*$_{N\Delta 159}$ pUT18C::*imuB*$_{C\Delta 136}$	This study
SAB103	*E. coli* BH101 with pKT25::*imuA*$_{N\Delta 159}$ pUT18::*imuB*$_{C\Delta 136}$	This study
SAB104	*E. coli* BH101 with pKT25::*imuA*$_{N\Delta 159}$ pUT18C::*imuB*$_{C\Delta 81}$	This study
SAB105	*E. coli* BH101 with pKT25::*imuA*$_{N\Delta 159}$ pUT18::*imuB*$_{C\Delta 81}$	This study
SAB106	*E. coli* BH101 with pKNT25::*imuA*$_{N\Delta 159}$ pUT18C::*imuB*$_{C\Delta 160}$	This study

SAB107	*E. coli* BH101 with pKNT25::*imuA*$_{N\Delta159}$ pUT18::*imuB*$_{C\Delta160}$	This study
SAB108	*E. coli* BH101 with pKNT25::*imuA*$_{N\Delta159}$ pUT18C::*imuB*$_{C\Delta136}$	This study
SAB109	*E. coli* BH101 with pKNT25::*imuA*$_{N\Delta159}$ pUT18::*imuB*$_{C\Delta136}$	This study
SAB110	*E. coli* BH101 with pKNT25::*imuA*$_{N\Delta159}$ pUT18C::*imuB*$_{C\Delta81}$	This study
SAB111	*E. coli* BH101 with pKNT25::*imuA*$_{N\Delta159}$ pUT18::*imuB*$_{C\Delta81}$	This study
SAB112	*E. coli* BH101 with pKT25::*imuA*$_{N\Delta159}$ pUT18C::*imuB*	This study
SAB113	*E. coli* BH101 with pKNT25::*imuA*$_{N\Delta159}$ pUT18C::*imuB*	This study
SAB114	*E. coli* BH101 with pKT25::*imuA*$_{N\Delta159}$ pUT18::*imuB*	This study
SAB115	*E. coli* BH101 with pKNT25::*imuA*$_{N\Delta159}$ pUT18::*imuB*	This study
SAB116	*E. coli* BH101 with pKT25::*imuA*$_{N\Delta222}$ pUT18C::*imuB*$_{N\Delta300}$	This study
SAB117	*E. coli* BH101 with pKT25::*imuA*$_{N\Delta222}$ pUT18::*imuB*$_{N\Delta300}$	This study
SAB118	*E. coli* BH101 with pKT25::*imuA*$_{N\Delta222}$ pUT18C::*imuB*$_{N\Delta321}$	This study
SAB119	*E. coli* BH101 with pKT25::*imuA*$_{N\Delta222}$ pUT18::*imuB*$_{N\Delta321}$	This study
SAB120	*E. coli* BH101 with pKT25::*imuA*$_{N\Delta222}$ pUT18C::*imuB*$_{N\Delta338}$	This study
SAB121	*E. coli* BH101 with pKT25::*imuA*$_{N\Delta222}$ pUT18::*imuB*$_{N\Delta338}$	This study
SAB122	*E. coli* BH101 with pKNT25::*imuA*$_{N\Delta222}$ pUT18C::*imuB*$_{N\Delta300}$	This study
SAB123	*E. coli* BH101 with pKNT25::*imuA*$_{N\Delta222}$ pUT18::*imuB*$_{N\Delta300}$	This study
SAB124	*E. coli* BH101 with pKNT25::*imuA*$_{N\Delta222}$ pUT18C::*imuB*$_{N\Delta321}$	This study
SAB125	*E. coli* BH101 with pKNT25::*imuA*$_{N\Delta222}$ pUT18::*imuB*$_{N\Delta321}$	This study
SAB126	*E. coli* BH101 with pKNT25::*imuA*$_{N\Delta222}$ pUT18C::*imuB*$_{N\Delta338}$	This study
SAB127	*E. coli* BH101 with pKNT25::*imuA*$_{N\Delta159}$ pUT18::*imuB*$_{N\Delta338}$	This study
SAB128	*E. coli* BH101 with pKT25::*imuA*$_{N\Delta222}$ pUT18C::*imuB*$_{C\Delta160}$	This study

SAB129	*E. coli* BH101 with pKT25::*imuA*$_{NΔ222}$ pUT18::*imuB*$_{CΔ160}$	This study
SAB130	*E. coli* BH101 with pKT25::*imuA*$_{NΔ222}$ pUT18C::*imuB*$_{CΔ136}$	This study
SAB131	*E. coli* BH101 with pKT25::*imuA*$_{NΔ222}$ pUT18::*imuB*$_{CΔ136}$	This study
SAB132	*E. coli* BH101 with pKT25::*imuA*$_{NΔ222}$ pUT18C::*imuB*$_{CΔ81}$	This study
SAB133	*E. coli* BH101 with pKT25::*imuA*$_{NΔ222}$ pUT18::*imuB*$_{CΔ81}$	This study
SAB134	*E. coli* BH101 with pKNT25::*imuA*$_{NΔ222}$ pUT18C::*imuB*$_{CΔ160}$	This study
SAB135	*E. coli* BH101 with pKNT25::*imuA*$_{NΔ222}$ pUT18::*imuB*$_{CΔ160}$	This study
SAB136	*E. coli* BH101 with pKNT25::*imuA*$_{NΔ222}$ pUT18C::*imuB*$_{CΔ136}$	This study
SAB137	*E. coli* BH101 with pKNT25::*imuA*$_{NΔ222}$ pUT18::*imuB*$_{CΔ136}$	This study
SAB138	*E. coli* BH101 with pKNT25::*imuA*$_{NΔ222}$ pUT18C::*imuB*$_{CΔ81}$	This study
SAB139	*E. coli* BH101 with pKNT25::*imuA*$_{NΔ222}$ pUT18::*imuB*$_{CΔ81}$	This study
SAB140	*E. coli* BH101 with pKT25::*imuA*$_{NΔ222}$ pUT18C::*imuB*	This study
SAB141	*E. coli* BH101 with pKNT25::*imuA*$_{NΔ222}$ pUT18C::*imuB*	This study
SAB142	*E. coli* BH101 with pKT25::*imuA*$_{NΔ222}$ pUT18::*imuB*	This study
SAB143	*E. coli* BH101 with pKNT25::*imuA*$_{NΔ222}$ pUT18::*imuB*	This study